Faculty of Science and Engineering

Exploring the Design of a Simultaneous, Parallel, Discrete Joint Control Orthosis for Hand Rehabilitation

Daniel Aidan Benson

0000-0002-9606-3027

This thesis is presented for the award of the Degree of

Masters of Philosophy (Mechanical Engineering)

of

Curtin University

April 2024

Declaration

To the best of my knowledge and belief this thesis contains no material previously published by any other person except where due acknowledgement has been made and works are cited.

This thesis contains no material which has been accepted for any other degree or diploma in any university.

Signature: ………………………………………….

Date: ……………24/4/2024

Abstract

Hands provide many crucial functions in day-to-day life, however there are many ways this can be compromised, such as brain injuries, local traumatic damage, or surgery. When hand function is compromised, rehabilitation can become a requirement for recovery. While many rehabilitation exercises and methods exist which permit therapy, the application of robotics to this is a growing field. This project explores the design of a hand orthosis for rehabilitation which builds upon several pre-existing designs. This project began by creating a novel mechanism which could provide targeted therapy to one or more nominated discrete joints, simultaneously, across the lower forearm.

This work incorporates extensive research into the development of a simulated full hand rehabilitative orthosis. The goal is to let therapists assist patents in carrying out the most common, frequently needed and widely referred physiotherapeutic exercises. For accomplishing this goal, this work contributes to four major aspects of exoskeleton design:

1. Design and development of a therapeutically derived, controllable hand model.
2. Development and objective simulation of a 26 degrees of freedom (DOF) mechanism capable of full hand controllability.
3. Design and functional simulation of the 26-DOF mechanism that would facilitate independent joint control operations.
4. Development of a multilevel ROS package in a distributed computing environment for simulating and automating (through programming) the designed mechanism.

Through these contributions, this work expands upon and improves the capabilities of hand orthoses to move beyond common design limitations such as controlling only entire fingers or immobilising crucial regions such as the wrist. Considering common physiotherapy exercises when designing this orthosis while permitting isolation of individual joints for targeted therapy will provide improved outcomes for the relevant patient demographics.

Contents

List of Figures

List of Tables

Notations

a_n	The distance from joint axes Z_n to Z_{n+1} measured along X_n
α_n	The angle between the axes Z_n and Z_{n+1} measured about X_n
d_n	The distance between axes X_{n-1} and X_n measured along the axes Z_n
θ_n	The angle between axes X_{n-1} to X_n measured about Z_n axes
x, y, z	Cartesian coordinates along the X, Y, Z axis respectively

Abbreviations

DIP	Distal Inter-Phalangeal
PIP	Proximal Inter-Phalangeal
MCP	Meta-Carpal Proximal
CMC	Carpo-Metacarpal
DP	Distal Proximal
DOF	Degree(s) of Freedom
URDF	Unified Robotic Description Format
DH	Denavit-Hartenberg

Chapter 1: Introduction

In this chapter the fundamental consequences of hand injury and its impact on an individual's quality of life are addressed, this is then followed by a discussion of the anatomy of the human hand. Objectives, and scope of this research are then presented.

1.1. Research Background

Muscular or motor control of the hand can become compromised through many ways, such as brain injury, direct injury or as a side effect of surgery. The inability to effectively manipulate objects or interact with the world causes a considerable reduction in the quality of life for an affected individual. As such, ensuring therapy outcomes provide at a minimum the ability to move again will provide a considerable improvement in patient wellbeing.

1.2. Human Hand Anatomy

1.2.1. Structure

The human hand typically consists of four fingers and a thumb, connected to the wrist and then to the forearm. The structure of the hand is provided by bones, these are interfaced by joints, comprising of ligaments, which are driven by tendons connected to muscles that are controlled by the brain via nerves.

1.2.1.1. Bone structure

There is a total of twenty-seven bones within the human hand, comprising of 3 per finger, 2 in the thumb, the 5 metacarpals and 8 carpals forming the wrist [1]. The carpal and metacarpal bones provide the palm while the joint to the fingers form the knuckles. The bone in each phalange which is linked to the metacarpal is known as the proximal phalanx, in the fingers these in turn are linked to the middle phalanx, with each phalange subsequently ending in a distal phalanx. The wrist is connected to both the radius and ulnar bones [2].

1.2.1.2. Joint structure

Each bone in the phalanges is connected to their functional neighbour via joints; this results in each finger possessing three joints while the thumb possesses 2. Joints in the fingers between the distal and middle bones are known as Distal interphalangeal (DIP), between the middle and proximal interphalangeal (PIP), while the joint between proximal and metacarpal is the metacarpophalangeal (MCP) [1]. The thumb possesses two slightly differently named joints; the distal phalangeal (DP) between the distal and proximal, and the proximal phalangeal (PP) between the proximal and metacarpal. The carpometacarpal joint lies between the metacarpals and the distal carpal bones of the wrist. Interfacing the radius of the forearm with the carpals is the Radiocarpal joint, with the distal radioulnar joint between the ulna and radius beneath it [2].

1.2.1.3. Tendons

Tendons provide connection between the muscles for each joint and the associated region of the corresponding bone, in this manner extensor tendons provide extension to the wrist and fingers while flexor tendons provide flexion [1]. The thumb possesses multiple additional tendons to permit abduction and adduction to the proximal metacarpal joint and the carpometacarpal joint.

1.2.1.4. Muscles

Motion of the joints in the hand are controlled by multiple groups of muscles, achieving abduction/adduction and flexion/extension as needed. For the index, middle and ring fingers,

abduction, and adduction is controlled by the interossei muscles, which are located between the metacarpal bones toward the dorsal face. In proximity with the interossei are the lumbricals, located beside the metacarpals toward the palm face, with the exclusion of the thumb, these muscles are responsible for flexion of the metacarpophalangeal joints and extension of the interphalangeal joints. The little finger possesses an additional group of muscles called the hypothenar muscles, consisting of the abductor digiti minimi, flexor digiti minimi brevis and opponens digiti minimi [1]. The abductor digiti minimi provides abduction of the finger along with flexion of the metacarpophalangeal joint [1]. The flexor digiti minimi brevis provides flexion of the metacarpophalangeal joint [1]. The opponens digiti minimi provides both flexion and lateral rotation of the metacarpophalangeal and interphalangeal joints [1]. The thumb possesses a group of muscles known as the thenar muscles, containing the abductor pollicis brevis, adductor pollicis, flexor pollicis brevis and opponens pollicis [1]. The abductor pollicis brevis and adductor pollicis provide abduction/adduction of the thumb at the carpometacarpal joint, while the flexor pollicis brevis provides flexion of the thumb at the metacarpophalangeal joint, and the opponens pollicis provides the opposition of the thumb [1].

1.2.1.5.   Nerves

The hand is innervated by three nerves: the radial, median and the ulnar [1]. The radial nerve provides sensation to the dorsal of the hand across the thumb, index finger and the middle finger. The median nerve provides sensation across the palmar region of the thumb, index finger, middle finger and partially the ring finger, along with providing control of the thenar muscles for the thumb. The ulnar nerve provides sensation to the little finger and ring finger along with control of the hypothenar muscles. The nerves carry signals from the brain to the muscles as well as sensations such as touch, pain, and temperature back to the brain [2].

1.2.1.6.   Ligaments

Ligaments are bands of connective tissue that connect bones while supporting and keeping them in place. There are 6 groups of ligaments: the interphalangeal collateral ligaments, the volar plate, the radial and ulnar collateral ligaments, the volar radiocarpal ligaments, the dorsal radiocarpal ligaments, and the ulnocarpal and radioulnar ligaments [1]. The interphalangeal collateral ligaments are present on both sides of the finger and thumb joints, preventing sideways motion. The volar plate is present on the palm side of the proximal interphalangeal joints, connecting the proximal phalanx to the middle phalanx, this ligament limits the joint to being straightened rather than bending backward. The radial and ulnar collateral ligaments connect the respective forearm bones to the sides of the carpal bones, this stabilises the sides of the wrist while limiting abduction/adduction. The volar radiocarpal ligaments connect the radius to multiple carpal bones, providing support to the palmar face of the wrist. The dorsal radiocarpal ligaments also connect the radius to carpal bones; however, it instead provides support to the back of the wrist. The ulnocarpal and radioulnar ligaments provide the main support for the wrist, connecting the radius and ulnar, as well as the ulnar and carpus [2].

1.2.2. Hand Functionality

Three pairs of motion are exhibited by the joints of the human hand, with each occurring about a different axis of rotation. The flexion/extension pair occurs via rotation about the horizontally perpendicular axis to the joint and bone orientation as seen in figure 1, abduction/adduction occurs about the vertical perpendicular axis, while pronation/supination occur about the parallel axis [3].
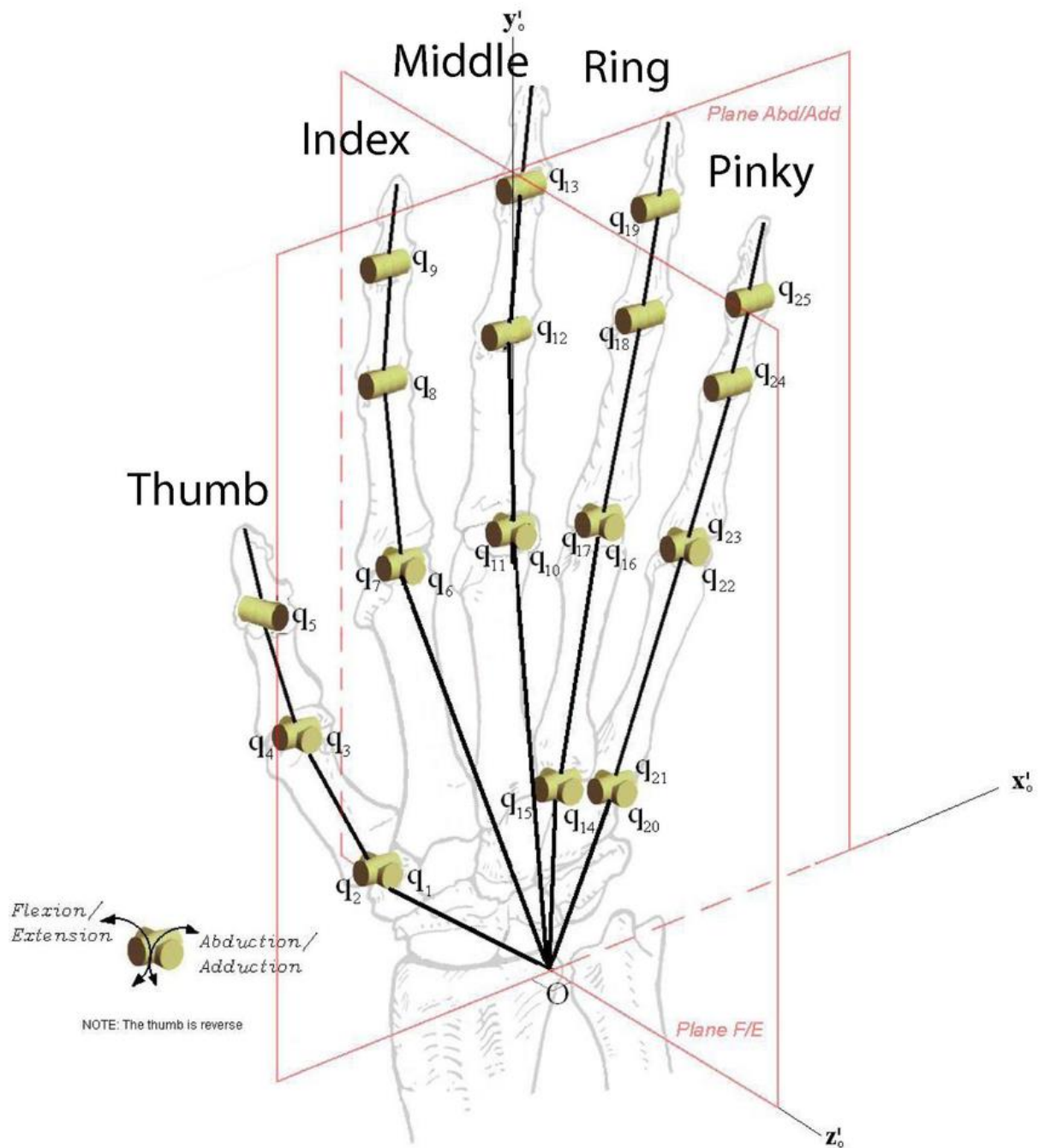
Figure 1: Hand Joint structure [3] indicating layout and orientation of bones, joints, and joint motion in the hand.

9 joints exhibit single-type motion, all permitting flexion/extension. These joints occur in three regions: the distal and proximal interphalangeal joints, and the thumb distal phalangeal joint. 6 joints exhibit double type motion, with all showing non pronation/supination. These joints occur in two groups: the proximal metacarpal joints and the distal radioulnar joint. The four remaining joint regions, the radioulnar joints, the little and ring carpometacarpal joints, and the thumb carpal metacarpal joint, do not conform to the same single or double type joint motion, rather they each exhibit individual characteristic motion. The pair of distal and proximal radioulnar joints combine to provide pronation/supination through combined relative motion. The thumb carpal metacarpal joint provides flexion/extension along the bone axis as other such joints, however it also provides a combined form of abduction/adduction and pronation/supination as a second, distinctive motion

type. Appendix D contains a layout of all joints in the forearm and hand, with each cylinder representing a DOF in each joint, thus resulting in 26 DOF in total [2].

1.2.3. Challenges affecting the rehabilitation process

The objective of rehabilitation is to recover the patient's mobility, with the aim to ensure self-sufficiency and the ability to interact with at the least general household needs, achieving this ensures the recovery of the patient quality of life, however the actual level of recovery is dependent on a number of factors, such as the type and location of injury, the complexity of associated rehabilitation exercises, and the ease of access to the therapist and associated therapy. Achieving rehabilitation requires a goal range of motion, such as the hand therapy motion ranges provided in Appendix A, achieving these motion capabilities ensure the patient can achieve a variety of grasp and motion forms such as those shown in Appendix B. Both documents have been provided by the School of Occupational Therapy [4], with the objective of demonstrating grasps which will ensure the patient can interact with the desired household needs.

The process of hand rehabilitation involves a variety of exercises, designed to engage multiple muscles at once, often with each exercise training a particular form of grasp, with some examples including the use of an elastic band for training simultaneous phalange extension and the use of a squeeze ball for training phalange flexion, both of these examples combine range of motion, force and muscle control, while being adjustable to train a varying number of phalanges. Supporting the use of interactive tools for training, the therapist can further guide the patient via direct application of force to targeted regions of the patient hand to provide supported training for smaller regions or single phalanges/joints which may be unsuitable to train via methods such as the examples given. Such direct methods also enable the therapist to observe any limitations or deviations present in the subject area.

The potential exists to use robotic orthoses to expand and improve upon therapeutic exercises however there are several factors which limit this potential. Following interviews with medical practitioners [5], multiple points of interest were identified; the addition of a therapeutic orthosis to the patient arm must avoid applying additional strain on the compromised area, otherwise it risks exacerbating the existing injury, furthermore its design must be of a form comfortable to the patient to encourage their interest in continuing its usage. The capacity to incorporate a more diverse range of exercises in the design would enable one device to provide a much greater rehabilitation effort than simpler methods, however the need remains for a therapist to observe and guide the associated exercises, this could be alleviated via remote therapy using methods such are internet connectivity however the quality of connection or even access to such utilities could influence the quality received, however this would otherwise serve to address existing limits arising from patients residing in remote areas which may not be readily accessible for the therapist.

Another limitation on the use of orthoses is the sheer diversity of therapeutic needs, as well as the variations between individuals. To avoid an excessive complexity of design an orthosis could be designed to only provide a limited form of therapy however this increases the number of devices required for full rehabilitation depending on the scope for the individual patient.

1.3. Research Significance

This work aims to explore theoretical and experimental challenges associated with the motion planning of robotic exoskeletons in occupational hand therapy. The analyses required for planning and designing exoskeletons' interactions and functionality would help in achieving the following objectives:

A. Building a robust model of a therapeutic hand exoskeleton,
B. Designing and constructing therapeutic robots,
C. Implementing behavioural routines that replicate desired human motion,
D. Simplifying the motion planning scheme and incorporating a distributed, low profile sensory system for reporting behavioural data in a diverse selection of sites, and
E. Developing a novel robotic system that can act upon, partially substitute, and assist human beings in hand therapy.

1.4. Scope of Work

In this project, the pursuit of the objectives will lead to the simulated operation of a robotic hand exoskeleton capable of inducing sufficient hand motion consistent with therapeutic requirements. This exploration can be achieved through a sequence of steps listed below.

1. Requirements Analysis: The initial task involves determining the complete motion characteristics of a healthy human hand, broken down to provide characteristics for each joint. This is a necessary first step for the modelling process as the provision of the motion requirements is the determining factor for the suitability of an exoskeleton.
2. Physical Representation Modelling: The second task involves the development of a model representation of the hand motion characteristics. To develop a suitable model using the determined requirements, a mathematical representation must be derived which incorporates dynamic and kinematic behaviour.
3. Exoskeleton Design: The third task involves the development of a model exoskeleton capable of facilitating motion in accordance with hand constraints. Developing a suitable model requires identification of appropriate actuator types and sizes, along with drive mechanisms to produce the desired motion.
4. Simulation Control Schema and Testing: The fourth task is the development of a simulated control system which can provide full control over the exoskeleton model. As this requires a method of response control, a suitable form of plant control which is readily tuneable and appropriate to this system must be determined. The overall system behaviour could be demonstrated by testing of the control schema through manipulating the modelled arm via the exoskeleton. To provide a basis for simulation and control methodology, the Robotic Operating System (ROS) will be used.

Chapter 2: Literature Review

The literature review presented in this chapter reviews recent developments in orthosis design, examining scope, actuation mechanisms, transmission methods, and support structures. The chapter then discusses mathematic representations and their applications to rehabilitation. This chapter closes with discussion of ROS, its applications to orthosis design, and subsequently rehabilitation.

2.1. Existing Orthosis Design Examination

A comprehensive survey of exoskeleton designs between 2009 and 2019 was conducted in Appendix E, it identified primary forms of structure and actuation used for rehabilitation. The primary methods of control for the designs utilised serial linkages, Bowden cables, tendon cables or in rarer cases pneumatics. Most exoskeletons were designed to control phalanges individually to perform simple grasps while regions such as the wrist and thumb metacarpal were often restrained as part of the support structure. Actuation was supplied via servomotor, with the location varying across designs, as such some designs carried actuators directly on the support structure while others utilised Bowden cables to offset the actuator from the exoskeleton structure.

2.1.1. Design scope range

2.1.1.1. Single phalange

Typically occurring as discrete sections of a larger structure, the single phalange mechanism provides a self-contained structure for controlling all joints required for the design scope within a single phalange, potentially the thumb or any other finger. This self-contained nature enables the given phalange to be controlled irrespective of neighbouring phalange mechanism states. Figure 2 is one such mechanism which uses four discrete mechanisms to each provide single phalange control.

2.1.1.2. Multiple phalange

The multi-phalange mechanism provides an alternative design to parallel single phalange designs, with particular emphasis on multiple phalanges being controlled by the same actuation supply, as opposed to the independent supplies of the single mechanisms. Dependant on the actuation needs, combining supplies can reduce the number required for the desired controllability, however this can also reduce the total controllability of the mechanism with respect to inter-phalange positioning. Figure 3 is a design containing a multi-phalange mechanism which controls both the index and
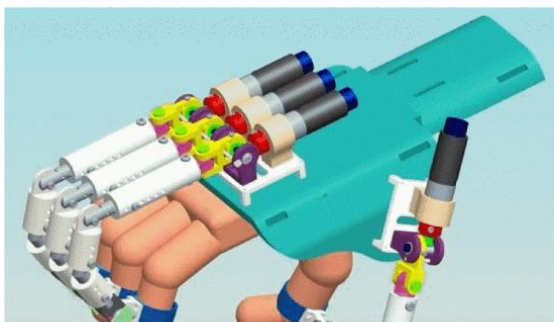
Figure 2: HEXOSYS-II [6] dorsal mounted orthosis controlling 4 phalanges using gear driven lever mechanism. ©2011 IEEE

middle finger with the same supply, along with the thumb being controlled by a separate, single phalange supply.
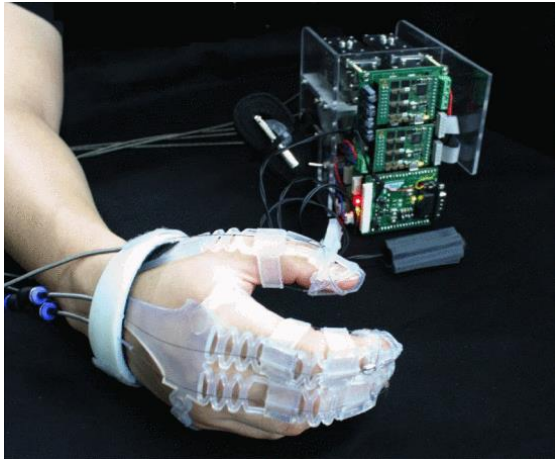
Figure 3: Exo-Glove Poly [7] externally supplied, tendon driven orthosis controlling 3 phalanges. ©2016 IEEE

2.1.1.3. Thumbless phalange

A variation of the multi-phalange mechanism, the thumbless phalange design typically utilises a structural element to constrain motion of the thumb rather than actuate it. Figure 4 is one such design which provides 4 phalange grasping control via multi-phalange mechanism while the thumb is restrained outside of the desired control space.

2.1.1.4. Phalange-only grasping motion.

When examining designs applying full hand grasping exercises, a major design distinction became apparent with respect to the wrist. Depending on the needs of the subject wrist, the supporting structure of the mechanism may potentially mechanically restrain the wrist, preventing undesirable motion. Figure 5 is one such mechanism which restrains the wrist, with this design using the larger dorsal region to support the actuation mechanism.
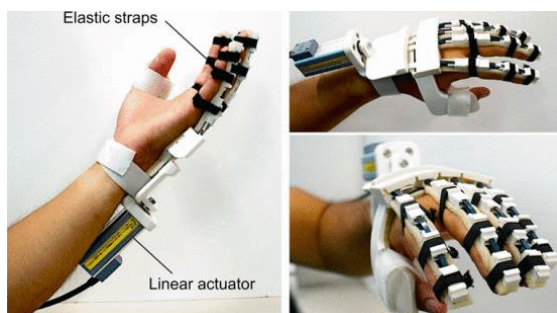
Figure 4: Layered Spring Exoskeleton [8] mounted on the hand dorsal region. ©2013 IEEE

Figure 5: Multi-finger Hand Exoskeleton [9] dorsal region forearm-mounted orthosis.

2.1.1.5.   *Forearm*

A further expansion to the premise of locking the wrist is locking of the forearm, this design decision is applied when motion of both the wrist and forearm are undesirable. Mechanical restriction of the forearm is required for any design in which rotation of this region is undesirable or detrimental to the design operation, such as seen in figure 6 which utilises restraint of the wrist and forearm to maintain hand alignment with the phalange control mechanisms.

2.1.2. Actuation mechanisms

Two forms of actuator motion supply have been observed: linear and rotation. Actuators supplying a form of linear motion typically interface in a manner which takes advantage of the change in length to act upon the orthosis, such as via Bowden cables or linkage-based designs such as Figure 5. Rotational motion is observed in designs which utilise the change of angular position as a driving mechanism, as used in gear-based mechanisms such as Figure 2.

2.1.2.1.   *Electric motors*

Driving most observed actuators, electric motors have been observed as the most common form of actuator supply for the observed orthoses, with both stepper and servo motors being used. Servomotors are commonly utilised to supply linear motion such as that seen in figure 7, while stepper motors are commonly used to provide rotational motion such as in figure 8.
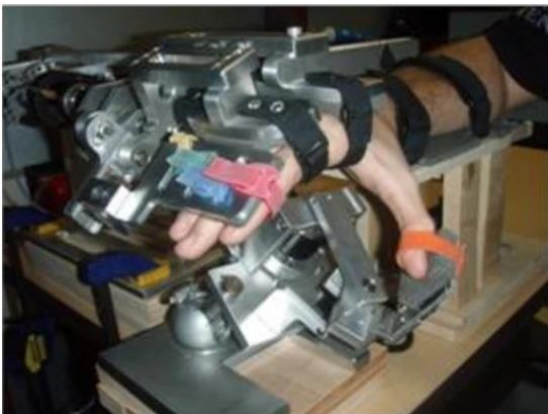
Figure 6: HEXORR Exoskeleton [10] controlling 5 phalanges in 2 groups. ©2015 IEEE
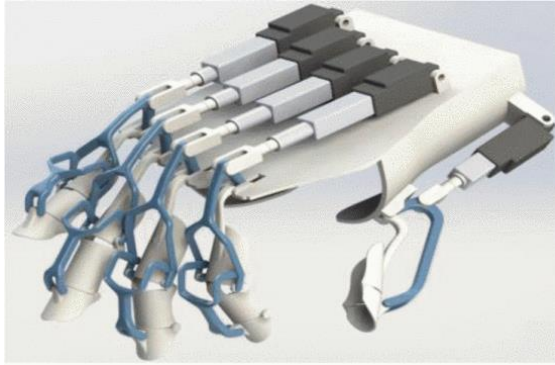
Figure 7: Exoskeleton CAD model [11] dorsal mounted, controlling 5 phalanges via linkage. ©2015 IEEE

2.1.2.2.   Pneumatic

The use of pneumatic actuation was observed in Figure 10, [19], and [22], during which controlled bladder deformation across joints was applied to control grasp-based phalange poses. The primary limitations encountered included actuation bulk, cumulative deformation, and pressure supply effectiveness.

2.1.2.1.   Electroactive polymer

Electroactive polymers provide change in shape in response to electrical stimuli, this provides the potential to function as a structural element while providing controlled actuation. Unfortunately, this form of actuation was not observed in use for orthoses in recent studies, past designs have explored its use however, those designs were studied in [14].

2.1.2.2.   Shape memory alloy

Like electroactive polymers, shape memory alloys provide controlled deformation in response to external stimuli, in the case of shape memory alloys this is heat. Again, like electroactive polymers the use of shape memory alloy as a form of actuation was not observed in recent designs of orthoses.
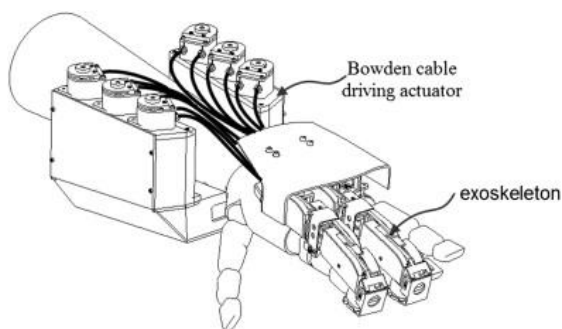
Figure 8: Local Bowden Exoskeleton [12] forearm and wrist dorsal mounted, controlling 2 phalanges via hybrid gear mechanism.
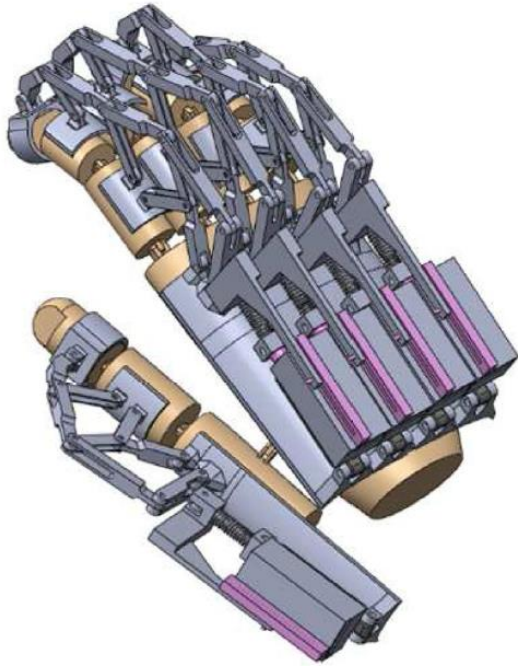
Figure 9: Exoskeleton CAD Model [9] dorsal mounted, controls 5 phalanges.
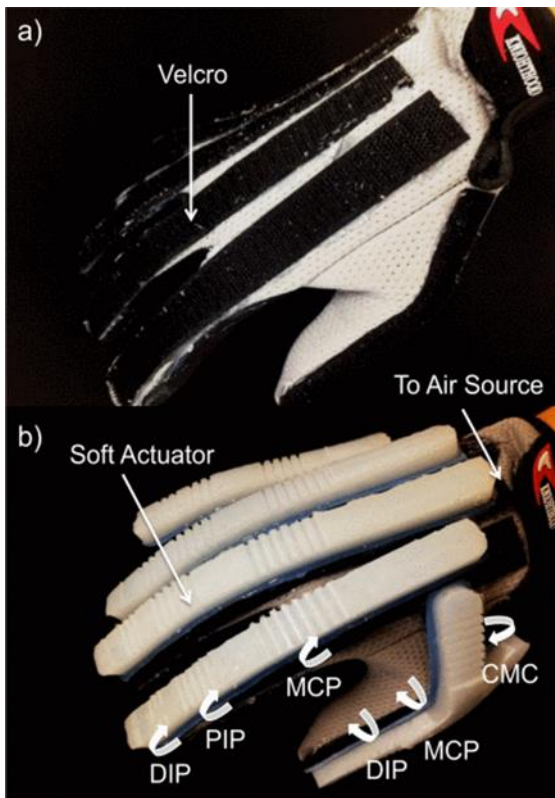
Figure 10: Exoglove Prototype [13] dorsal mounted, controls 5 phalanges via controlled pneumatic bladder deformation. ©2015 IEEE
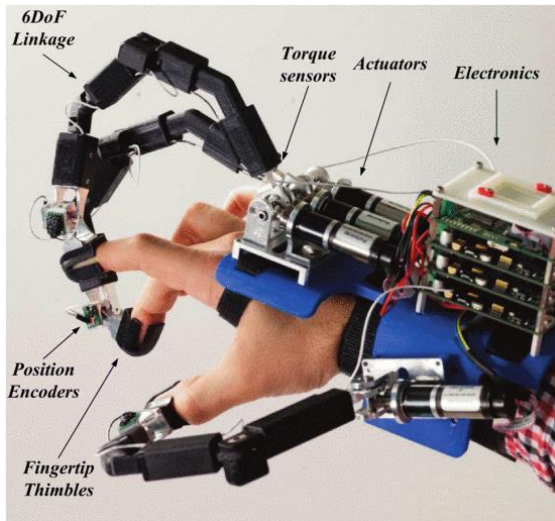
Figure 11: HEXOTRAC Prototype [15] dorsal mounted, controls 3 phalanges via gear driven mechanism. ©2016 IEEE

2.1.3. Transmission

2.1.3.1. Linkage series

Typically applied to control multiple joints simultaneously, linkage style mechanisms are applied in parallel for use in grasping exercises with each phalange controlled by a single series. These linkages operate by controlling at least one joint, usually multiple, simultaneously realigning them as the linkage itself reorientates in response to actuation, as seen in Figure 9.

2.1.3.2. Lever

While linkages are often applied to directly control multiple joints, lever-based designs are used to provide directed control to an individual location, such as seen in Figure 11, this can yield indirect joint control via passive joint motion of uncontrolled joints.

2.1.3.3. Spring

The use of a spring-based mechanism was observed in Figures 4 and 12, in which three leaf springs were layered such that one was passive, one fixed and one actuated. Lateral motion of the actuated spring caused controlled deformation of regions controlling each joint in the affected phalange, effectively providing analogous control to a conventional full phalange linkage mechanism.
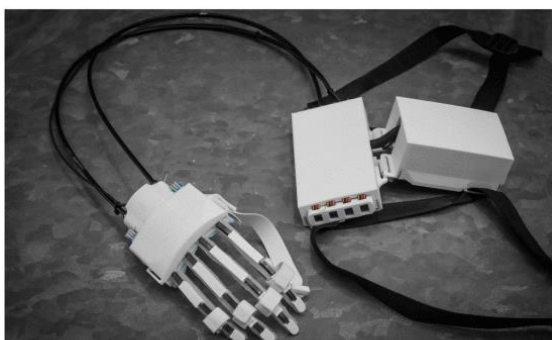
Figure 12: Portable Layered Spring Exoskeleton [16] externally supplied, dorsal mounted orthosis, controls 5 phalanges in 2 groups via parallel spring mechanism. ©2016 IEEE

21
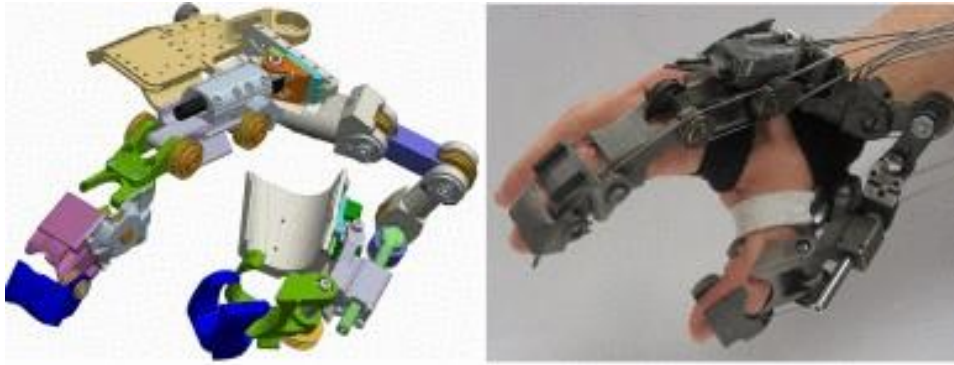
Figure 13: HX Exoskeleton [17] dorsal mounted, controls 2 phalanges via Bowden cable mechanism. ©2014 IEEE

2.1.3.4. Bowden cable

A tendon-based mechanism was observed in Figure 3, using the change in length of a cable to act upon all affected joints, thus enabling multiple joints and phalanges to be controlled by a single source. Unlike the tendon-based mechanism, Bowden cables serve as an intermediary element, often seen as a method to supply indirect actuator output to another mechanism, as seen in Figure 12 which applied the use of Bowden cables to delocalise the actuation supply used in its prior design Figure 4.

2.1.3.5. Deformation

Serving as the transmission mechanism for the pneumatically actuated design in Figure 10, the deformation element uses a pneumatic bladder as a source of activated deformation with a designed pattern of reactive regions in the surrounding body to provide an outlet for the bladder change, resulting in targeted deformation of the overarching structure at predesigned locations such as the phalange joints.

2.1.4. Support structure

2.1.4.1. Localised

In many observed designs with few actuators, such as Figures 4 and 11 with single or four respectively, it may be favourable for the actuators to be mounted on the orthosis, enabling their output to act directly on the transmission mechanism and subsequent target body region.

2.1.4.2. Delocalised

The delocalised structure provides a site for actuator mounting which is not located on the orthosis directly, as such an intermediary transmission method is required to interface the orthosis motion and the actuation supply. In designs such as Figures 12 and 13, this is often achieved via Bowden cable.

2.1.5. Existing Exoskeletons Features' Comparison

To facilitate an effective evaluation of extant orthosis, Table 1 contains a comparison of the subsystems and operation mechanisms for each of the examined orthoses between 2012 and 2023. This table compares the following properties: primary structural support location, number of phalanges controlled, phalange control mechanism, motion drive mechanism, motion type produced, relative actuation supply location, and total DOF controllable. These characteristics enable a comparison of design scope, orthosis design elements, and capabilities, to ensure a fairer comparison between designs during examination.

Table 1 Performance comparison for examined orthoses from Appendix E and more recent.

Orthosis	Support region	# Phalanges target	Phalange control mechanism	Drive mechanism	Motion type	Actuation supply location	Total DOF
CAD [11]	Hand dorsal	5	Linkage	Linear actuator	Grasp	Hand dorsal	5
Bowden [12]	Full forearm	2 fingers	Linkage	Bowden	Discrete	Forearm underside	6
HES	Full arm	4 fingers	Linkage	Direct rotation	Grasp	Arm dorsal	4
BRAVO	Hand dorsal	5	Linkage	Direct rotation	Grasp	Hand dorsal	2
Fine Finger	Hand dorsal	5	Linkage	Linear actuator	Grasp	Hand dorsal	5
HEXORR [10]	Full forearm	5	Linkage	Direct rotation	Grasp	Adjacent	2
HANDEXOS	Hand dorsal	5	Linkage	Bowden	Grasp	External	5
HEXOSYS-II [6]	Hand dorsal	4	Lever	Direct rotation	Grasp	Hand dorsal	4
iHandRehab [31]	Hand dorsal	2	Lever	Bowden	Discrete	External	8
Layered Spring [8]	Hand dorsal	4 fingers	Spring	Linear actuator	Grasp	Hand dorsal	1
Portable Spring [16]	Hand dorsal	5	Spring	Bowden	Grasp	External	2
HX [17]	Hand dorsal	2	Lever	Bowden	Discrete	External	4
Exo-Glove [7]	Hand	3	Cable	Bowden	Grasp	External	3
Intention	Hand dorsal	5	Linkage	Linear actuator	Grasp	External	5
Multi-Finger [9]	Full forearm	4 fingers	Linkage	Linear actuator	Grasp	Hand dorsal	4
Exoskeleton CAD [9]	Hand dorsal	5	Linkage	Linear actuator	Grasp	Hand dorsal	5
SAFE	Hand dorsal	5	Lever	Direct rotation	Discrete	Hand dorsal	10
HEXOTRAC [15]	Full forearm	3	Lever	Direct rotation	Grasp	Full forearm dorsal	3
Exoglove [13]	Hand dorsal	5	Deformation	Pneumatic	Grasp	External	5
Fuzzy [18]	Hand	4 fingers	Cable	Direct rotation	Grasp	Adjacent	2
Soft [19]	Hand Dorsal	5	Deformation	Pneumatic	Grasp	External	5
Robotic Device [20]	Full Forearm	5	Linkage	Direct rotation	Grasp	Adjacent	1

Robotic Exoskeleton [21]	Full forearm	4 fingers	Linkage	Direct rotation	Grasp	Adjacent	1
Soft Glove [22]	Hand dorsal	5	Deformation	Pneumatic	Grasp	External	5
HandMATE [23]	Hand Dorsal	5	Linkage	Linear actuator	Grasp	Hand dorsal	5
RobHand [24]	Full forearm	5	Lever	Linear actuator	Grasp	Hand dorsal	5
Exoskeleton Robot [25]	Full forearm	5	Lever	Linear actuator	Grasp	Hand dorsal	6
Rehabilitation Exoskeleton [26]	Full forearm	5	Linkage	Linear actuator and tendon	Grasp	Forearm and hand dorsal	8
Flexohand [27]	Hand dorsal	5	Cable	Bowden cable	Grasp	External	5

Given the human hand and forearm combined contains 26 DOF[2], creating a suitable orthosis capable of controlling this number of joints requires selection of suitable elements based on their performance as examined in Table 1. The first and most impactful limitation is the need to facilitate discrete joint control, this would provide the most comprehensive and largest scope of control compared to phalangeal control methods, most notable from the DOF column in which HX, SAFE and iHandRehab orthoses possess discrete joint control alongside a higher DOF count than the number of phalanges targeted, indeed iHandRehab and SAFE possess the highest DOF. A target of 26 DOF thus inclines toward similarly discrete joint control.

2.2. Motion Planning
2.2.1. Kinematics

In the application of pose driven robotics, the use of forward and reverse kinematics provides important mechanisms for identifying both resultant poses and required component orientations to achieve desired poses. The application of cumulative kinematic transformations takes advantage of controllable joint orientations and typically fixed linkage dimensions to produce appropriate transformation matrices for each component. Two important applications of robot kinematics are configuration space and collision detection [28].

The configuration space of a given robot is the full region which can be achieved across all available poses. Any pose within the configuration space in a workspace which aligns a component with either an obstacle or another subcomponent will produce a collision. Equation (2.1) provides a conventional representation by which DH parameters can be utilised to produce a transformation matrix (T_n) for a given joint and eventually program the robot. Equation (2.1) is further expanded by (2.2) to permit computation of end position P for a sequence of joints from a given frame F, via matrix multiplication.

$$T_n = \begin{pmatrix} \cos\theta_n & -\sin\theta_n\cos\alpha_n & \sin\theta_n\sin\alpha_n & a_n\cos\theta_n \\ \sin\theta_n & \cos\theta_n\cos\alpha_n & -\cos\theta_n\sin\alpha_n & a_n\sin\theta_n \\ 0 & \sin\alpha_n & \cos\alpha_n & d_n \\ 0 & 0 & 0 & 1 \end{pmatrix} \qquad (2.1)$$

$$T_{F-P} = \left(\prod_{n=b}^{a} \begin{bmatrix} \cos\theta_n & -\sin\theta_n\cos\alpha_n & \sin\theta_n\sin\alpha_n & a_n\cos\theta_n \\ \sin\theta_n & \cos\theta_n\cos\alpha_n & -\cos\theta_n\sin\alpha_n & a_n\sin\theta_n \\ 0 & \sin\alpha_n & \cos\alpha_n & d_n \\ 0 & 0 & 0 & 1 \end{bmatrix} \right) \qquad (2.2)$$

2.2.2. Convex Polyhedra

To improve upon the collision detection identifiable via poses, a volumetric representation is required. This can be achieved via convex decomposition, which will produce a convex polyhedron for each mobile element. A convex polyhedron is a 3D point cloud bounded by a network of 2D planes, this produces a surface containing the entirety of the object known as a convex hull. The convex hull improves upon the kinematic identification of collisions by identifying the positions of not only the joints but the edges of the bounded space of each subsection, thus permitting more precise collision detection and/or avoidance. Collision avoidance is not necessarily the only application of collision identification, as object interaction such as grasping requires contact and therefore collision to occur, as such a volumetric analysis of the region occupied by a robotic system would permit more effective pose identification for the purpose of grasping and other such interactions where collision is not only wanted but desirable. Combining the point cloud nature of a convex polyhedron with kinematics permits a further improved posing mechanism to achieve not only joint state control but vertex positional control as any point within a subsection cloud can be mathematically handled in the same manner as an end effecter to control its pose [28].

2.2.3. Capability map

Further refining the configuration space is the capability map, an improved pose identification which builds upon the configuration space to provide a calculable representation of the versatile workspace, describing how readily regions of the workspace are reachable following the application of all joint limits, structural limitations, and environmental factors. The capability map enables the visual representation of a robot's safely achievable motion range [28].

2.2.4. Therapeutic application

The capability map of a robot describes the full range of kinematic capabilities within a given workspace, thus all achievable poses following design constraints are incorporated into the resulting space. Given that the exercises in Appendix B can be considered a collection of hand poses, the necessary robotic orthosis arrangement for each can be considered a configuration within its capability map which must be present to facilitate that exercise. The incorporation of motion limits in the subject hand will limit the motion ranges for the orthosis, as such the initial capability map will be constrained by the individual joint capabilities for the hand undergoing rehabilitation. As therapy proceeds and joint motion is restored, the resulting expansion of the orthosis configuration space and capability map for the subject hand should thereby approach that of a comparably sized healthy hand.

2.3. Application of ROS to orthosis design

ROS is an open-source framework for robotic software development, providing users with a method for controlling and interacting with both simulated and physical robotic systems while being available across multiple platforms and programming languages [29].

2.3.1. Communication methodology

ROS uses two main methods of communication: messages, and services. Messages are structured data packages formatted according to topics which can be published or subscribed to, in this manner any node responsible for a specific message type being produced can publish it to the topic which will then be received by all nodes which are subscribed to that topic. Services are a form of function call which is provided by a server to run its service as needed when called by other nodes, rather than running perpetually. These two aspects of interaction between nodes enable both data and operations to be conveyed during the overall package operation[29].

2.3.2. Interactive tools

Ros contains multiple useful interactive tools, including methods for viewing the operational and communication structure of a workspace, as well as multiple simulation software's such as RViz and Gazebo. By default, the RQT graph can be utilised to observe the node and topic structure of a workspace, showing publishers, subscribers, and the active topics. RViz provides a motion simulation system for robots, allowing the user to view and simulate motion planning for a given design, however it does not provide a physics engine. Gazebo is a physics engine which can be utilised to simulate a robotic design within a workspace, enabling both environmental configurations and inter-object interaction [29].

2.3.3. Orthosis design

The design methodology of ROS holds multiple avenues for beneficial application to the design of robotic orthoses; at its most basic the use of topics can be directly applied to the generation of joint pose lists with a given message containing the complete configuration of a robot, alternatively the goal configuration can be generated and published, in this manner a control algorithm can utilise the received goal state message to call the appropriate service to operate a motion planning server to produce the necessary series of configurations to achieve the goal state, as an example. The use of RViz enables the verification of the orthosis design, allowing the user to control and view the pose of the design to ensure unwanted collisions do not occur as well as observe the resulting poses and path planning motion. Gazebo provides a means to use the motion planned robot in an environment with physics enabled, allowing the user to observe the interactions between an orthosis design and other objects, for example the use of an exercise ball to verify the orthosis pose will interact with the ball as intended. Overall, these are just example uses of the various elements described pertaining to ROS, there is further capacity for ROS to interact with external input such as controllers, sensors, or even physical robots, as such ROS provides a versatile means to visualise, control and interact with robotic designs [29].

Chapter 3: Exoskeleton Subject Analysis

To provide an accurate reflection of natural human motion it is desirable that the simulated orthosis act upon a model of a human hand, this ensures that any characteristics such as size and motion range limits are applied to the subject model to function as limits for the orthosis motion as well as proportions for sizing components. Developing such a model hand requires measuring the following: bone length, joint location, subsection volume, and joint limits, with additional analysis of any anomalous characteristics present which may need to be addressed. For the ease of access, the author's left hand, as seen in Figure 14, was used as the modelling subject. For the development of all 3D models, Autodesk Fusion 360 was used.

3.1. Subject hand analysis

Important anomalies to identify include dimensional, structural and motion. The subject hand can be seen with a noticeable distortion in the little finger, affecting alignment due to bones not being parallel as expected, in turn this affects phalange length. The same phalange exhibits behavioural anomalies in the proximal metacarpal joint as it demonstrates jerky motion, most notably when extended beyond parallel. The ring proximal metacarpal joint demonstrates a behavioural anomaly in that its position is strongly tied to the position of the little finger, however this only affects motion range when the little undergoes flexion at which point the ring finger cannot demonstrate extension beyond parallel. Overall, these motive anomalies occur only outside the motion ranges specified in Appendix A, as such the subject hand remains capable of the typical range of healthy motion, while the structural deviation only affects alignment for individual bones rather than their sizing as such measurements between joint locations will still give a viable length measurement for the little intermediate bone while its alignment in the simulated form can be applied in a corrected manner.

Figure 14 Author left hand. Note little finger PIP joint shape.

Further to anomaly analysis, the motive range limitations of the subject hand must be measured to provide both confirmation of adherence with expected norms as well as to complete ranges for elements not included in Appendix A, such as thumb carpal metacarpal and proximal metacarpal joints, abduction/adduction for the phalanges, and carpal metacarpal motion for the little and ring fingers. The motion ranges for joints present in Appendix C meet or exceed the anticipated ranges.
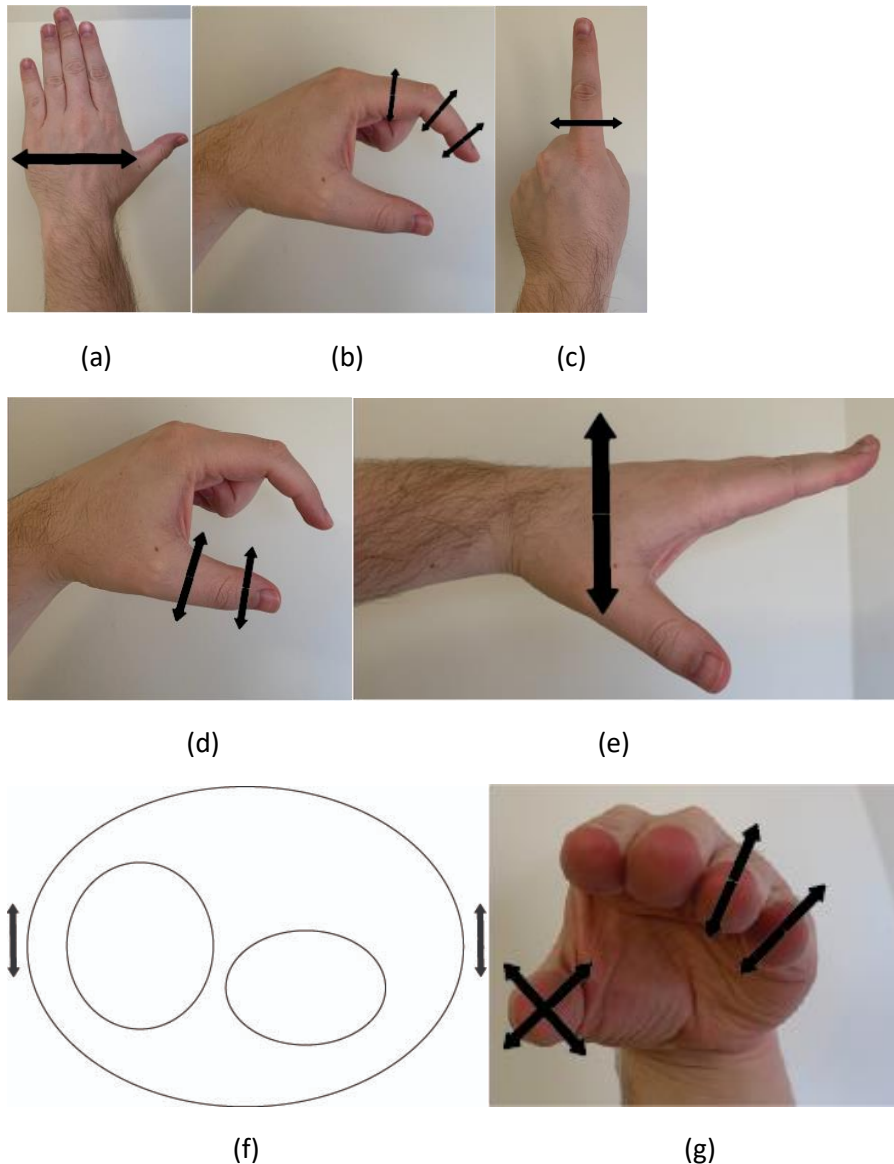
Figure 15: Force Application Requirements.(a) wrist radial/ulnar deviation. (b) non-thumb phalange flexion/extension for proximal, intermedial and distal regions. (c) proximal adduction/abduction. (d) thumb flexion/extension for proximal and distal, note that thumb proximal also has abduction/adduction perpendicular to shown arrows. (e) wrist flexion/extension. (f) radius/ulnar pronation/supination. (g) metacarpal motion indicating thumb rotation and flexion/extension, as well as ring and little metacarpal flexion/extension.

To provide a basis for component sizing, the distances between joint centres of motion have been approximated per Appendix D, this permits an estimate for individual bones and sections such as the carpals which incorporates any non-bone components which are involved in operation. By using both measured locations for carpal metacarpal joints as well as identified edges the approximate size of the carpal structure was measured, enabling an approximated model which neglects intercarpal motion.

To provide complete motive capabilities for the subject hand, a complete examination of the required target areas must be conducted. As can be seen in figure 15(b), 15(c) and 15(d), each non-thumb phalange requires four directed applications of force to provide the necessary flexion/extension and adduction/abduction, while the thumb requires three. To provide the motive requirements of the metacarpal region, as can be seen in figure 15(g), the little and ring phalanges

require one directed force application while the thumb requires two, resulting in the complete chain of little and ring fingers requiring five force applications alongside four for the index and middle fingers, and the thumb also requiring five. From figure 15(a) and 15(e) the wrist requires two sets of force application, one providing flexion/extension and the other adduction/abduction. To provide the forearm radioulnar revolution a single source of rotational force is required, shown in figure 15(f) as tangential forces [30].

3.2. Subject model design

Applying the evaluation of the subject hand, modelled components for each bone as well as supporting elements were produced. Figure 16 contain the bone models for the phalanges from proximal to distal, in which it is important to note the two types of joints present. The distal, proximal, and intermediate bone models each contain joint elements for 1 DOF joints facilitating PIP, DIP and DP flexion/extension, with structural prevention of unnatural adduction/abduction. The metacarpal and proximal bone components contain additional elements for facilitating 2 DOF joints enabling both flexion/extension and adduction/abduction in the MCP and CMC joints, with the addition of a supporting interface element to combine the two 1 DOF joints forming the joint design.
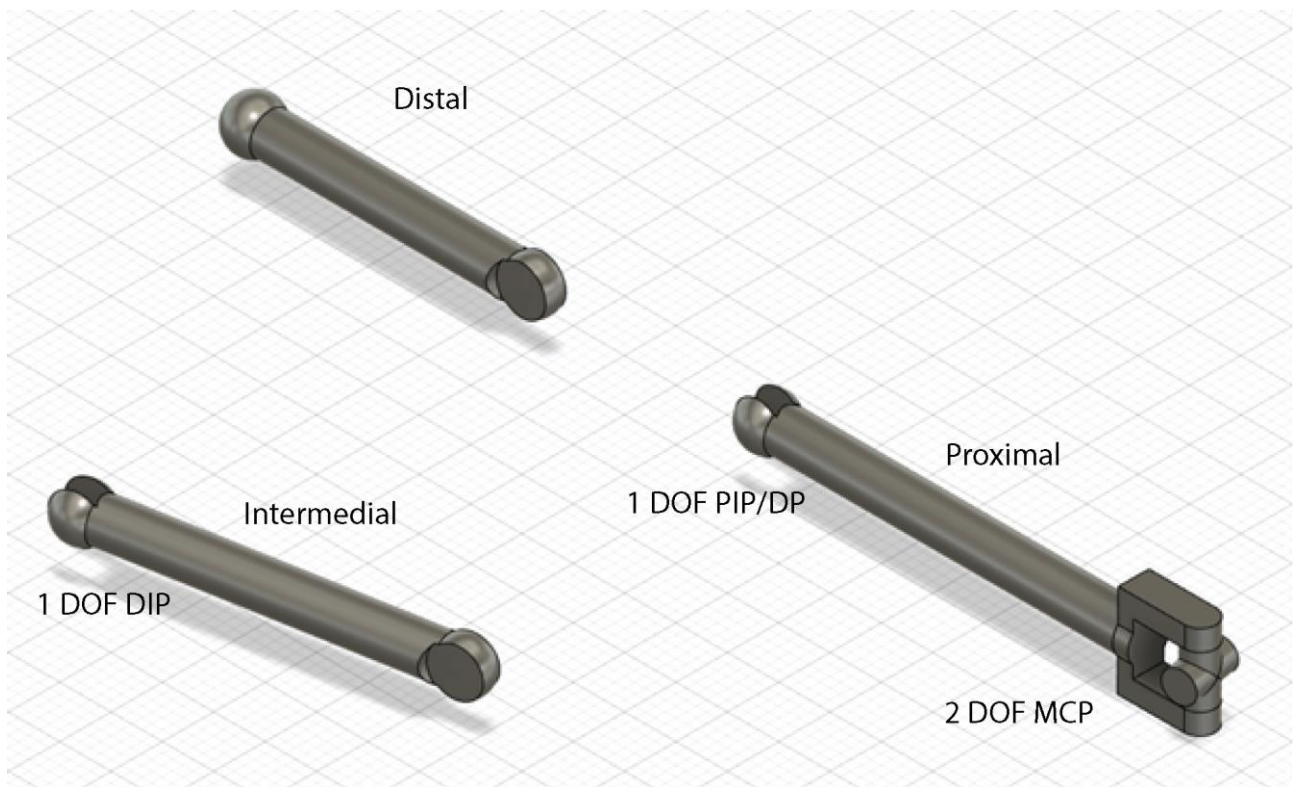
Figure 16: Hand Model Phalange Components.
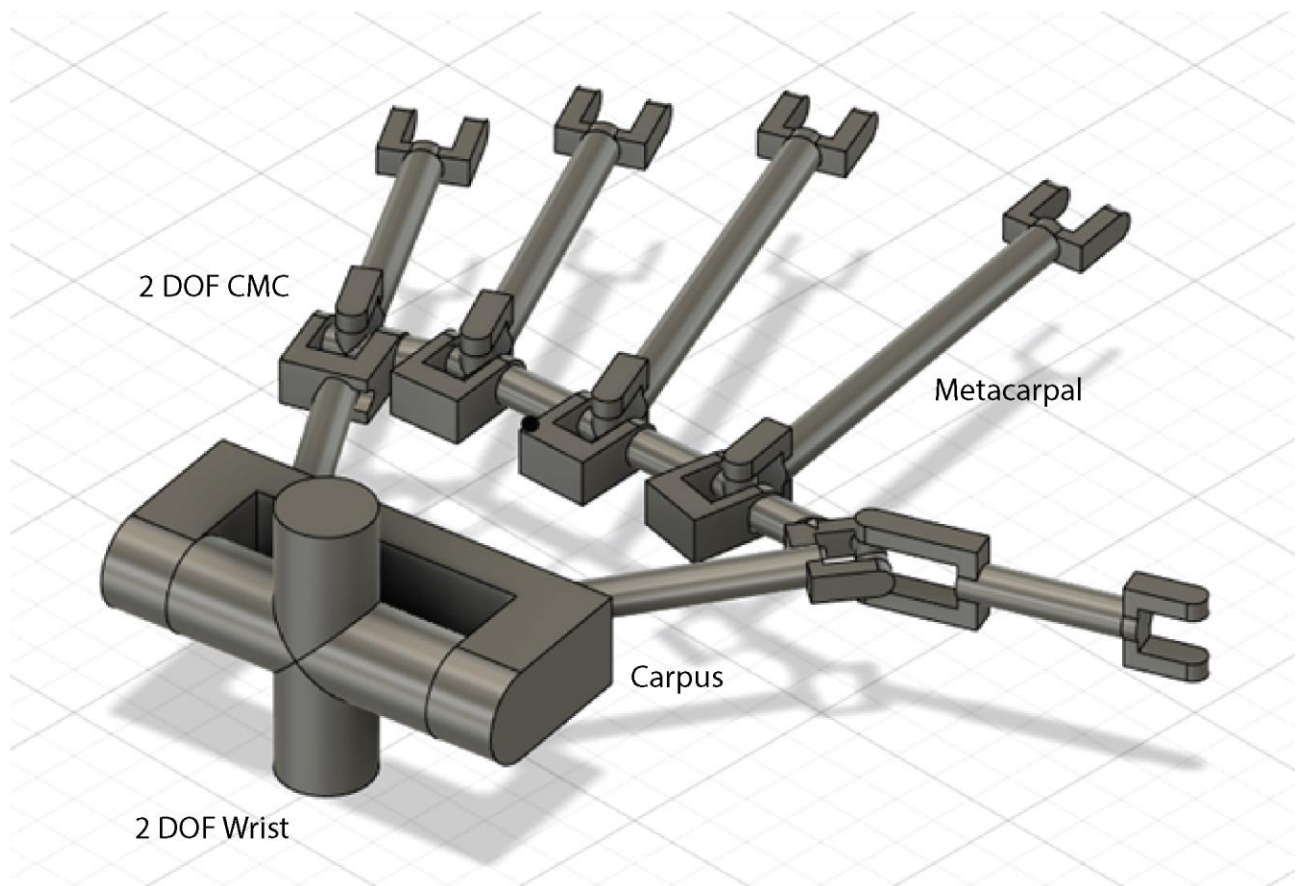
Figure 17: Hand Model Meta/Carpals Region. Note index and middle phalange CMC interface is actuated for orientation tuning only.

The carpal region and forearm radius/ulnar region have been modelled as combined structures rather than individual bone models, for the carpus this is due to the insignificant motion between carpal bones enabling the carpus to be modelled based off the measurements for joint locations in Appendix D, yielding the model shown in figure 17, this model contains joint elements enabling the 2 DOF joints for the CMC and wrist joints in the same style as the MCP joints, facilitating a model comparable to Figure 1. The forearm was split into two components based on a different design to that of the other bone elements, due to the complexity of motion internal to the forearm region the decision was made to split the overall body according to the relative location in which motion between the radius and ulnar occurs, as such the proximal radioulnar region reflects the relatively immobile region while the distal radioulnar region contains the region rotated as a result of the radioulnar joint rotation, furthermore both regions were measured according to the subject body measurements rather than bone measurements which results in the models being relatively larger as seen in figure 18.
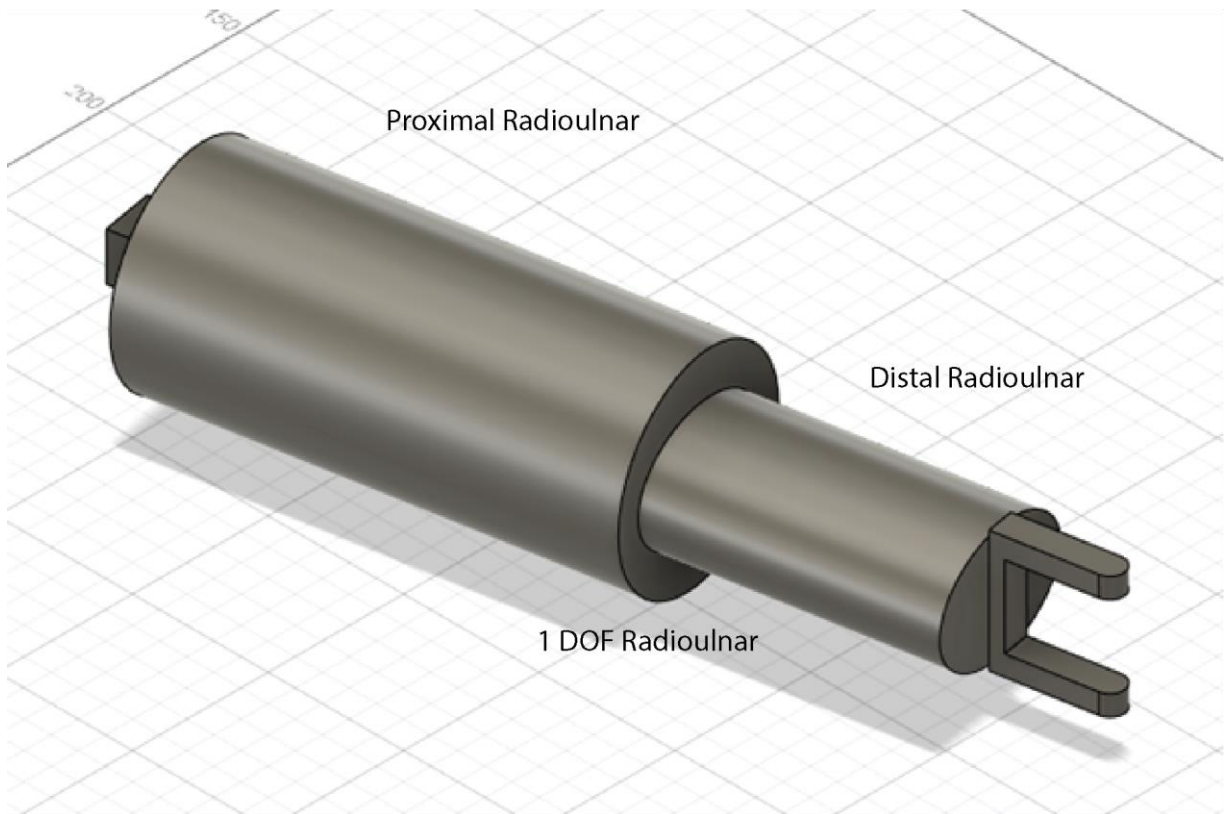
Figure 18: Hand Model Forearm Region.

3.3. Assembly

Combining all bone and supporting models yields the design shown in figure 19, this model takes advantage of the joint connection process in Fusion 360 model assembly to incorporate the joint motion limits outlined in Appendix A, yielding both a full-scale model proportional to the subject, as well as motion limits consistent with therapeutic goals.
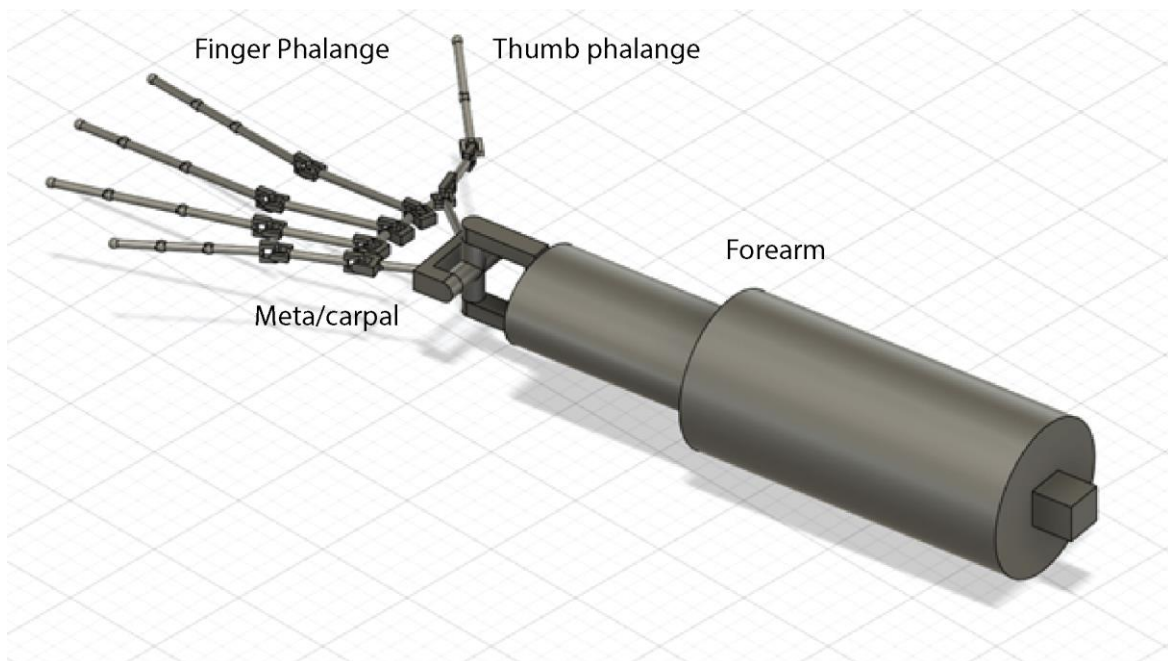
Figure 19: Complete Hand Model Assembly, Isometric view.

Chapter 4: Exoskeleton Design and Implementation

To produce an effective orthosis design, multiple substructures must be addressed: a means of actuation supply, an actuation transmission method, a structural support mechanism, and an end effector interface. For this purpose, the transmission method serves to convert the actuator output into a form suitable to supply localised actuation structures present on the orthosis, which will subsequently act upon end effector bodies of the orthosis to manoeuvre the subject hand. Note that the orthosis design and execution of various poses included in this chapter are based on the common, widely used and recommended therapeutic regimens.

4.1. Subject hand analysis

From the observed actuation forms, only the use of motors such as stepper or servos would be suitable, this is a result of few comparable designs for electroactive or shape memory materials as well as the explored deficiencies in pneumatic designs. Multiple designs such as [15] and [17] have shown the use of several types of electric motor for use in targeted joint control, as such their use in this application would be suitably comparable. Given the objective to control each joint independently, the orthosis design must support 26 individual actuators, this cannot be feasibly supported on the hand or forearm without impacting the volume and weight of the orthosis, as such a mechanism is required which would facilitate externalising the actuation supply without compromising the orthosis volume. From the observed design elements, the use of Bowden cables was selected as it would allow many cables to run in parallel between the orthosis and actuation supply, this would further enable actuators to be mounted on a more suitable region of the patient's body for mobility purposes, or externally in applications where worn travel is not required.

To provide mechanical interfaces for controlling each joint, it is necessary that a structural element is present for each bone or bone region. For the phalanges this is achieved via an element for each proximal, distal, and intermediary component. For the metacarpal region, the index and middle regions can be treated as a single combined bone region, this is due to the absence of relative motion observed during hand motion, as such only four elements are required to support the ring, little, thumb and combined metacarpal regions. For the forearm region the structural element must permit motion within the region, as such two structural elements would suffice [30].

4.2. Orthosis subsystem design

To meet the needs of the force diagrams shown in figure 15, linkage elements have been selected such that end points of actuation align with the directed force arrows, as shown in figure 20. In this manner Figure 20(a) and 20(b) meets the needs of Figure 15(b) and 15(c) via lever mechanism supplying the proximal flexion/extension, rotational linkage supplying intermediate and distal flexion/extension and rotational linkage applied to the proximal lever to supply proximal adduction/abduction. Figure 20(f) meets the needs of figure 15(g) via the use of lever mechanisms to provide directed force, with the ring and little metacarpals supplied by over-actuated mechanisms to provide the single directed force required, while the thumb metacarpal is supplied by a similar, fully actuated mechanism to provide the two perpendicular forces required. Figure 20(e) also contains the use of push-pull pulley mechanisms to provide stroke-limited applications of tangential force, with mechanisms present on both sides to provide even, mirrored forces. Like figure 20(e), Figure 20(c) and 20(d) contains the use of paired pulleys providing push-pull applications of force to facilitate wrist flexion/extension and adduction/abduction.
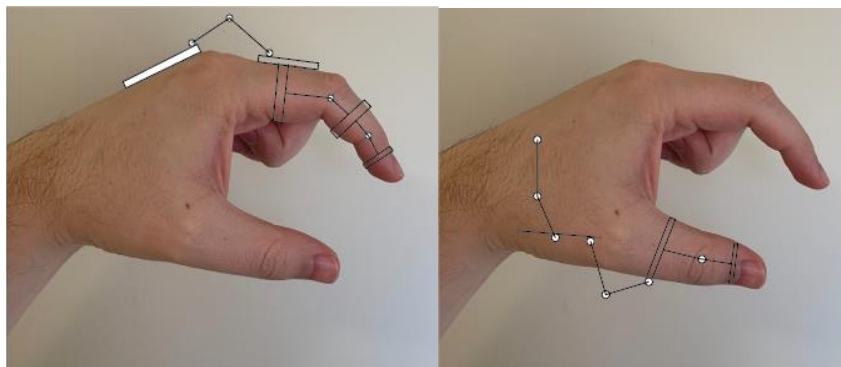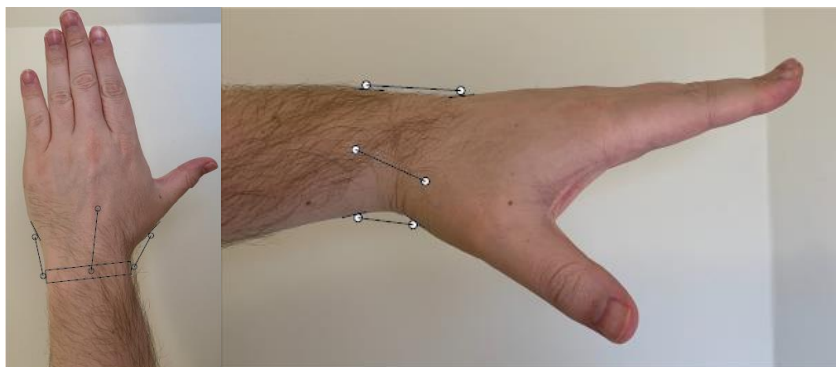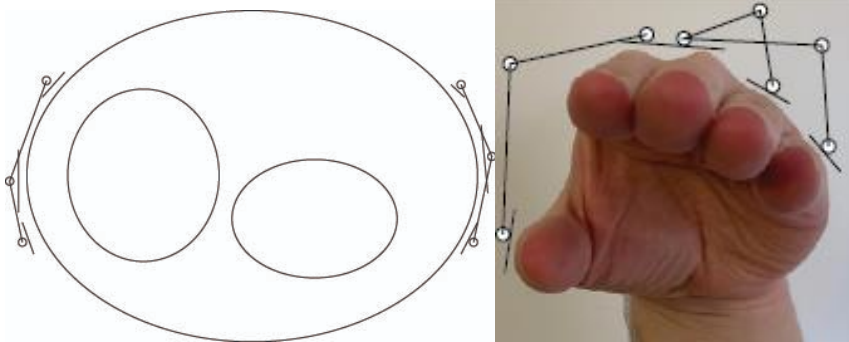
Figure 20: Orthosis Interaction Points. (a) lever mechanism providing proximal flexion/extension and adduction/abduction, targeted rotation mechanism providing intermedial and distal flexion/extension. (b) thumb arrangement for proximal lever mechanism and distal flexion/extension rotation mechanism. (c) mechanism providing wrist radial/ulnar deviation. (d) mechanism providing wrist extension/flexion. (e) mechanism providing forearm supination/pronation. (f) lever mechanism providing flexion/extension for orthosis-controlled metacarpals.

4.2.1. Tension regulation

To facilitate delocalised actuation, a structural element is required which provides both back mounted transport and a common start point for the Bowden cable transmission. To further support
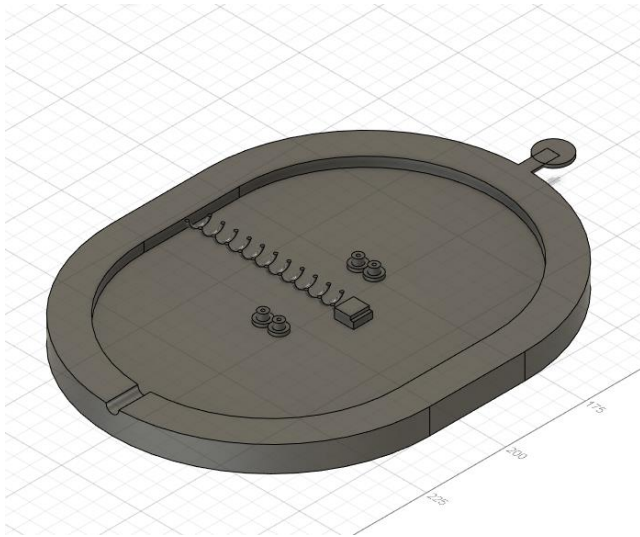
Figure 21: Tension Passive Regulation Mechanism.

the Bowden cable aspect, multi-layer cable protection is required to prevent interference between individual cables as well as minimise the overall volume of the mechanism, the use of an umbilical style arrangement ensures no cables can be caught on external objects. A further structural element required for the Bowden cable mechanism is the inclusion of aa mechanism which serves to regulate variations in tension, figure 21 contains a design for a passive tension regulation mechanism which is intended to absorb slack on individual cables occurring as a result of changes in path length caused by motion of downstream joints, such as the effect of flexion/extension of the wrist on the path length for the DIP joint.

4.2.2. Motion Mechanism Selection

To interface the individual support elements and provide required actuation, end effector interfaces must account for the variations in joint structure and motion characteristics. Of the required motions, the distal radioulnar joint is the only region to require rotation exclusively, as such a distinctive mechanism is required. The remaining regions can be split according to volumetric importance, with the palmar dorsal region being freely available while the phalange dorsal regions are involved in multiple grasps per Appendix B, as such this distinction requires both regions to utilise differing actuation mechanisms.

The absence of significant requirements for dorsal volume enables the use of linkage and lever-based elements to be used for the joints within the metacarpal regions. Given the typical size of observed linkage mechanisms, the use of smaller lever style elements as used in Figure 22 enables each mechanism to control a single joint via single actuator, in the cited design the paired motion requirements for the proximal metacarpal joints were met by combining the lever mechanism with an additional rotational mechanism of the same style supply, this same style of actuation can be further applied to supply both the carpometacarpal joint motion for the little, ring and thumb phalanges.
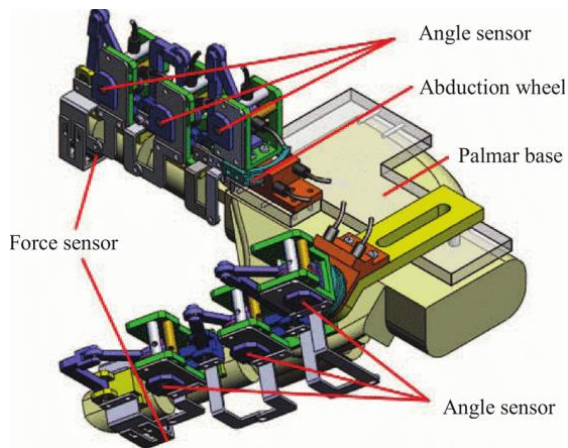
Figure 22: iHandRehab CAD Model [31] dorsal mounted, controls 6 joints across 2 phalanges using cable driven lever mechanisms for each joint. ©2011 IEEE

For the DIP, DP and PIP joints, the requirement of dorsal volumetric freedom renders both lever mechanisms and linkage mechanisms ill-suited, however lower profile designs such as the tendon and leaf spring are not observed as capable of providing the required individual joint control, however the self-aligning orthosis design depicted in Figure 13 shows a possible mechanism for controlling the joints in an independent manner potentially without significantly impacting volumetric accessibility, specifically the mechanism controlling the DIP and PIP joints. In the original design both joints are controlled by a common actuator for the index phalange however if these joints were decoupled it would facilitate full independent joint control for the phalanges while volumetric accessibility for the phalanges would only be limited by the size of the frame for each region as well as the interfacing mechanism, as such with a sufficiently compact mechanism and frame the impact would be minimal.

The provision of rotation for the forearm region requires the design of a mechanism able to act tangentially to the radioulnar region. By using a similar concept to the tendon component of Figure 3, a bidirectional pulley style mechanism can take advantage of the relative immobility of the upper forearm to serve as the base while the distal radioulnar region can be used as the end effected subject, this then permits the forearm to exhibit bidirectional rotational motion.

To provide the actuation supply, a rotational supply such as a stepper motor can be used. To interface the rotational supply with the linear behaviour of Bowden cables, a pair of pinned arms can be utilised, this not only enables varied arm lengths based on required linear motion length needs for each joint, but it also ensures that pairs of cables are directly supplied by the same actuator, providing even push-pull cable motion.

4.3. Design modelling

Designed with respect to Figure 12, the distal and intermedial phalanges utilise a structural element which wraps about the bone region and provides joint interfaces in line with the subject phalangeal joint centre of motion. As can be seen in figure 23, the intermedial element contains two differing sizes of joint interface as corresponding to the differing size of the distal and proximal interphalangeal joints. The distal element contains only a single joint interface for the DIP/DP joint while the other end of the structure continues and covers the end of the region. The proximal element contains two joint interfaces, however only one is of the design for the PIP joint, the other is applied to the dorsal of the element to provide an interface for the lever mechanism providing the MCP joint.
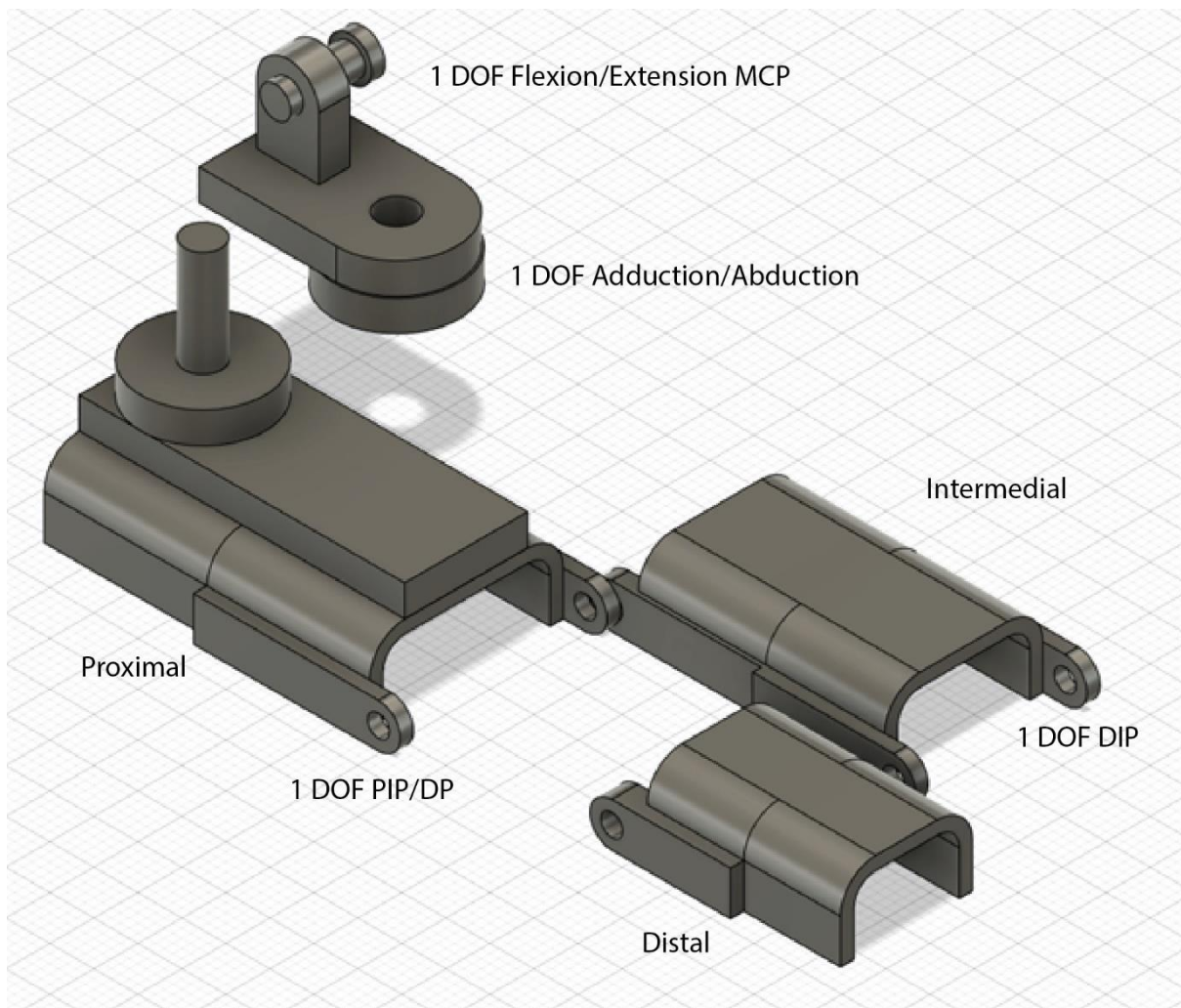
Figure 23: Orthosis Phalange Structure Model.

Due to the lack of designs observed to control the metacarpal bones of the ring and little finger, the decision was made to utilise a similar mechanism to the MCP joint mechanism. Taking advantage of the absence of limiting factors on design volume in the dorsal palm region, a mechanism able to provide 1 DOF for the little and ring phalanges was designed while a variation able to provide 2 DOF was utilised for the thumb. Figure 24 shows a subassembly containing both a lever mechanism for the carpal region and an MCP joint lever mechanism in series.
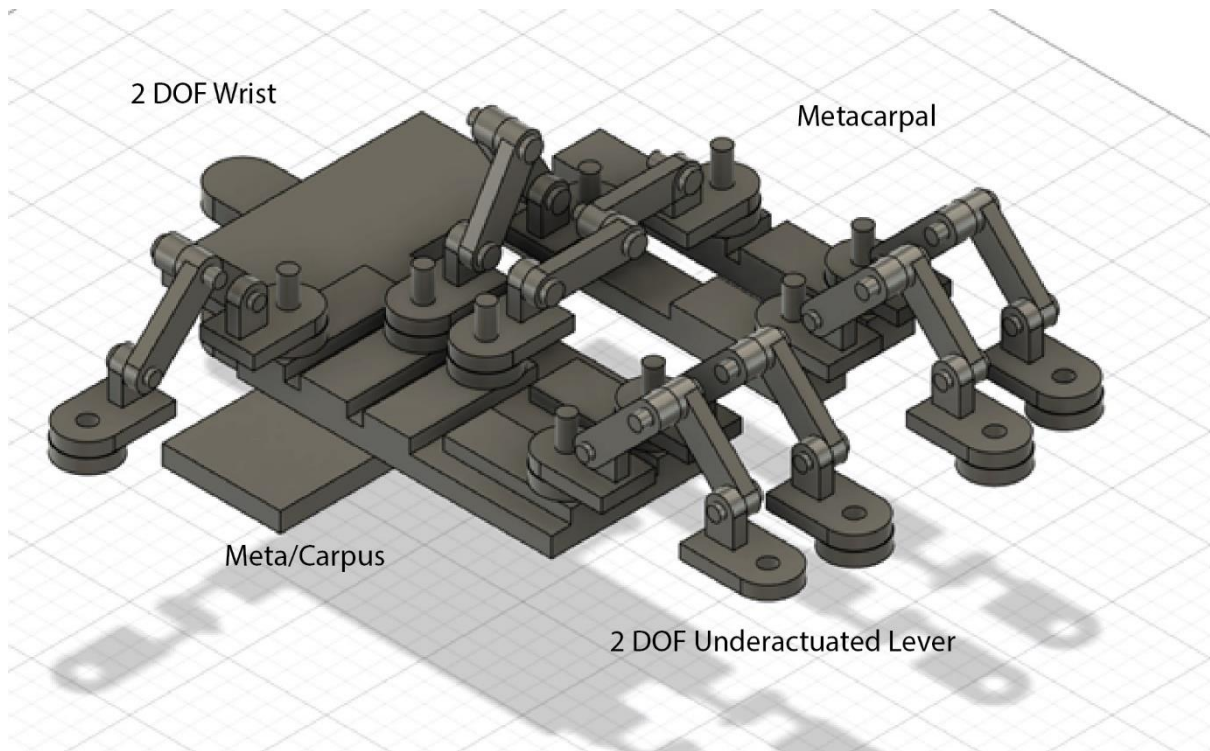
Figure 24: Orthosis Meta/Carpal Structure Model.

To produce the wrist flexion/extension an additional element on the palmar side of the carpal region was incorporated, this serves to provide a connection point for a push-pull mechanism which applies to both the dorsal and palmar regions of the carpus, enabling actuation and the resulting tension to act upon the wrist. A similar mechanism is present for the little and thumb carpal regions to provide similar connection points to facilitate abduction and adduction. Applying the design elements of Figure 8, the subassembly depicted in figure 25 provides end points for actuation to apply to the distal radioulnar structure, enabling even application of motion to opposing sides of the forearm and facilitating the necessary rotation.
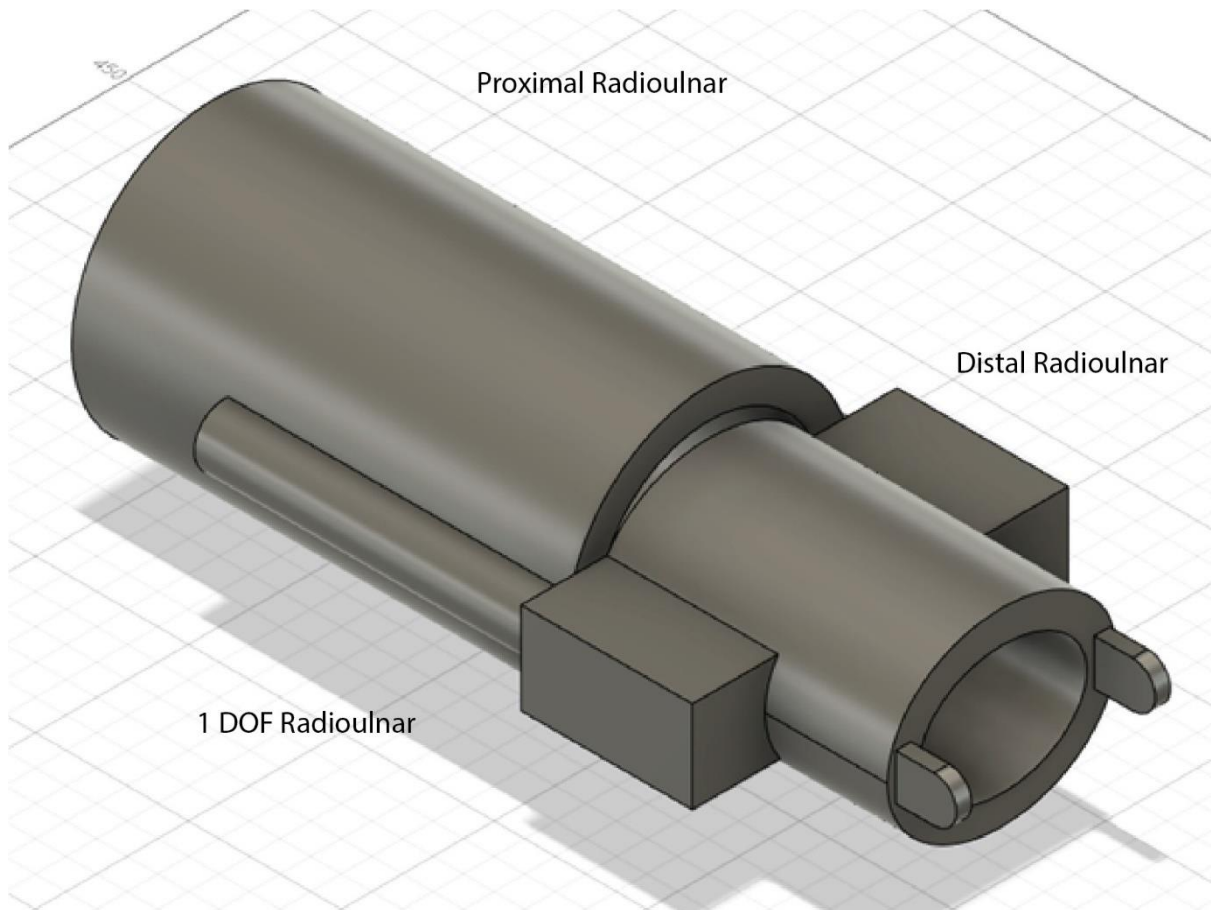
Figure 25: Orthosis Forearm Structure Model.

4.4. Assembly

Figure 26 depicts the combined assembly of the orthosis model with an additional structural element in the wrist serving as a placeholder for the subject hand to enable the wrist structural elements to produce the desired motion, this is due to the need in Fusion 360 for two bodies to be in contact for a joint to be assembled.
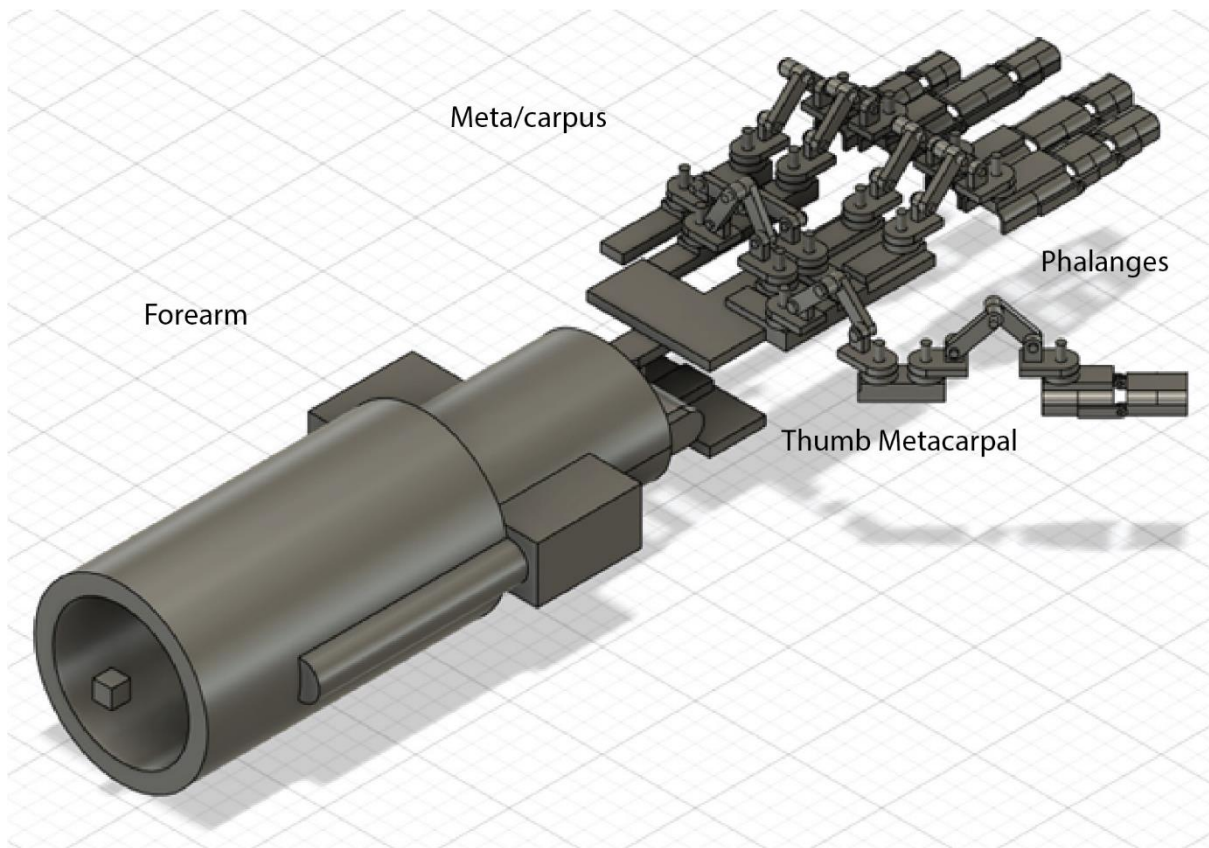
Figure 26: Complete Orthosis Model Assembly, with wrist interface component. Isometric view.

Building upon the requirements established in Figure 15, Figure 27 depicts the force requirements for motive needs and how they will be met by the associated subsections of the orthosis design, as developed by Figure 20. Figure 27(a) shows a top view of the phalangeal structure as utilised for each non-thumb phalange, with force direction arrows consistent with 15(c) and the need for adduction/abduction. 27(b) shows a side view of the non-thumb phalangeal structure, with force arrows providing the required flexion/extension of 15(a). Figure 27(c) shows a top view of the thumb and adduction/abduction of the proximal region as well as the metacarpal, while the side view is like that of 27(b) with respect to the lever mechanism for both the thumb metacarpal and proximal, while the distal flexion/extension is also like that of 27(e). Figure 27(d) depicts the forearm region and the mechanism utilised to provide supination/pronation per 15(f). Figure 27(e) depicts a side view of the structure providing flexion/extension of the little and ring phalanges, as required by 15(g). Figure 27(f) depicts the result of forces applied in 27(d) to provide flexion/extension and radial/ulnar deviation, as required for 15(a) and 15(e).
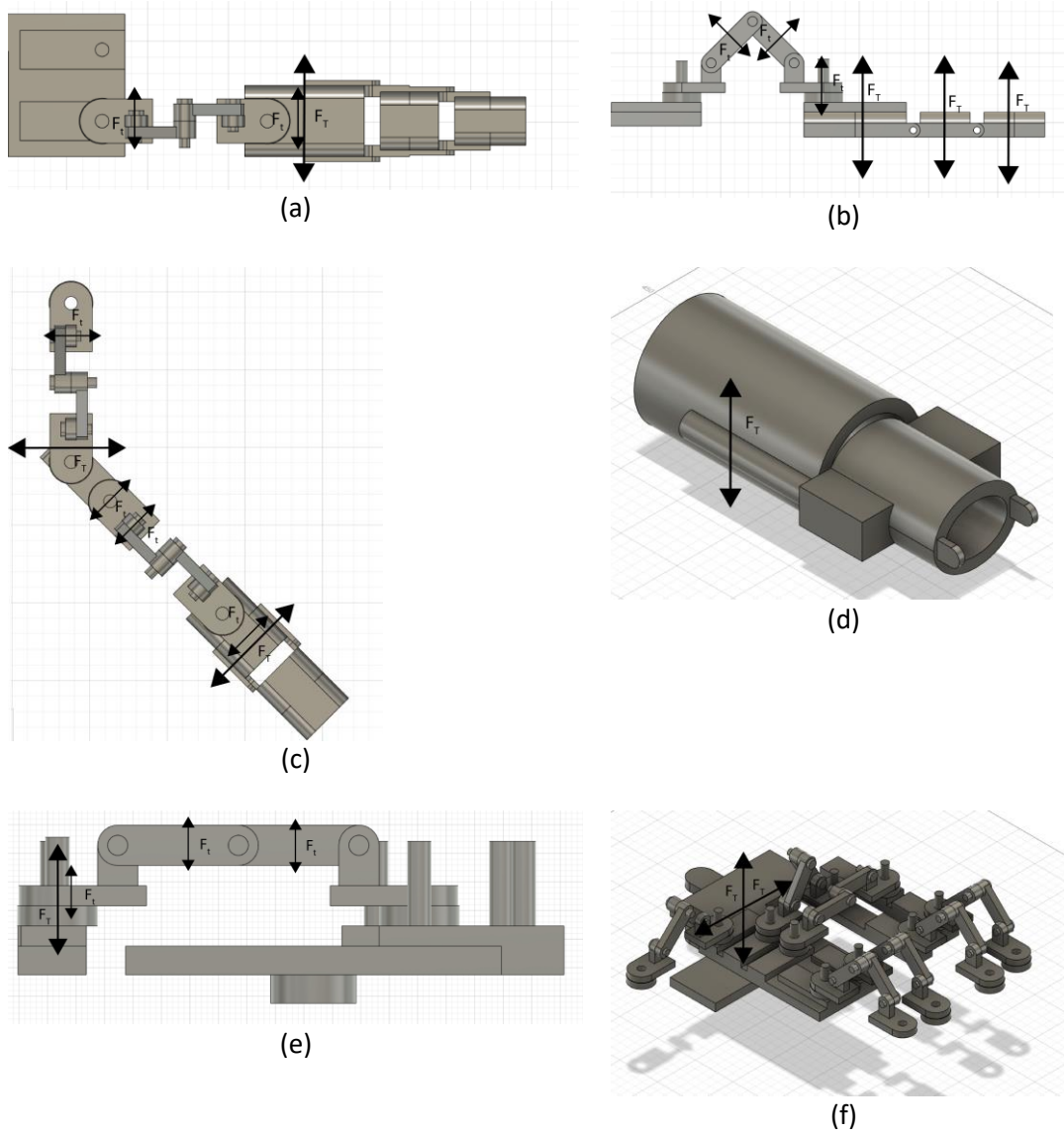
Figure 27: Orthosis Force Applications. (a) non-thumb phalangeal adduction/abduction. (b) flexion/extension for all phalanges, note the thumb does not possess an intermedial flexion/extension component. (c) thumb adduction/abduction for proximal and rotation driving force for metacarpal. Thumb proximal and metacarpal also includes a force component identical to the lever component in (b). (d) supination/pronation of radioulnar region. (e) flexion/extension of ring and little metacarpals. (f) flexion/extension and radius/ulnar deviation. Note in all diagrams small arrows indicate mechanism contributions while large arrows indicate region force outcome. F_t indicates mechanism tangential force contribution; F_T indicates subsection force application.

Chapter 5: ROS Compatible Design of the Exoskeleton

To provide a ROS-compatible control and visualisation scheme, an open-source script [32] was used to produce an appropriate package for each assembly, as seen in Appendix F. Appendix F(1) shows the script requirement of a base link, which serves as a world anchor for the orthosis model. In F(2) the script is activated in Fusion360, producing a structured package as seen in F(3). F(4-6) contain the contents of the launch, URDF, and mesh folders respectively. As the script maintains the joint configurations from the Fusion360 models, joint limits derived from Appendix A are preserved.

5.1. Hand model

Utilising the developed URDF, the hand model can be visualised in RViz by running the associated launch file. As seen in figures 28-29, this produces the assembly alongside a simple GUI enabling control over the position of each joint along with displaying motion limits as specified in the original model and included in the URDF. Alongside RViz, a launch file is available to permit simulation in Gazebo however this model is not effective by itself as it demonstrates instability arising from inconsistencies in requirements for modelling between Fusion360 and Gazebo, with the result that components of the assembly do not remain stationary when undriven, this has the effect of producing chaotic outcomes in which the hand model was observed bouncing around the workspace and many phalangeal components consistently left their joints and exceeded limits. This undesired behaviour resulted in Rviz being utilised exclusively.
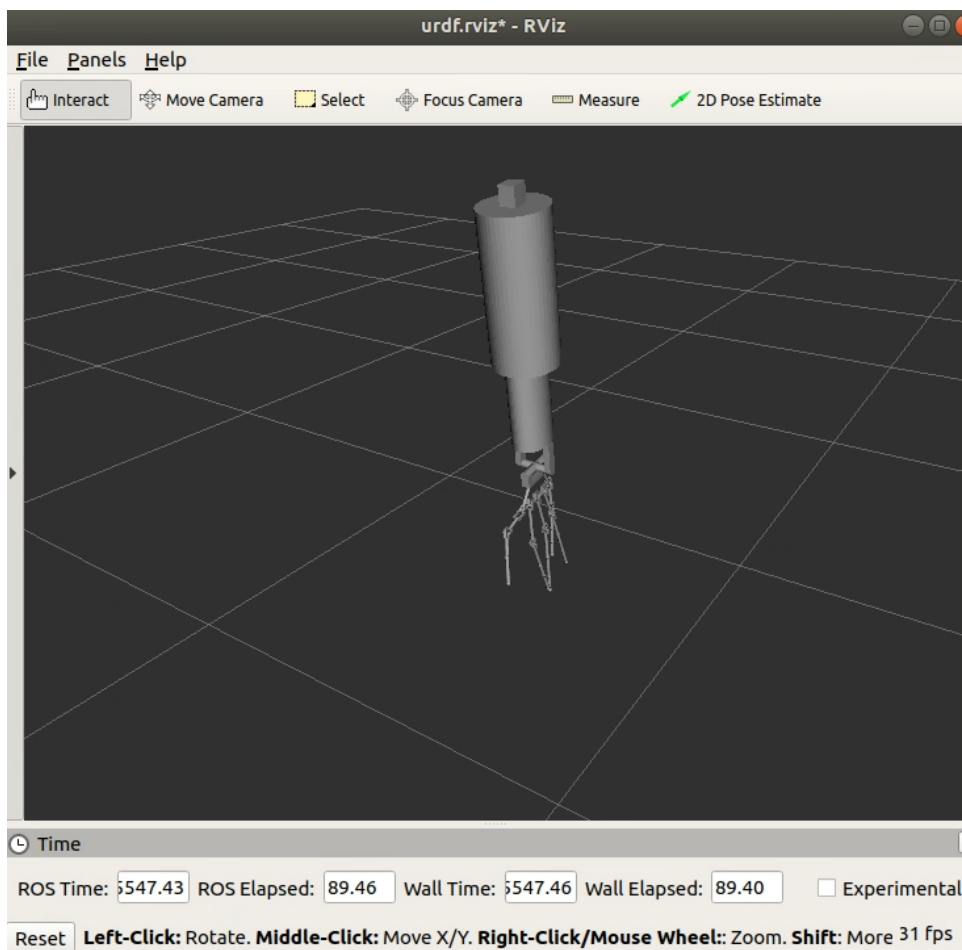
Figure 28: ROS RViz Hand Model.

Figure 29 ROS RViz Hand Model full GUI. Contains both desired and tuning joint control.

The simple control GUI provided with the package enables simple but effective pose examination for the hand, with which each joint can be controlled readily via associated labelled sliders, however due to the considerable number of joints present, as well as the numerous tuning joints, this GUI becomes cumbersome to use. The immediately beneficial usage of this GUI is to verify and tune individual poses, with those included in Appendix B serving as effective examples to replicate.

By itself, the hand model package provides a means to examine the arrangement of individual bones in the human hand, with exceptions for the wrist and forearm due to their design. Combined with the ability to position individual joints as well as predefined motion limits this serves to represent a simulated hand. With improvements such as applying MoveIt to the initial URDF, improvements can be made such as defining types of joints to remove elements which are not required for motion control, including converting tuning joints into fixed joints, as well as applying further motion control elements. Overall, this provides the necessary improvement to the imported model to facilitate both pose control and some path planning simulation for the hand model.

5.2. Orthosis
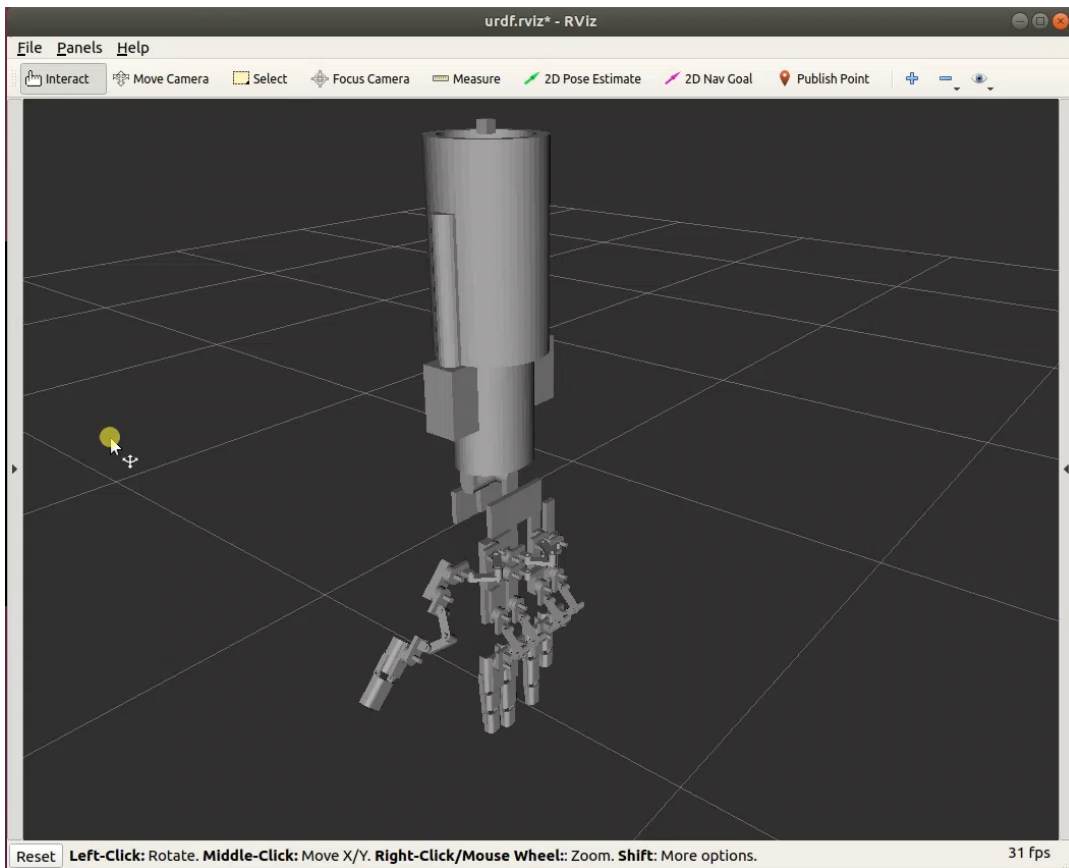
Figure 30: ROS RViz Orthosis Model.

As with the hand model, the developed orthosis model package contains two launchers, with the Gazebo simulation demonstrating similarly unwanted behaviour. As seen in Figures 30-31, the RViz simulation is again like the hand model, however it contains an even greater number of joint controllers on the GUI, with this design containing not only additional tuning elements but additional intermediary joints which are not intended to be directly actuated, as such the base GUI shows an exaggerated quantity of slider joint controllers compared to that of the hand.

Figure 31 ROS RViz Orthosis Model full GUI. Contains desired, intermediate, and tuning joint control.

Experiencing the same limitations as the hand model base GUI, the orthosis model is further hindered in its useability due to the intermediary joints, with multiple joints such as the proximal and metacarpal joints each containing as many as 2 additional joints which must be carefully controlled to ensure realistic posing, as such this GUI is significantly less convenient for simple viewing and posing compared to the hand model.

Even with the application of MoveIt, the cumbersome nature of selecting angles when configuring poses significantly impacts the useability of the orthosis model, combined with the multitude of intermediary joints which need to be carefully adjusted manually, this yields an awkward to use control scheme which overloads the user with information.

5.3. Overall model evaluation

Overall, both aspects of the orthosis model provide a means to control both the subject hand and the orthosis itself, providing both calibration for accuracy and full independent joint control. The range of motion for all joints is further capable of being calibrated to suit the desired range, with the
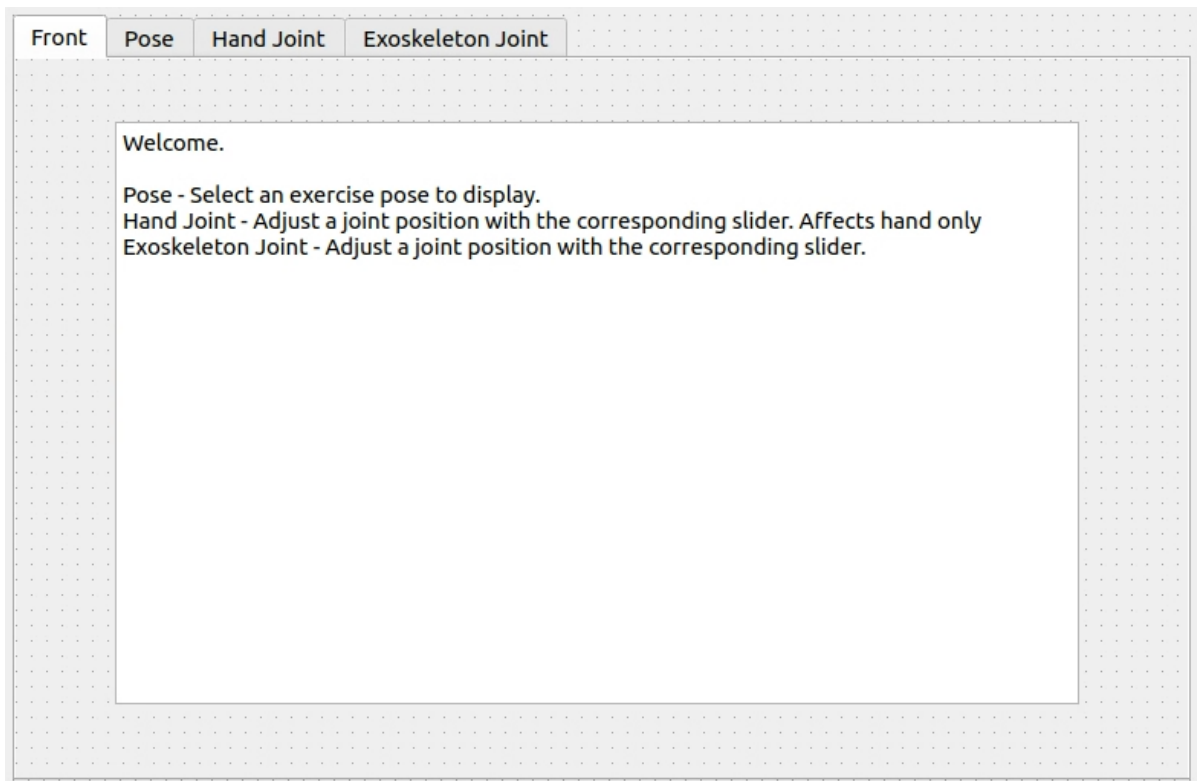
Figure 32: Revised ROS GUI Front Panel with simple user instructions.

depicted model utilising a combination of therapeutically derived values from Appendix A as well as measured approximations from the example subject hand listed in Appendix C, this enables the range of control to be defined by the desired subject and their capabilities.

As it currently stands, the control mechanism for the orthosis provides excessive information to the user, resulting in excess information compared to the controllability required for simulated verification, for the individual joint controllability to become user-friendly it must be condensed such that only the target subject joints are visible for usage, with all passive and tuning joints rendered invisible to mitigate potential confusion as well as to simplify the display.

5.4. Enhanced control algorithm design

With the goal of overcoming the limitations of the existing control system, a new GUI was designed which would both address the needs of the user and incorporate solutions to the drawbacks of the previous design. To address the multiple forms of control desired, the multiple existing GUIs have been condensed into multiple tabs in a single GUI, while the excess information has been removed via abstraction with all internal and tuning joints removed from the user's control.

The proposed design contains 4 modes of operation selectable by the user, enabling a selection between pose control, hand joint control, orthosis joint control and external joint data control. Pose control contains predefined configurations derived from Appendix B, providing the user with a selection of therapeutic exercises to replicate as seen in Figure 33. As can be seen in Figures 34 and 35, both hand and orthosis joint control modes provide a similar display to the user, the difference in operation is that hand joint control provides a configuration goal for the hand to achieve without the orthosis while the orthosis control permits configuration of the hand goal configuration as manipulated by the orthosis. Unlike the prior joint control GUI in figures 29 and 31, only the joints which are intended to be controlled are shown, while sliders are arranged consistent with the layout of joints in the hand. The external input mode is intended to facilitate control methods such as
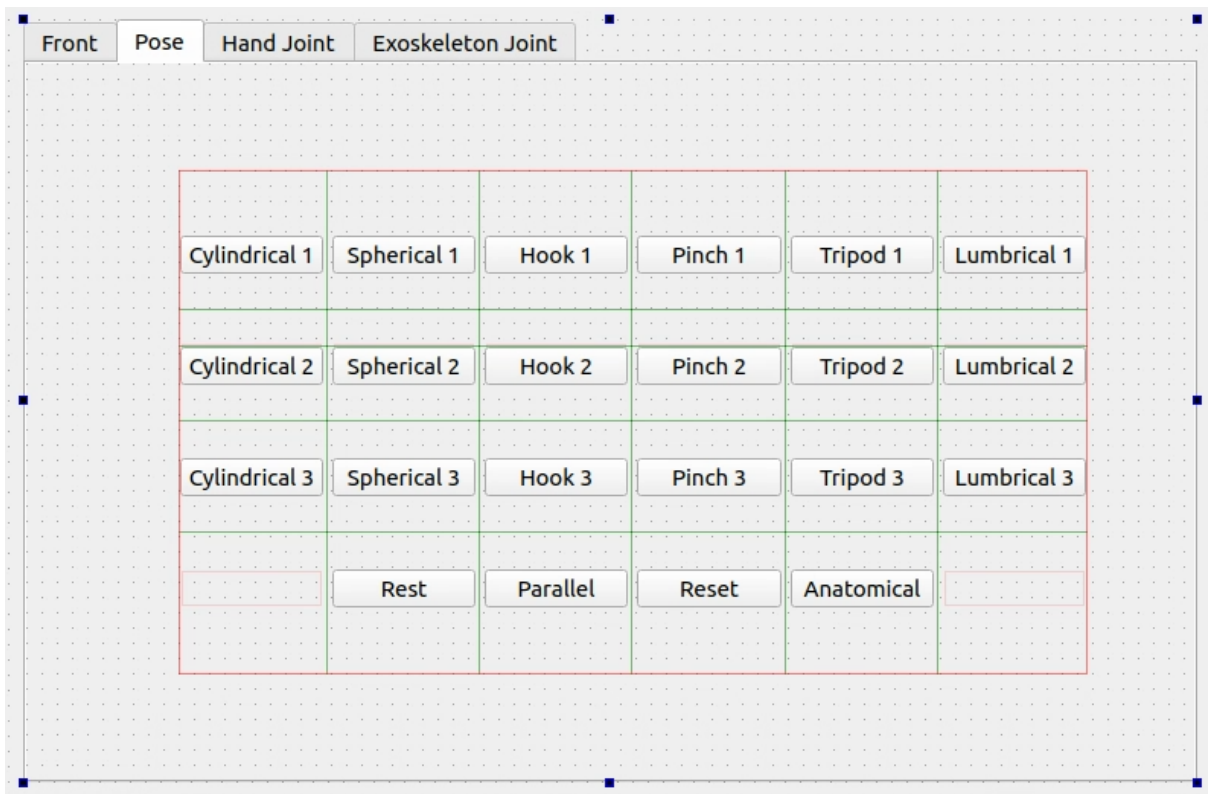
Figure 33: Revised ROS GUI Pose Panel showing predefined exercise state selection per Appendix B.

dynamic pose control, in which case a sensory mechanism such as the Leap Motion Controller would record the motion of the controlling physical hand then supply the resulting joint state values to the orthosis controller, this would enable simultaneous joint data input rather than individual slider input while also enabling further exercise duplication without requiring modification of predefined exercise poses.

As part of improving motion characteristics of the controller, a motion planning element must be incorporated to enable a diverse joint motion controller, this must be capable of generating differing response rates and motion patterns for each individual joint. ROS has the capacity for incorporating PID control mechanisms for joint control however this can be further modified by incorporating a step based shifting control point for each joint, in this manner the individual joint motion characteristics can be incorporated by applying an appropriate formula indicating the control point at a given step thus allowing control over motion start time as well as implementing partial equation controllability and nonlinear equation control.
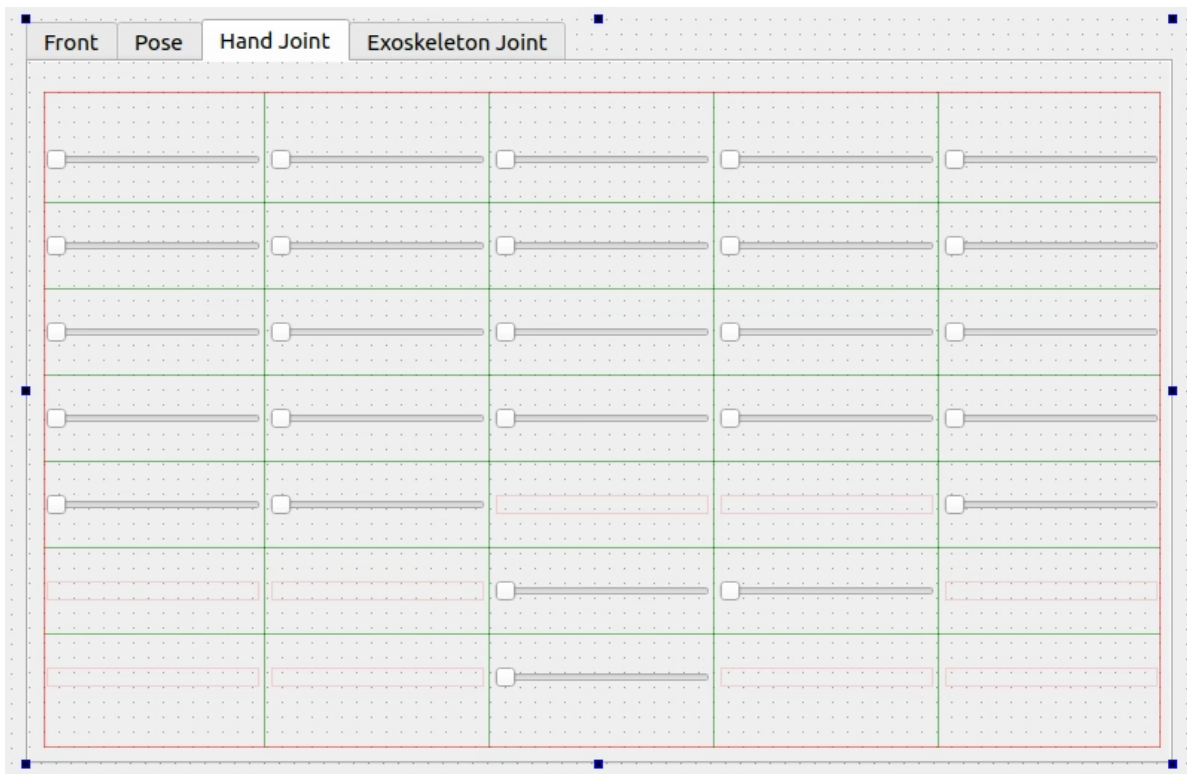
Figure 34: Revised ROS GUI Hand Control Panel showing arranged joint sliders.
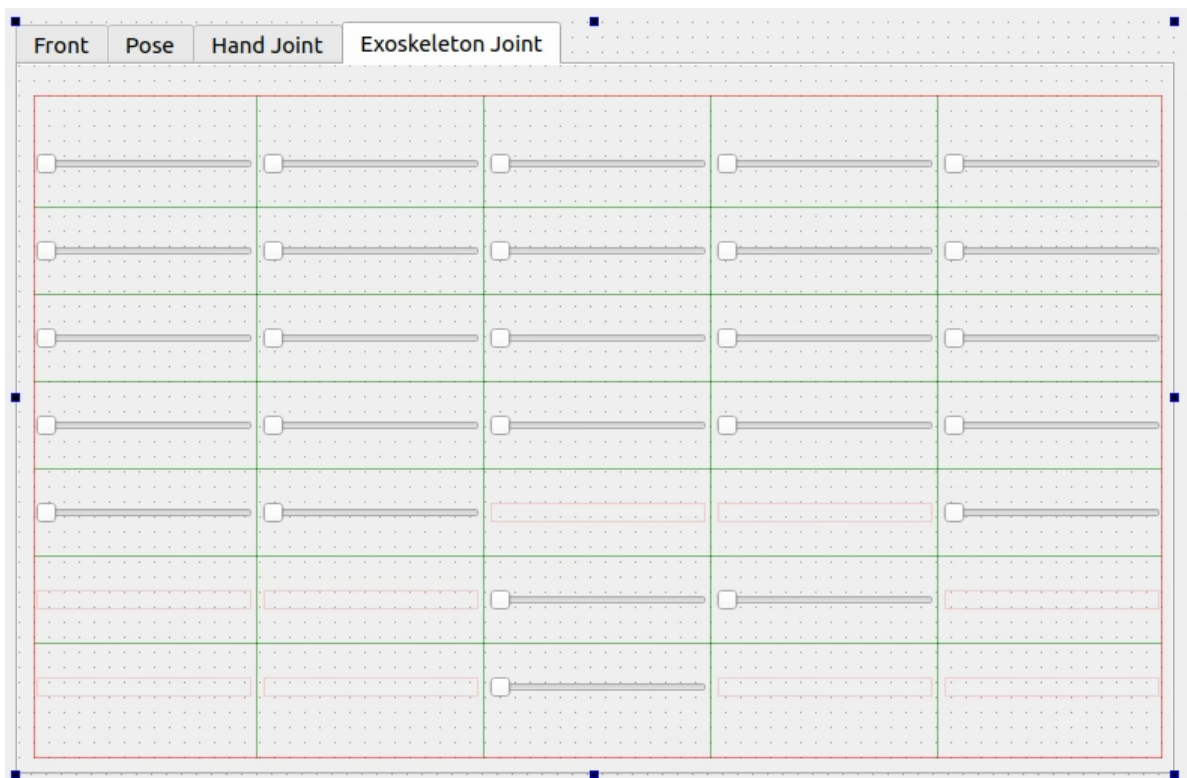
Figure 35: Revised ROS GUI Orthosis Control Panel showing arranged joint sliders.

Chapter 6: Kinematic Analysis of the Exoskeleton

Verifying the motive capabilities of the orthosis and skeleton models can be achieved via a combination of modelling methods, such as forward kinematic analysis (and its mathematical representations) shown earlier in Chapter 2, or via simulation model demonstrations in ROS RViz. In this way the capacity for the modelled designs to replicate common rehabilitation exercises and poses can be ascertained.

As exoskeletons are required to help in performing muscular functions, their smooth and unobstructed movements need to be determined a priori. DH parameters allow swift and accurate manipulators' movement analysis and obstacle avoidance investigations for developing multiple degrees of freedom mechanisms [33]. Also, to perform the life-essential tasks, a human hand needs a high level of dexterity. DH parameters, because of a reduced number of required variables, make it easy to perform the exoskeleton kinematic analyse [34, 35]. DH parameters also enable easy and robust coding for controlling the joint motion [36]. This work therefore used DH parameters for kinematic analysis and motion planning of the hand skeleton.

Furthermore, to avoid the computational complexities associated with spherical joints, this work focused on analysing the hand movements by investigating the joint interconnections between the limb segments. This enables axes of rotations of three-dimensional joints in a simple manner using the appropriate DH parameters [35, 37].

The following paragraphs detail the employed kinematic analysis approach.

6.1. Hand Kinematics

To facilitate independent movement of each joint in every finger and thumb during the rehabilitative therapy and flexion and extension exercises, natural movements of joints in the hand, each finger and thumb were extensively studied. Based on the anatomical understanding and previous exoskeleton designs, a close-to-nature and human-friendly modular exoskeleton design was perceived [38-41].

Having a good understanding of the anatomical structure of human hand, attention was paid to map finger, thumb, and hand-joints' rotations and the resulting poses and overall hand configurations during the common power and precision exercises. The power and precision exercises are conducted during the hand rehabilitation. Figure 36 shows the common power exercises recommended by therapists and corresponding natural poses of the hand, fingers, and thumb, widely required for the hand rehabilitation. Figure 37 shows the common precision exercises and naturally occurring hand-, finger- and thumb-poses required for the hand rehabilitation.
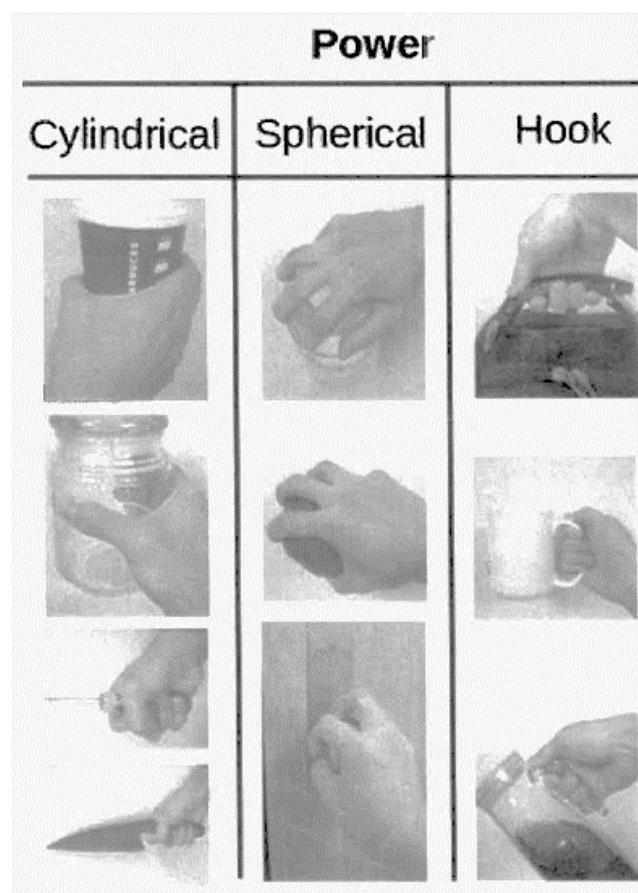
Figure 36: Ten common power exercises and natural poses of the hand, fingers, and thumb, required for the hand rehabilitation.[4]

49
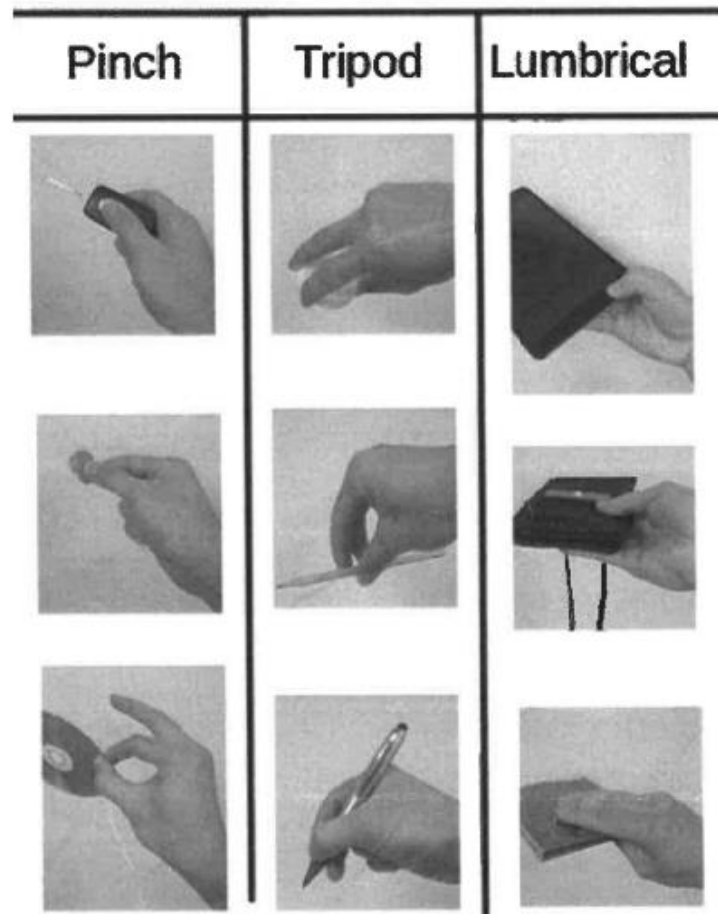
Figure 37: Nine common precision exercises and natural poses of the hand, fingers, and thumb, required for the hand rehabilitation.[4]

As suggested in [38] and obvious in Figures 36 and 37, a comfortable exoskeleton design would require each finger to have 1-DOF for abduction and/or adduction and 3-DOF for finger extension and flexion. Hence, each finger would require 4-DOF. The thumb in our design would need 1-DOF for abduction and/or adduction and 2-DOF for finger extension and flexion. Figure 38 below shows the kinematic arrangement of the index finger and thumb. Utilising the DH parameters from Tables 2-4 enables the application of the transformation matrix depicted in Equation (2.1), yielding the forward kinematic transformation between any two sequentially adjacent joints. By further utilising Equation (2.2), the position of any desired joint or end effector can be obtained with respect to the base of the forearm.

Link	θ_i	d_i	a_i	α_i
F_0-F_1	0	0	47	0
F_1-F_2	-40	0	35	0
F_2-P_1	45	0	32	0
F_0-F_4	40	0	57	100
F_4-F_5	-60	0	42	0
F_5-F_6	45	0	23	0
F_6-P_2	15	0	27	0
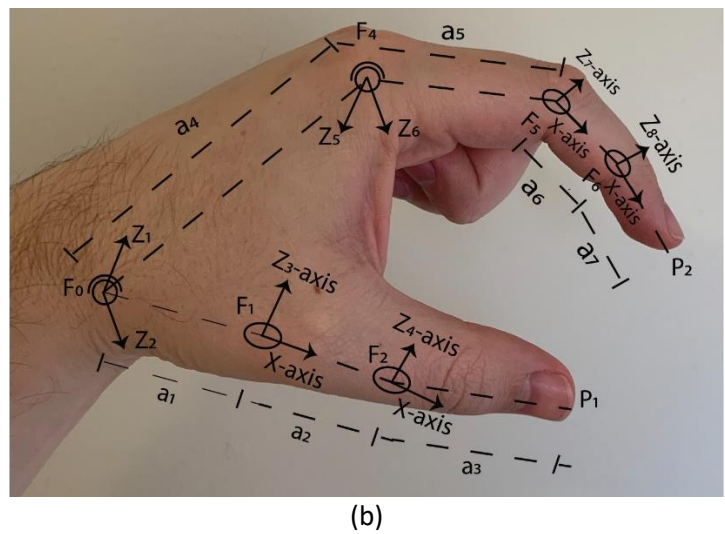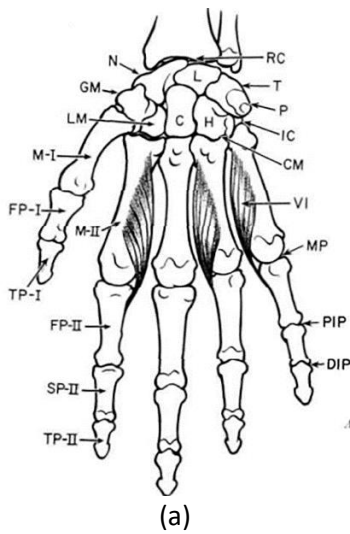
Figure 38: (a) The volar view of human hand showing bones, articulations, and interosseous muscles [40]. (b) Simple 2 phalange pinch pose

Figure 38(a) shows the volar view of the human hand, containing bones, joints, and interosseous muscles. Figure 38(b) shows the kinematic arrangements of joints and links in a simple pinch pose, with index finger joint Z_5 showing the axis of abduction and/or adduction, Z_6, Z_7 and Z_8 show the 3-DOF for finger extension and flexion, while Z_1 shows the axis of abduction and/or adduction, Z_2, Z_3 and Z_4 show the 3-DOF for thumb extension and flexion. Note that a 2-axis joint has a wheel-like symbol, and a single-axis joint is shown as an elliptical shape. Equations (6.1) and (6.2) apply (2.1) and (2.2) to the kinematic representation detailed in Figure 38(b) and Table 2, providing the cartesian coordinates of the end effector phalange tips P_1 for thumb and P_2 for index, with respect to the origin F_0, following frames F_0, F_1, then F_2 for P_1, and F_0, F_4, F_5, then F_6 for P_2.

$$P_1 = \begin{bmatrix} 0.7071 & -0.7071 & 0 & 22.6274 \\ 0.7071 & 0.7071 & 0 & 22.6274 \\ 0 & 0 & 1 & 0 \\ 0 & 0 & 0 & 1 \end{bmatrix} * \begin{bmatrix} 0.766 & 0.6428 & 0 & 26.8116 \\ -0.6428 & 0.766 & 0 & -22.4976 \\ 0 & 0 & 1 & 0 \\ 0 & 0 & 0 & 1 \end{bmatrix} \qquad (6.1)$$

$$* \begin{bmatrix} 1 & 0 & 0 & 47 \\ 0 & 1 & 0 & 0 \\ 0 & 0 & 1 & 0 \\ 0 & 0 & 0 & 1 \end{bmatrix} * \begin{bmatrix} 0 \\ 0 \\ 0 \\ 1 \end{bmatrix} = \begin{bmatrix} 104.3154 \\ 29.7742 \\ 0 \\ 1 \end{bmatrix}$$

$$P_2 = \begin{bmatrix} 0.9659 & -0.2588 & 0 & 26.08 \\ 0.2588 & 0.9659 & 0 & 6.9881 \\ 0 & 0 & 1 & 0 \\ 0 & 0 & 0 & 1 \end{bmatrix} * \begin{bmatrix} 0.7071 & -0.7071 & 0 & 16.2635 \\ 0.7071 & 0.7071 & 0 & 16.2635 \\ 0 & 0 & 1 & 0 \\ 0 & 0 & 0 & 1 \end{bmatrix} \qquad (6.2)$$

$$* \begin{bmatrix} 0.5 & 0.866 & 0 & 21 \\ -0.866 & 0.5 & 0 & -36.3731 \\ 0 & 0 & 1 & 0 \\ 0 & 0 & 0 & 1 \end{bmatrix}$$

$$* \begin{bmatrix} 0.766 & 0.1116 & 0.633 & 43.6645 \\ 0.6428 & -0.133 & -0.7544 & 36.6389 \\ 0 & 0.9848 & -0.1737 & 0 \\ 0 & 0 & 0 & 1 \end{bmatrix} * \begin{bmatrix} 0 \\ 0 \\ 0 \\ 1 \end{bmatrix} = \begin{bmatrix} 123.2445 \\ 63.5456 \\ 0 \\ 1 \end{bmatrix}$$

Figure 39: Corresponding to Figure 37(b), the putty is kept between the index finger and the thumb.[40]

The pose example in Figure 39 shows how the putty is kept between the index finger and the thumb for a simple therapeutic exercise (finger pinch) shown in Figure 54 below. Keeping the power and precision exercises related poses and hand configurations, a flexible hand exoskeleton was designed such that each joint would have the ability to move independently. A kinematic representation of the full hand skeleton is shown in Figure 40.
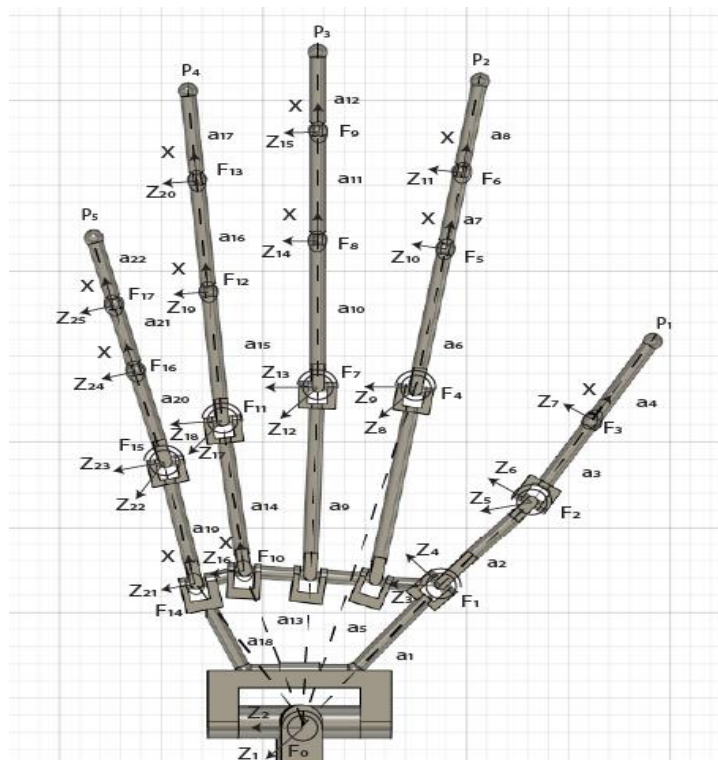
Figure 40: The kinematic representation of the complete hand skeleton showing one- and two-degrees of freedom of each joint.

Link	θ_i	d_i	a_i	α_i
F_0-F_1	θ_1 (Z_1)	0	0	90
	θ_1 (Z_2)	0	51	-90
F_1-F_2	θ_2 (Z_3)	0	0	90
	θ_2 (Z_4)	0	33	-90
F_2-F_3	θ_3 (Z_5)	0	0	90
	θ_3 (Z_6)	0	32	-45
F_3-P_1	θ_4	0	28	0
F_0-F_4	θ_5 (Z_1)	0	0	90
	θ_5 (Z_2)	0	45	-90
F_4-F_5	θ_6 (Z_8)	0	0	90
	θ_6 (Z_9)	0	42	-90
F_5-F_6	θ_7	0	23	0
F_6-P_2	θ_8	0	27	0
F_0-F_7	θ_9 (Z_1)	0	0	90
	θ_9 (Z_2)	0	41	-90
F_7-F_8	θ_{10} (Z_{12})	0	0	90
	θ_{10} (Z_{13})	0	43	-90
F_8-F_9	θ_{11}	0	32	0
F_9-P_3	θ_{12}	0	23	0
F_0-F_{10}	θ_{13} (Z_1)	0	0	90
	θ_{13} (Z_2)	0	41	-90
F_{10}-F_{11}	θ_{14}	0	46	0
F_{11}-F_{12}	θ_{15} (Z_{17})	0	0	90
	θ_{15} (Z_{18})	0	38	-90
F_{12}-F_{13}	θ_{16}	0	33	0
F_{13}-P_4	θ_{17}	0	26	0
F_0-F_{14}	θ_{18} (Z_1)	0	0	90
	θ_{18} (Z_2)	0	45	-90
F_{14}-F_{15}	θ_{19}	0	38	0
F_{15}-F_{16}	θ_{20} (Z_{22})	0	0	90
	θ_{20} (Z_{23})	0	20	-90
F_{16}-F_{17}	θ_{21}	0	20	0

6.2. Orthosis Kinematics

Due to the complexity of the structure, the kinematic representation of the orthosis design presented in Figure 26 has been split into multiple subsections, Figures 41, 42, 43, and 44 illustrate the kinematic representations of the forearm, the metacarpal region of the hand, the index finger, and the thumb, respectively. Although the full assembly in Figure 26 contains the complete arrangement of components, the illustrated diagrams show each distinct kinematic arrangement, as the structural design for the ring/little metacarpals and all finger proximal-distal are the same barring individual length differences, sharing identical motion behaviour. For kinematic representation, Table 4 uses P_2 from Figure 41 as F0 for all chains, in this way the series for each phalange is consistent in origin and end point with Figure 40. To combine the exoskeleton diagrams indicated in figures 42-44 the combined carpal-metacarpal region of figure 42 serves as the common region, with the index and middle phalange chains connecting via MCP components while the little and ring metacarpal linkages connect as shown in figure 41 for the little metacarpal, with the thumb chain shown in figure 44 similarly connecting in its entirety from the corresponding carpal joint. All 4 fingers utilise similar structures to that shown in figure 43, with differences for sizing only.
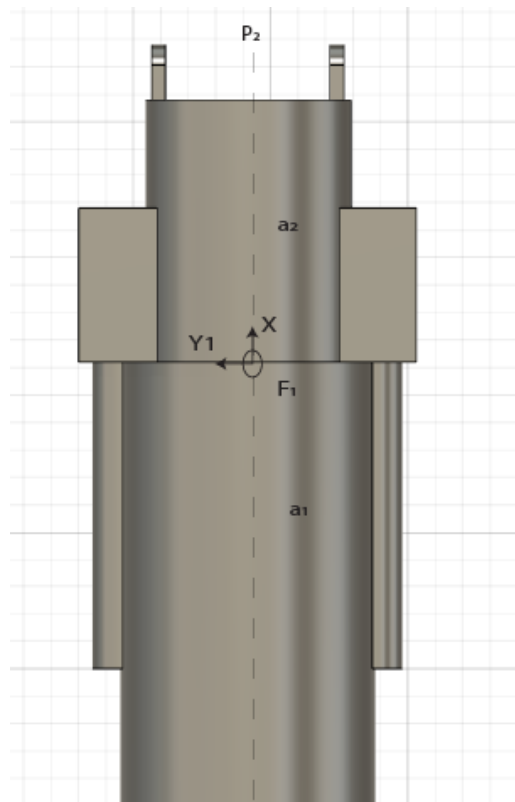
Figure 41: The kinematic representation of the Forearm, top view.
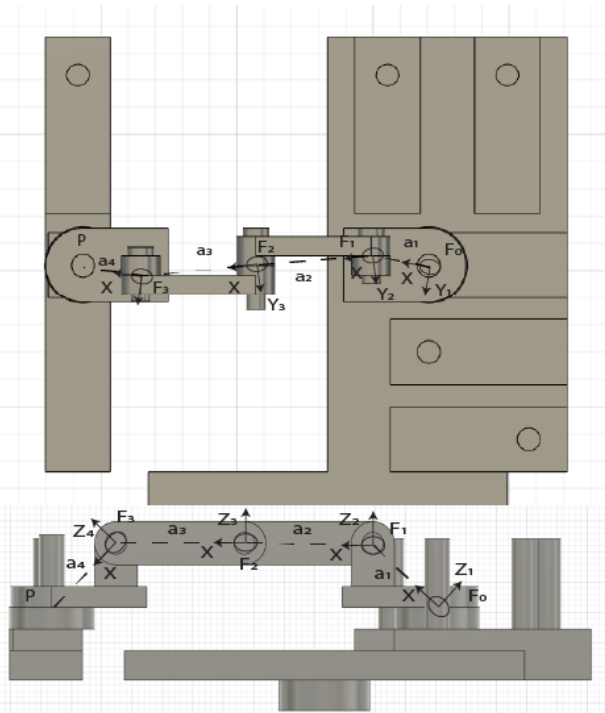
Figure 42: The kinematic representation of the Metacarpal region of the hand. Identical ring metacarpal structure not shown.
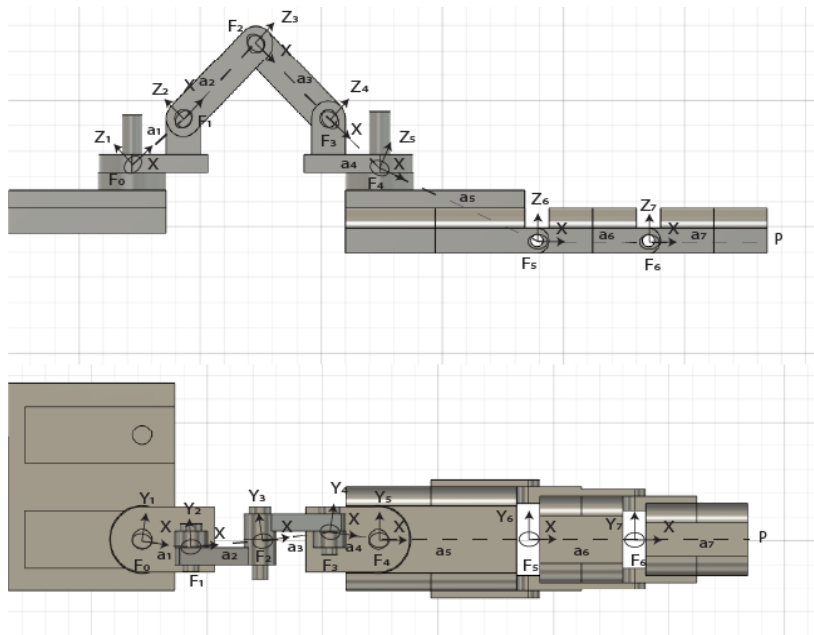
Figure 43: The kinematic representation of the index finger. Middle, ring and little phalange structures are identical post metacarpal structure.
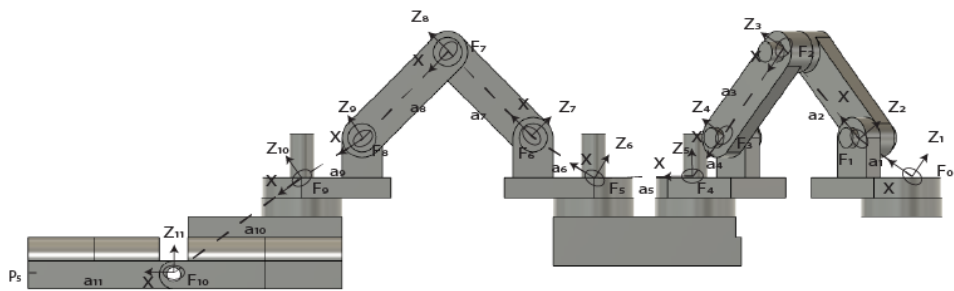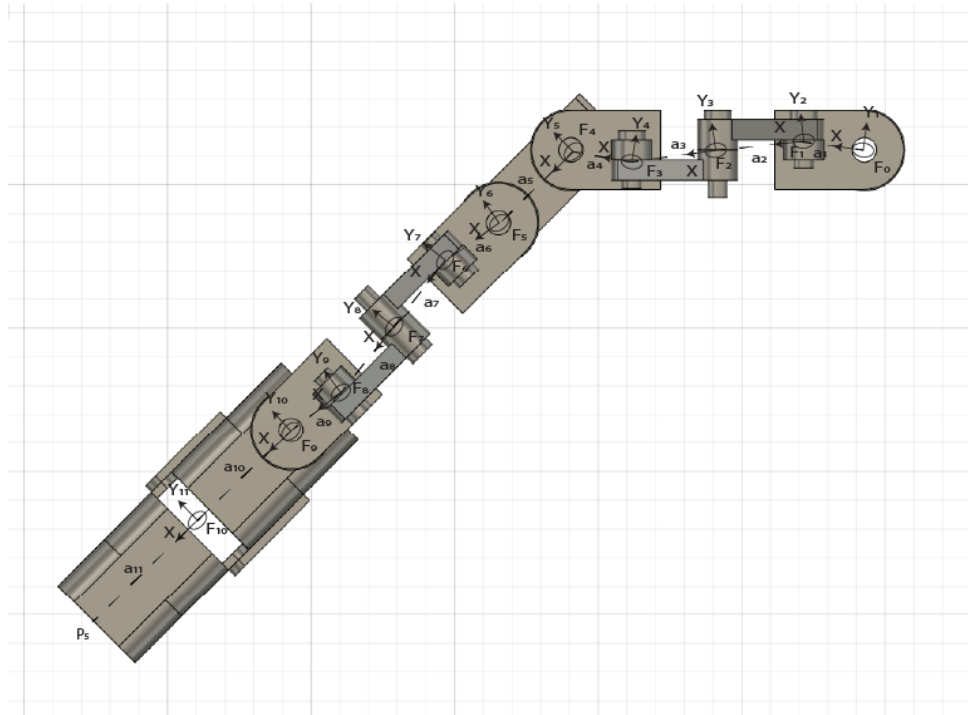
Figure 44: The kinematic representation of the thumb subsection. Top and side view.

Table 4: DH parameters for the Orthosis configuration shown in Figures 41-44.

Link	θ_i	d_i	a_i	α_i
F_0-F_1	θ_1 (Z_1)	0	0	90
	θ_1 (Z_2)	27.53	60.97	-90
F_1-F_2	θ_2	14.12	10.59	90
F_2-F_3	θ_3	0	21.18	0
F_3-F_4	θ_4	0	21.18	0
F_4-F_5	θ_5	10.59	14.12	-90
F_5-F_6	θ_6	-4.27	9.88	-90
	45	7.94	4.27	90
F_6-F_7	θ_6	14.12	10.59	90
F_7-F_8	θ_7	0	21.5	0
F_8-F_9	θ_8	0	21	0
F_9-F_{10}	θ_9	14.12	10.59	-90
F_{10}-F_{11}	θ_{10}	-10.03	22.44	90

F_{11}-P_1	θ_{11}	0	25.5	0
F_0-F_{12}	θ_{12} (Z_1)	0	0	90
	θ_{12} (Z_2)	27.53	120.07	-90
F_{12}-F_{13}	θ_{13}	14.12	10.59	90
F_{13}-F_{14}	θ_{14}	0	21.18	0
F_{14}-F_{15}	θ_{15}	0	21.18	0
F_{15}-F_{16}	θ_{16}	10.59	14.12	-90
F_{16}-F_{17}	θ_{17}	-13.56	32.44	90
F_{17}-F_{18}	θ_{18}	0	23	0
F_{18}-P_2	θ_{19}	0	24.5	0
F_0-F_{19}	θ_{20} (Z_1)	0	0	90
	θ_{20} (Z_2)	27.53	115.96	-90
F_{19}-F_{20}	θ_{21}	14.12	10.59	90
F_{20}-F_{21}	θ_{22}	0	21.18	0
F_{21}-F_{22}	θ_{23}	0	21.18	0
F_{22}-F_{23}	θ_{24}	10.59	14.12	-90
F_{23}-F_{24}	θ_{25}	-10.03	33.94	90
F_{24}-F_{25}	θ_{26}	0	33	0
F_{25}-P_3	θ_{27}	0	20.5	0
F_0-F_{26}	θ_{28} (Z_1)	0	0	90
	θ_{28} (Z_2)	27.53	64.5	-90
F_9-F_{27}	θ_{29}	14.12	10.59	90
F_{10}-F_{28}	θ_{30}	0	21.18	0
F_{11}-F_{29}	θ_{31}	0	21.18	0
F_0-F_{30}	θ_{32}	10.59	14.12	-90
F_{30}-F_{31}	θ_{33}	0.2	50.95	0
F_{31}-F_{32}	θ_{34}	14.12	10.59	90
F_{32}-F_{33}	θ_{35}	0	21.18	0
F_{33}-F_{34}	θ_{36}	0	21.18	0
F_{34}-F_{35}	θ_{37}	10.59	14.12	-90
F_{35}-F_{36}	θ_{38}	-10.03	28.44	90
F_{36}-F_{37}	θ_{39}	0	33	0
F_{37}-P_4	θ_{40}	0	23.5	0
F_0-F_{38}	θ_{41} (Z_1)	0	0	90
	θ_{41} (Z_2)	27.53	84.68	-90
F_{38}-F_{39}	θ_{42}	14.12	10.59	90
F_{39}-F_{40}	θ_{43}	0	21.18	0
F_{40}-F_{41}	θ_{44}	0	21.18	0
F_{41}-F_{42}	θ_{45}	10.59	14.12	-90
F_{42}-F_{43}	θ_{46}	0	34.94	0
F_{43}-F_{44}	θ_{47}	14.12	10.59	90
F_{44}-F_{45}	θ_{48}	0	21.18	0
F_{45}-F_{46}	θ_{49}	0	21.18	0
F_{46}-F_{47}	θ_{50}	10.59	14.12	-90
F_{47}-F_{48}	θ_{51}	-10	18.44	90
F_{48}-F_{49}	θ_{52}	0	20	0
F_{49}-P_5	θ_{53}	0	17.5	0

6.3. Exercise Poses' Kinematics Demonstration

To demonstrate the capabilities of the hand skeleton model and orthosis model with respect to replicating the needs of hand therapy, the exercises in figures 36 and 37 have been replicated via a combination of subject hand posing, skeleton ROS model posing, and orthosis ROS model posing.

6.3.1. Cylindrical

The cylindrical power grasps apply fundamentally parallel non-thumb phalange orientation across the controlled object, with subsequent adjustment for each joint to match the surface geometry of the object, in this way both cylindrical, conical, and similar irregular objects can be manipulated, with the thumb completing the grasp by being aligned in opposition to the fingers. Figures 45 and 46 show the fingers aligned for a regular shaped object while the thumb is visibly aligned to act on the object in the opposite direction to ensure a grasp. Figure 47 shows a differing cylindrical grasp in that while the fingers are parallel and applied directly upon the object, the thumb is instead acting upon the index phalange, resulting in both phalanges applying force on the object and it being opposed by the metacarpals rather than another phalange.

Figure 45: The kinematic representation of the Power exercise 1, Cylindrical 1.

Figure 46: The kinematic representation of the Power exercise 2, Cylindrical 2.

Figure 47: The kinematic representation of the Power exercise 3, Cylindrical 3.
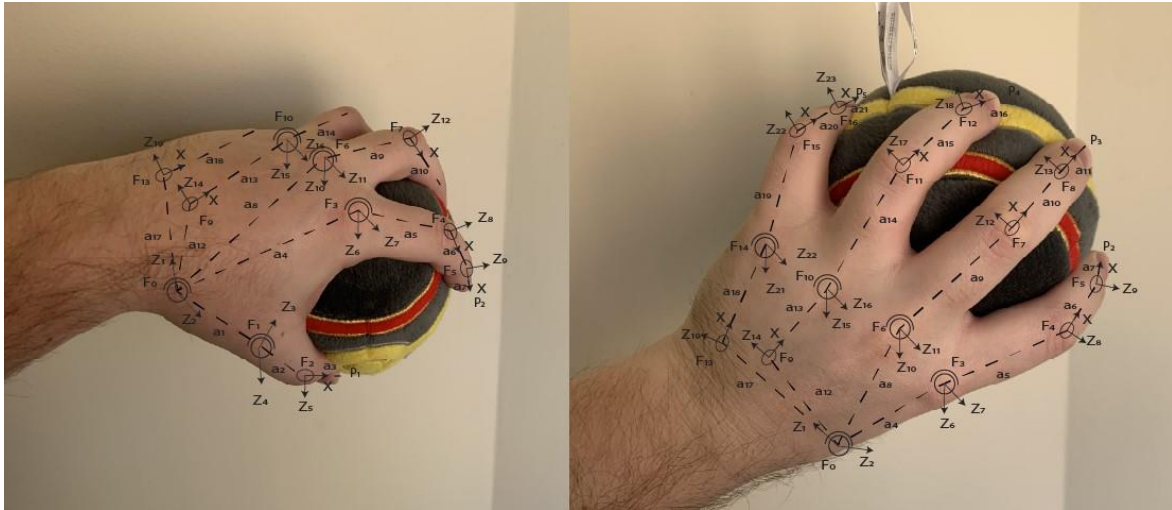
Figure 48: The kinematic representation of the Power exercise 5, Spherical 1.

6.3.2. Spherical

As a power grasp, the spherical grasps distribute the phalanges across the geometry of the manipulated object, with the resulting fore applied via arm motion being distributed across the object, particularly useful for objects such as the lid shown in figure 49 or handles of a similar shape to the object shown in figure 48.

6.3.3. Hook

The hook exercises utilise the non-thumb phalanges being arranged in parallel about the manipulated object handle with the metacarpal region utilised in some instances as an additional point of control, while the thumb is aligned with the manipulated handle. Figures 51 and 52 demonstrate the hook grasp being utilised to control the global orientation of the manipulated object, with the thumb and little finger combining to control alignment in figure 51 while the metacarpals participate in figure 52. Figure 50 shows a different application of the hook grasp in which the thumb applies antagonistic motion to that of the controlled object while the hooked phalanges control the position of the object. Equation (6.3) applies (2.1) and (2.2) to Figure 50, utilizing Table 3 and measurements from Appendix A to provide a kinematic representation, in this case the cartesian coordinates of the index finger relative to the wrist.
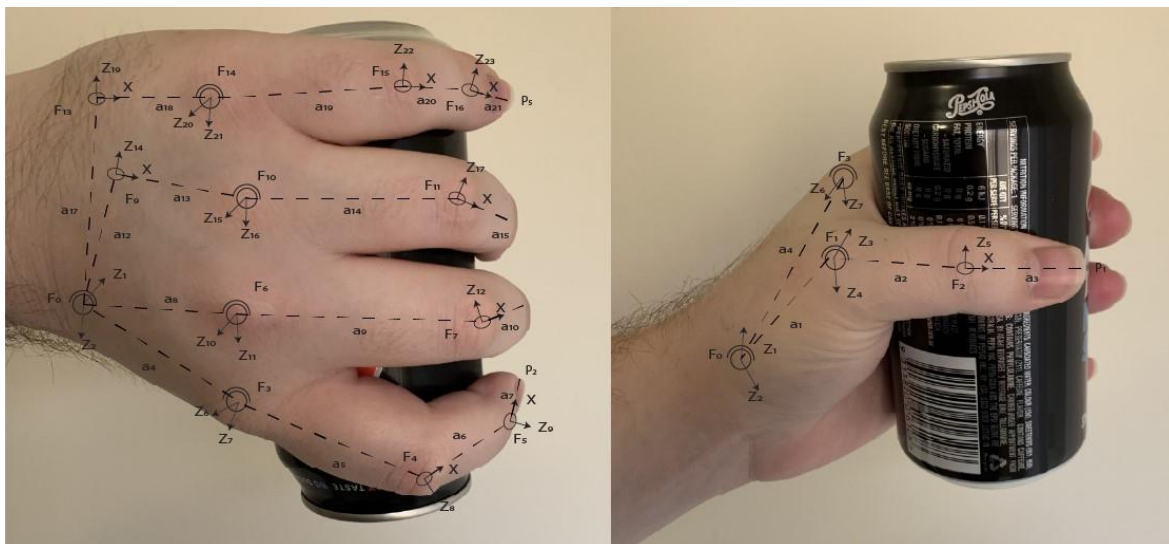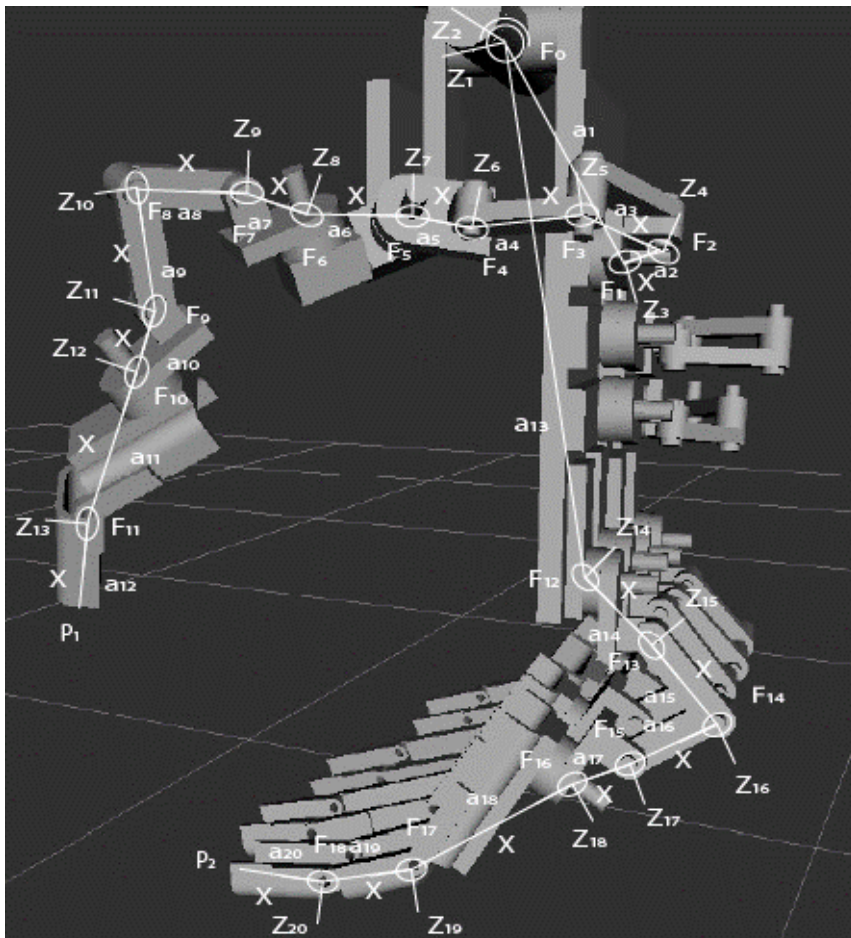

Figure 49: The kinematic representation of the Power exercise 6, Spherical 2.

Figure 50: The kinematic representation of the Power exercise 8, Hook 1.

$$P_2 = \begin{bmatrix} 0.17 & 1 & 0 & 4.69 \\ -0.98 & 0.17 & 0 & -26.6 \\ 0 & 0 & 1 & 0 \\ 0 & 0 & 0 & 1 \end{bmatrix} * \begin{bmatrix} 0 & 1 & 0 & 0 \\ -1 & 0 & 0 & -23 \\ 0 & 0 & 1 & 0 \\ 0 & 0 & 0 & 1 \end{bmatrix}$$

$$* \begin{bmatrix} 0.09 & 0 & 1 & 3.66 \\ 1 & 0 & -0.09 & 41.84 \\ 0 & 1 & 0 & 0 \\ 0 & 0 & 0 & 1 \end{bmatrix} * \begin{bmatrix} 1 & 0 & 0 & 0 \\ 0 & 0 & 1 & 0 \\ 0 & -1 & 0 & 0 \\ 0 & 0 & 0 & 1 \end{bmatrix}$$ (6.3)

$$* \begin{bmatrix} 0.71 & 0 & 0.71 & 31.8 \\ 0.71 & 0 & -0.7 & 31.8 \\ 0 & 1 & 0 & 0 \\ 0 & 0 & 0 & 1 \end{bmatrix} * \begin{bmatrix} 1 & 0 & -0.1 & 0 \\ 0.09 & 0 & 1 & 0 \\ 0 & -1 & 0 & 0 \\ 0 & 0 & 0 & 1 \end{bmatrix} * \begin{bmatrix} 0 \\ 0 \\ 0 \\ 1 \end{bmatrix}$$

$$= \begin{bmatrix} 20.17 \\ -101.3 \\ 0 \\ 1 \end{bmatrix}$$
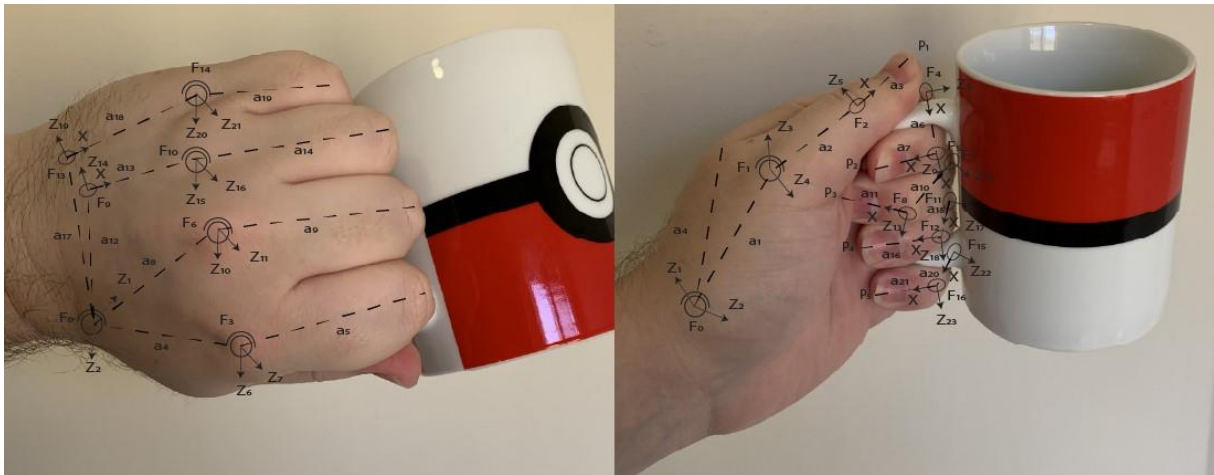
Figure 51: The kinematic representation of the Power exercise 9, Hook 2.

6.3.4. Pinch

The pinch exercise utilises balanced antagonistic force application between the index and thumb phalanges to provide a grasp over various objects. As shown in figures 54 and 55 utilise only the index and thumb phalanges while the remaining phalanges are free to fold or extend as seen, respectively. Figure 53 is similar in position of all phalanges to figure 54 however the middle phalange is noticeably participating for object stabilisation. Equation (6.4) applies (2.1) and (2.2) to Figure 55, utilizing Table 3 and measurements from Appendix A to provide a kinematic representation, in this case providing the cartesian coordinates for the index finger relative to the wrist.

Figure 52: The kinematic representation of the Power exercise 10, Hook 3.

Figure 53: The kinematic representation of the Precision exercise 1, Pinch 1.

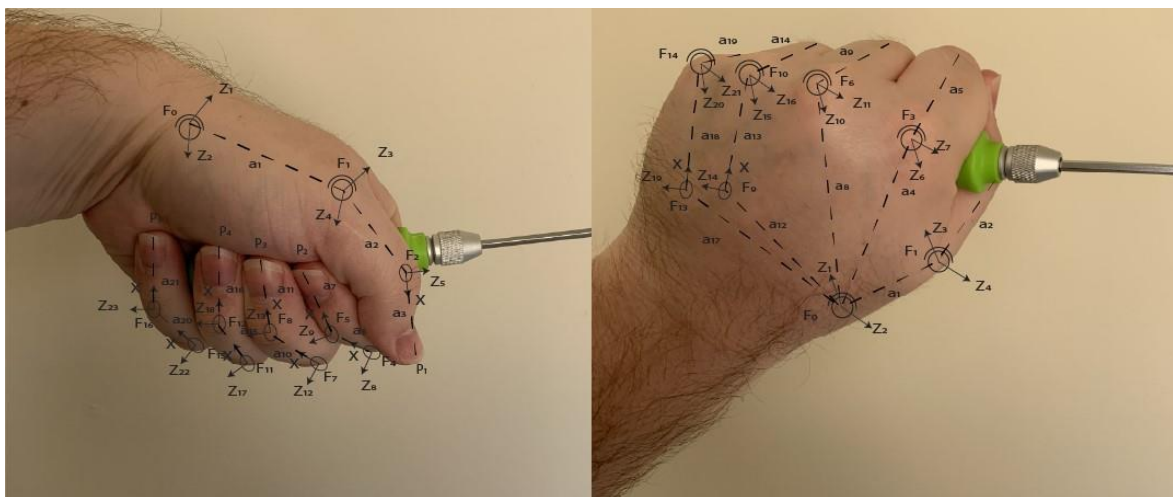Figure 54: The kinematic representation of the Precision exercise 2, Pinch 2.

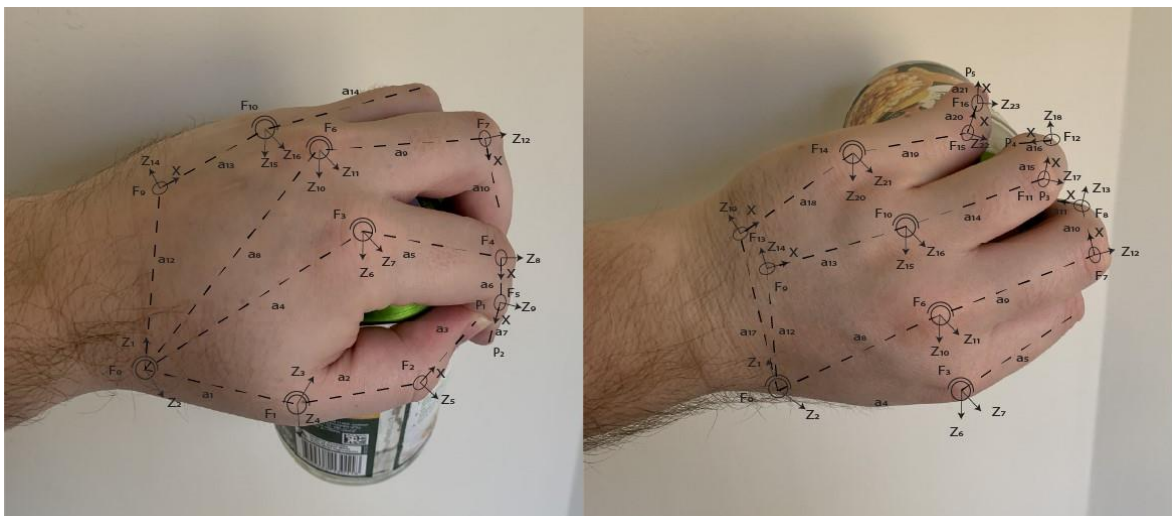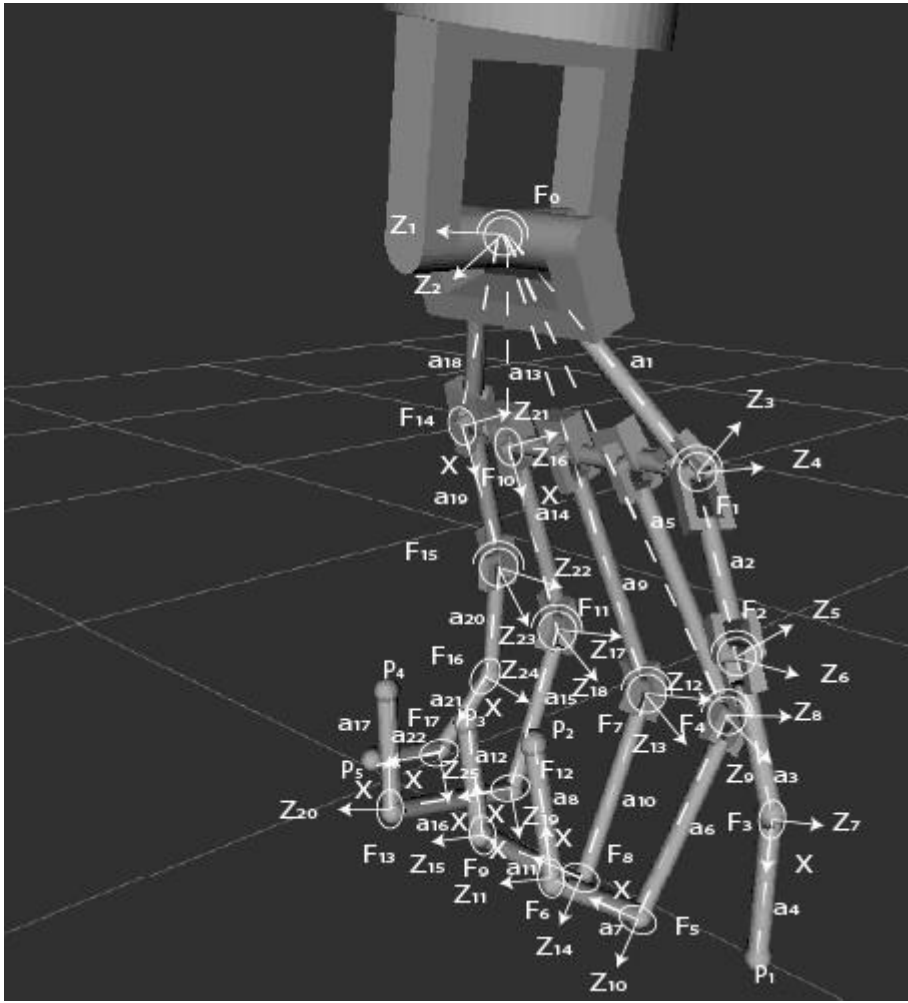*Figure 55: The kinematic representation of the Precision exercise 3, Pinch 3.*

$$P_2 = \begin{bmatrix} 1 & 0.09 & 0 & 26.9 \\ -0.09 & 1 & 0 & -2.35 \\ 0 & 0 & 1 & 0 \\ 0 & 0 & 0 & 1 \end{bmatrix} * \begin{bmatrix} 0 & 0.7 & 0 & 0 \\ -0.71 & 0 & 0 & -16.3 \\ 0 & 0 & 1 & 0 \\ 0 & 0 & 0 & 1 \end{bmatrix} \tag{6.4}$$

$$* \begin{bmatrix} 0.17 & 0 & 0.98 & 7.29 \\ 0.98 & 0 & -0.17 & 41.36 \\ 0 & 1 & 0 & 0 \\ 0 & 0 & 0 & 1 \end{bmatrix} * \begin{bmatrix} 1 & 0 & 0 & 0 \\ 0 & 0 & 1 & 0 \\ 0 & 1 & 0 & 0 \\ 0 & 0 & 0 & 1 \end{bmatrix} * \begin{bmatrix} 0.94 & 0 & 0.34 & 42.3 \\ 0.34 & 0 & -0.9 & 15.4 \\ 0 & 1 & 0 & 0 \\ 0 & 0 & 0 & 1 \end{bmatrix}$$

$$* \begin{bmatrix} 1 & 0 & 0 & 0 \\ 0 & 0 & 1 & 0 \\ 0 & -1 & 0 & 0 \\ 0 & 0 & 0 & 1 \end{bmatrix} * \begin{bmatrix} 0 \\ 0 \\ 0 \\ 1 \end{bmatrix} = \begin{bmatrix} 85.87 \\ -23.47 \\ 0 \\ 1 \end{bmatrix}$$
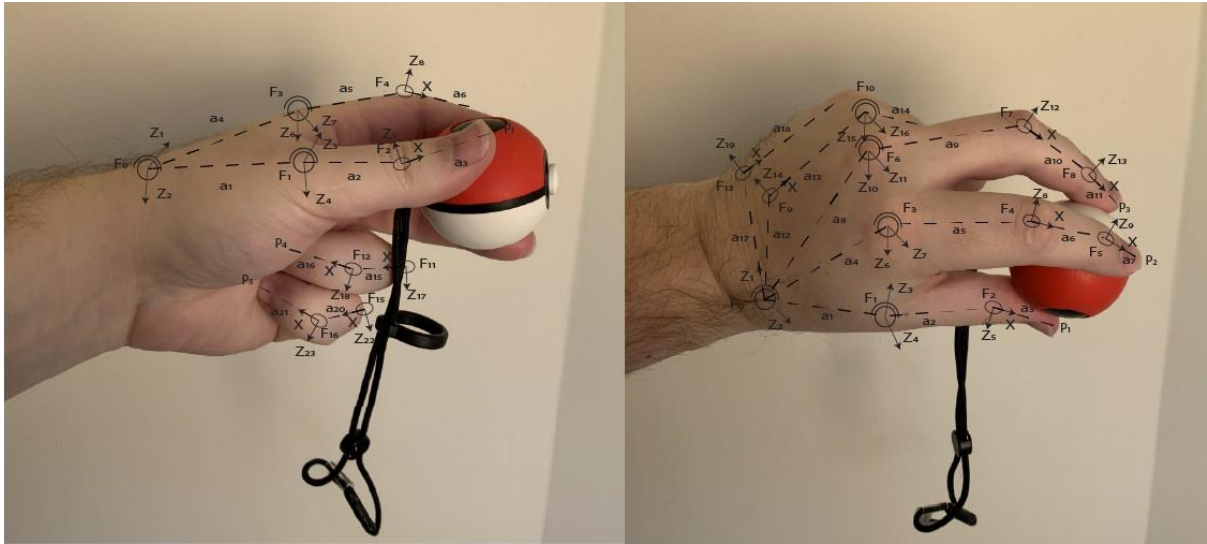
Figure 56: The kinematic representation of the Precision exercise 4, Tripod 1.

6.3.5. Tripod

As the name suggests, the tripod exercises utilise triangulated force application to the manipulated object via the index, middle and thumb phalanges, with the ring and little phalanges free to rest as comfortable for the patient. Figures 56 and 57 show the little and ring phalanges being curled up fully while the index, middle and thumb phalanges are applied evenly distributed around the manipulated objects.

6.3.6. Lumbrical

Exercises under the lumbrical category utilise the thumb, finger MCP joints, wrist, and forearm. As shown in figures 58 and 59 the MCP flexion/extension and adduction/abduction is utilised to conform to the shape of the object then the thumb applied in opposition. As shown in figure 60, the resulting orthosis induced position retains parallel positions of the fingers and the thumb positioned opposite the space which would be occupied by the object. Equation (6.5) applies (2.1) and (2.2) to Figure 60, utilizing Table 3 and measurements from Appendix A to provide a kinematic representation, in this case providing the cartesian coordinates for the thumb relative to the wrist.
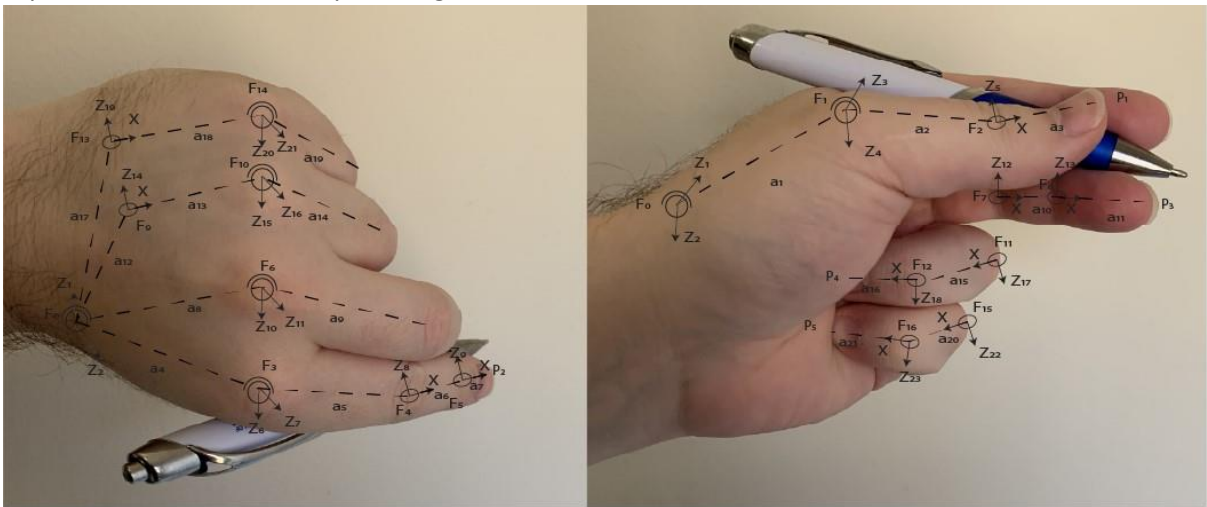
Figure 57: The kinematic representation of the Precision exercise 6, Tripod 3.
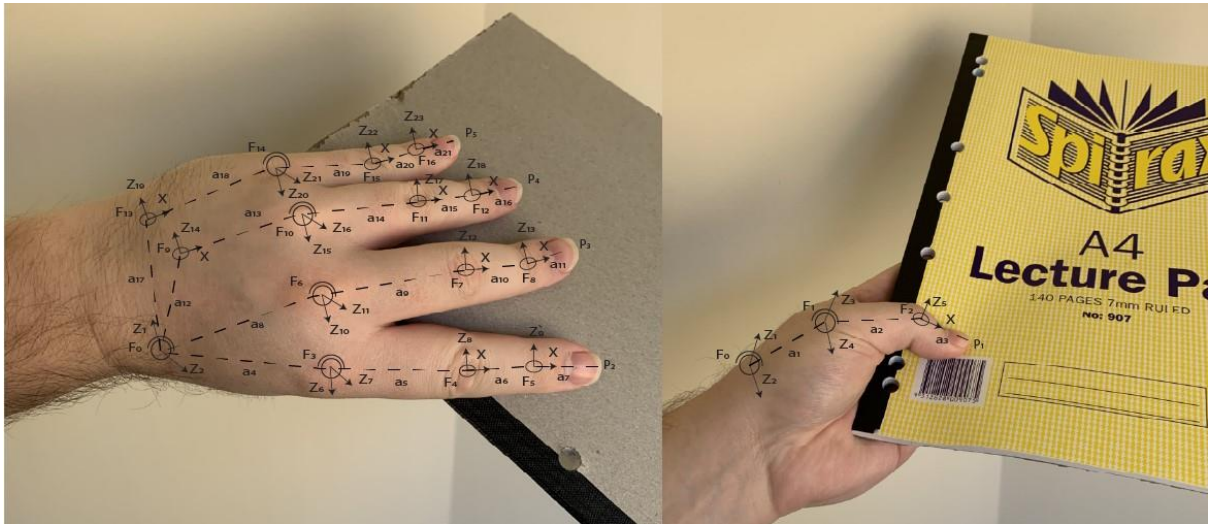
Figure 58: The kinematic representation of the Precision exercise 7, Lumbrical 1.
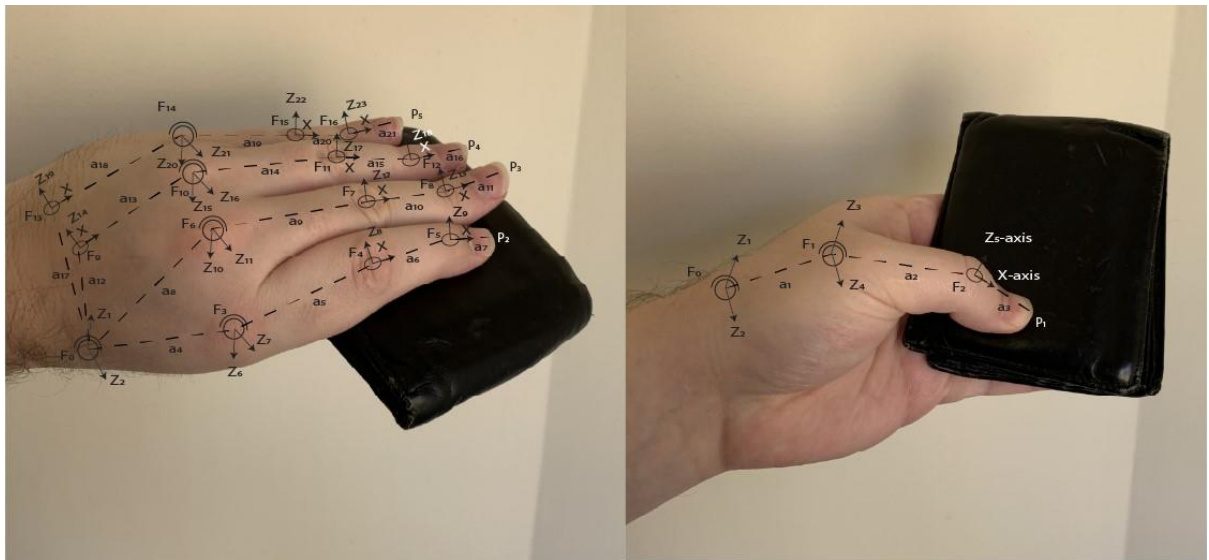
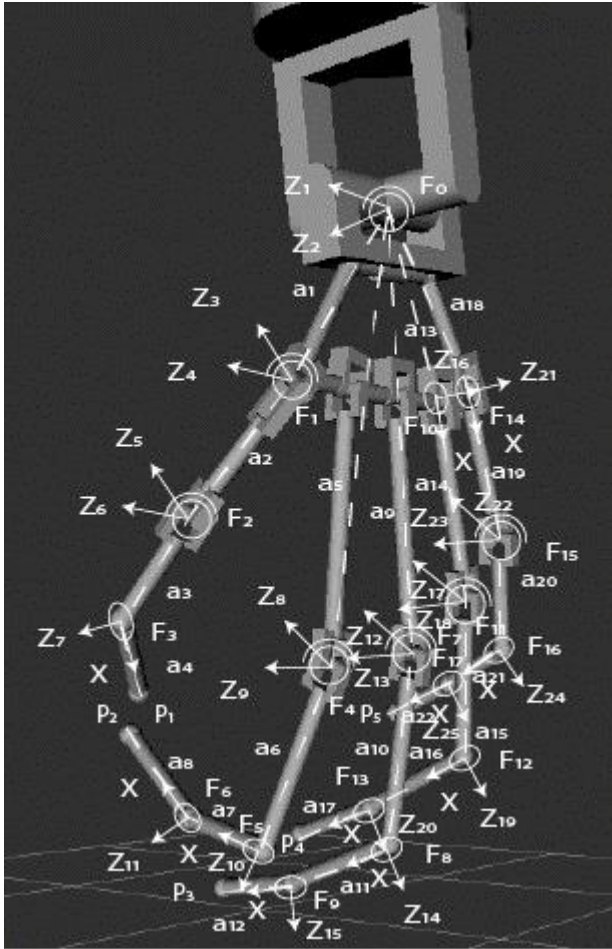*Figure 59: The kinematic representation of the Precision exercise 8, Lumbrical 2.*
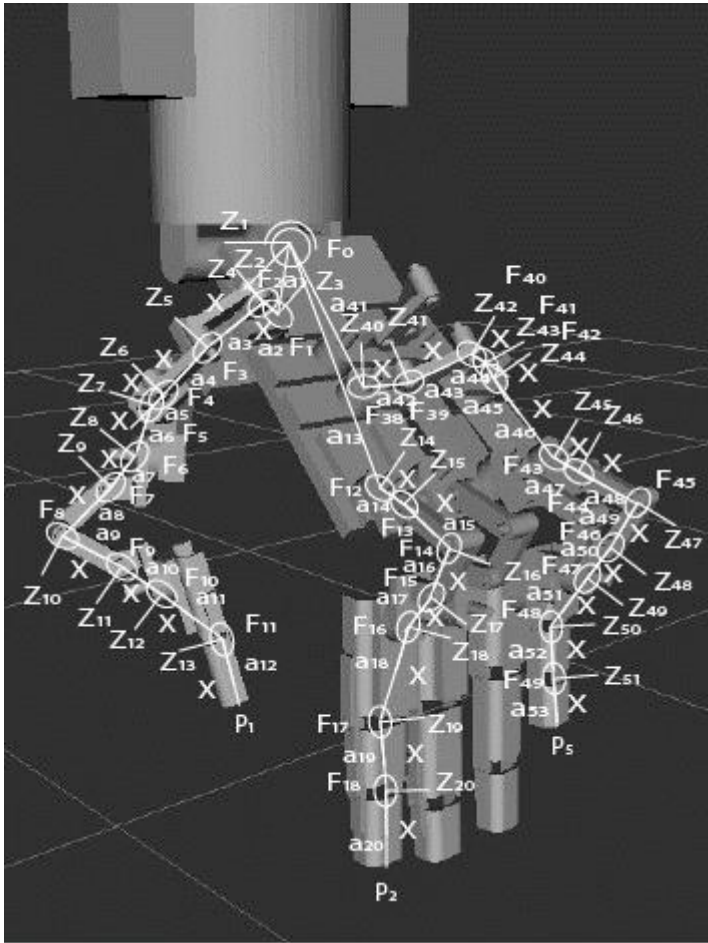
Figure 60: The kinematic representation of the Precision exercise 9, Lumbrical 3.

$$P_1 = \begin{bmatrix} 1 & 0 & 0 & 28 \\ 0 & 1 & 0 & 0 \\ 0 & 0 & 1 & 0 \\ 0 & 0 & 0 & 1 \end{bmatrix} * \begin{bmatrix} 1 & 0 & 0 & 32 \\ 0 & 1 & 0 & 0 \\ 0 & 0 & 1 & 0 \\ 0 & 0 & 0 & 1 \end{bmatrix} * \begin{bmatrix} 0 & 0 & 0.5 & 0 \\ -0.5 & 0 & 0 & 0 \\ 0 & -1 & 0 & 0 \\ 0 & 0 & 0 & 1 \end{bmatrix} * \begin{bmatrix} 1 & 0 & 0 & 33 \\ 0 & 0 & 1 & 0 \\ 0 & -1 & 0 & 0 \\ 0 & 0 & 0 & 1 \end{bmatrix} \tag{6.5}$$

$$* \begin{bmatrix} 0.5 & 0 & -0.87 & 0 \\ 0.87 & 0 & 0.5 & 0 \\ 0 & -1 & 0 & 0 \\ 0 & 0 & 0 & 1 \end{bmatrix} * \begin{bmatrix} 0.34 & 0 & 0.66 & 17.4 \\ 0.94 & 0 & -0.2 & 47.9 \\ 0 & 0.71 & 0 & 0 \\ 0 & 0 & 0 & 1 \end{bmatrix}$$

$$* \begin{bmatrix} 0.94 & 0 & 0.34 & 0 \\ -0.34 & 0 & 0.9 & 0 \\ 0 & -1 & 0 & 0 \\ 0 & 0 & 0 & 1 \end{bmatrix} * \begin{bmatrix} 0 \\ 0 \\ 0 \\ 1 \end{bmatrix} = \begin{bmatrix} 67.55 \\ -20.86 \\ -47.9 \\ 1 \end{bmatrix}$$

6.4. Summary

The comparison of exercise poses shown in figures 45-60 demonstrate the capabilities of both the skeleton and orthosis models in duplicating rehabilitation exercises, as required to meet the design goal for the orthosis in replicating human motion. Furthermore, kinematic representations have been presented which enable DH parameter utilisation for forward kinematic modelling for both the skeleton and orthosis utilising therapeutic motion requirements.

Chapter 7: Design Variant Exploration

During the process of designing the presented orthosis, multiple subsystem variants were explored with the goal of either simplifying mechanisms or expanding performance scope capabilities. Such designs included an alternative joint control mechanism, an alternative drive supply mechanism to reduce actuator count, and an expanded/alternative control algorithm.

7.1. Joint control mechanism

Given the design objective of providing independent control for all joints, the selected position control mechanism must be capable of either controlling only single joints or controlling multiple without internal interference. Further, the prevalence of linkage-based structures led to the exploration of a modified linkage structure able to provide control over all joints in the phalange independently. By facilitating a larger range of input actuation, the controllability for phalange poses increases, allowing for each phalange to exhibit a more diverse range of configurations, given current designs providing only a varied proportion of one pose being applied.

Conceptually designed as multiple parallel linkages, this linkage design would receive multiple inputs to permit multiple control state outputs, through the inclusion of passive elements, the distal and intermediate regions would be unaffected by neighbouring joint motion, enabling intermediate and proximal joint movement without inducing inter-joint motion, this would enable a fully actuated mechanism rather than typical underactuated linkages.

7.1.1. Benefits vs Limitations

The increased controllable degrees of freedom facilitated by this design would allow a more dynamic control system, allowing for a much wider range of poses achieved by an affected phalange. Compared to typical single actuated linkages, a fully actuated phalange mechanism would require amendments to the nearby support structures to carry the additional permitted actuators, especially as the additional weight may impact the supportability of the structure itself. The inclusion of additional actuators for a linkage without delocalisation could increase stress on the patient hand due to weight while the increased volume could impact controllability of other areas due to the need to support the second or further actuators.

7.1.2. Outcome

Compared to other design mechanisms, the explored design yielded increased complexity for the same output, along with pre-existing impacts on range of motion due to the dorsal region volumetric impact, as such the exploration of this mechanism was ceased in favour of other designs.

7.2. Drive mechanism

Given the predominant observed actuation supply involved either bidirectional linear motion via linear actuation, or rotational motion supplied via servo or stepper motor, a method was explored which would apply an intermediary mechanism to the drive series with the intention of both providing a non-typical mechanism and to potentially reduce the number of actuators required. A non-typical mechanism would provide a novel development however the reduction in actuation count would be highly beneficial given this application required 26 DOF to be fully actuated, which numbered higher than other existing designs observed.

To achieve the goal of reducing the number of actuators involved in the supply mechanism, a design must produce several simultaneous outputs greater than the number required to operate the mechanism itself. With this objective in mind a camshaft style was explored which would take advantage of the drive shaft orientation controlling the position-based output of several elements, with the shaft itself being controlled by a single drive actuator. A shaft containing 26 motion elements manoeuvred on the same shaft this way would provide a 26:1 output/input mechanism from which all outputs are controlled by a single actuator, which is a significant reduction compared to the full 26 DOF using 1:1 which observed design methods would utilise.

The explored design for this control mechanism consisted of three major elements: the supply shaft, the position structure, and the output receivers. As mentioned, the supply shaft is primarily controlled via a single rotational supply such as a belt drive with the purpose of controlling the supply shaft position. The position structure provides an interface between the supply shaft and the output receiver, with one unit per output along the shaft, output is achieved via a variable radius disc with the surface profile of the disc corresponding to the range of output states required. The output receiver interfaces with the position disc for each output via measuring the current radius at the point of contact between the driven element of the interface and the disc, with the interface driven to contact the profile of the disc via opposing spring. The combined result of these three subsections is a scalable array of simultaneously controlled linear outputs corresponding to a single input rotational actuator, with variable states produced according to the mechanically designed profiles of each control disc and their corresponding relative positions of other discs. To provide the motion behaviour characteristics of the outputs, each disc profile is subdivided into multiple regions with each containing a range from a resting neutral state through to fully engaged for a different pose, as such each given range on a cam corresponds to the collective motion required for all associated outputs to achieve the desired pose range for that configuration.

7.2.1. Benefits vs Limitations

The largest benefit of this explored design is the potential to compress the actuation supply for an exoskeleton from a potentially large count down to a smaller number with a mechanically designed controller providing control logic. Although this design would reduce the quantity of actuators required, the proportionally larger load placed upon the supply shaft actuator would potentially require a larger actuator compared to more typical design mechanisms for this application. This disadvantage can be offset via multiple, smaller supply mechanisms however this would negate the overall objective of reducing actuator count. Another disadvantage of this design is the need to redesign camshafts to suit any given motion range limit, particularly given a subject undergoing rehabilitation who would ideally increase their range of motion in affected areas.

The weight of the camshaft design is strongly affected by the number of cams controlled, with the largest design potentially requiring a larger drive motor, while even smaller designs will be affected by the larger quantity of actuators needed to supply motion, as such this increased weight could impact or otherwise limit portability and ease of use. The inter-cam pose limitations also reduces the true controllability of the mechanism, producing false independent joint control which may affect the scope of control for a given cam layout.

7.2.2. Outcome

Due to complexity in designing cams and cam interface as well as potential reduction in controllability, this design was abandoned in favour of parallel Bowden cables driven by individual actuators. The mechanism itself may have merit in other control schemes however the needs for this orthosis are not met via camshaft designs.

7.3. Teleoperation

As part of efforts to design an element to overcome concerns regarding needs for therapy to occur under direct supervision, the application of teleoperation was explored as a potential to facilitate remote therapy with a physical medium and digital intermediary. To provide data regarding hand motion from both the therapist and patient the concept of a sensorised glove was explored, using localised bands of sensors applied to each joint alongside a digital twin hand.

The use of sensorised bands across each joint permits live data acquisition of the observed hand's motion, with two key applications depending on the wearer. On the hand of the patient the data provides both immediate positioning and ongoing behavioural such as movement trends as well as potentially elements such as speed and force, thus providing a measurable understanding of the patient hand rehabilitation status. On the hand of the therapist it provides a form of dynamic input in that the therapist can produce any desired motion or pose via their own hand in their presence for observation which would then be useable as control data for the remote orthosis, such as providing dynamic pose control beyond fixed exercise regimes, Applied immediately this would potentially enable the therapist to directly control the patient hand toward the pose desired by the therapist.

To minimise impact on the subject hand's motion, it is important that the glove be both low profile and firm, thus reducing loss of motion range due to collision and reducing dampening of orthosis actuation. To provide recording of motion the use of flex sensor bands was considered suitable for many joints, particularly those undergoing flexion/extension and adduction/abduction.

7.3.1. Benefits vs Limitations

The ability to facilitate remote therapy would help address transit related ease of access to therapists, while the ability to dynamically record both patient and therapist data would facilitate further enumerated therapy via data driven adjustments to rehabilitation plans.

The addition of further material across the patient hand will increase its volume, potentially limiting motion ranges of elements such as the phalanges given collisions will occur at proximities driven by the glove rather than the hand. Furthermore, the glove itself may interfere with orthosis operation due to changes in the motion response when actuated by the orthosis, in particular any pose for the patient hand will require the orthosis to account for and as such dampen its pose goal to compensate for the glove volume adjustment. For applications involving remote therapy, this design is impacted by ease of access and quality of internet connection, especially remote regions may not possess sufficiently stable connections to provide safe operation during live motion.

7.3.2. Outcome

Although the physical design was discontinued, the dynamic control elements were further explored as part of the revised control mechanism. The inclusion of a form of dynamic pose input is of considerable interest as it permits dynamic pose control which could be further improved to become real time, enabling the therapist to adjust exercises on an as needed basis without the need for modifying preconfigured poses.

Chapter 8: Conclusion

This chapter concludes discussion of the works carried out in this thesis, discussing the models produced, their novel developments, and provides recommendations for potential future works.

This project has produced two models for hand rehabilitation; a subject hand compliant with rehabilitation requirements and modelled on a realistic subject hand, and an orthosis designed for use in full-hand and lower forearm rehabilitation. The mathematical representations for these models have utilised DH parameters to provide a simplified mechanism for applying kinematic analysis to each. Both models have subsequently been simulated in ROS utilising Rviz visualisation software, with subsequent comparisons to the goal therapeutic exercise requirements.

8.1. Novel Developments

Throughout this project, research into the development of a simulated full hand rehabilitative orthosis has yielded four novel developments:

- Therapeutically derived, controllable hand model
- 26 DOF mechanism capable of full hand controllability
- Independent joint control operations
- ROS-based multilevel control package

The first novel development of this project is the hand model providing a simulated replica of the human left lower forearm. This model serves to demonstrate the simulated replication of natural human motion sourced from a combination of subject measurements, biomedical parameters, and therapeutic requirements. Through these combined characteristics a simulated subject has been created for use with orthosis simulations while providing motion behaviours and characteristics consistent with an analogous physical subject.

The second novel development is that of the range of controllability afforded by the orthosis design. To supply the necessary controllability for the lower hand, the produced orthosis design contains the necessary actuation to provide 26 DOF control across the entire hand and lower forearm, thus ensuring the developed hand model can be fully controlled across all joints. This design ensures both that all desired joint regions are controllable, and that no regions have been sacrificed for design simplicity.

The third novel development pertains to the simultaneous independence of joint control operations. Further to the area of effect of the orthosis design, each joint is controlled independently of its neighbours, permitting simultaneous parallel joint control. This design aspect ensures there is minimal impact on range of motion arising from neighbouring areas while increasing controllability scope compared to designs controlling entire regions such as phalanges simultaneously.

The fourth novel development is the multilevel nature of the ROS-based control package. Given the diverse forms of controllability desirable for hand therapy, the control algorithm has been designed to provide selectable modes of operation to suit a versatile scope of operation for the orthosis. Available modes operate both for visualising the hand model in motion as well as the orthosis interacting with the hand, with available modes including individual joint control for a joint-by-joint basis, preconfigured pose control for replicating rehabilitation exercises, and external input to permit dynamic pose control, wherein any pose within physical healthy ranges can be supplied via

sensory input to control the simulation poses. This multilevel control system facilitates simulation of a diverse range of therapeutic exercises and includes the capacity to visualise additional exercises beyond those preconfigured, via dynamic input.

From the works contained within this document, and Appendix E, a paper is being prepared for conference submission, encapsulating the novel developments of this project and the assessment of existing literature.

8.2. Future Research Potential

8.2.1. Conversion to physical orthosis

This project has explored the design of a simulated orthosis, a potential avenue of expansion for this design would be to convert it into a physical orthosis which would then permit it to act upon physical subjects and conduct rehabilitation exercises rather than visualising as is presented.

8.2.2. Relocation of target region

The scope for this design has been that of the lower forearm, however the design principles and components can be applied to different regions of the body to provide a rehabilitative orthosis with a different subject. For example, designing an orthosis for the human knee would require acknowledging the new geometry and relatively lower controllability requirement, while applications of existing knee therapy would replace the hand behaviour characteristics used, the assessed variations of actuation and control mechanisms would still be applicable however the selection criteria will be affected due to the change in behaviour such as collision between subsections.

8.2.3. Conversion from orthosis to bionics

The proposed orthosis design uses independent joint control to facilitate full hand discrete controllability, by applying these mechanisms to a design lacking the subject hand it would be possible to develop a bionic hand rather than an orthosis. With the actuation structures contained within the hand rather than mounted upon it, modifications would be necessary to the palm and forearm areas to internalise the structure however this would yield a robotic hand capable of the full range of natural motion without external structural components interfering with its pose capabilities.

References

[1]   Kenhub. "Learning Human Anatomy with Kenhub."

[2]   A. Kumar, T. S. Mundra, and A. Kumar, "Anatomy of Hand," in *Encyclopedia of Biometrics*, S. Z. Li and A. Jain Eds. Boston, MA: Springer US, 2009, pp. 28-35.

[3]   E. Pena-Pitarch, "Virtual Human Hand: Grasping Strategy and Simulation," 2010.

[4]   D. S. Keesing, "Interviewing a Rehabilitation Expert," D. Benson, Ed., ed, 2019.

[5]   D. J. Khan, "Interviewing a medical professional," D. Benson, Ed., ed, 2019.

[6]   J. Iqbal, N. G. Tsagarakis, and D. G. Caldwell, "A multi-DOF robotic exoskeleton interface for hand motion assistance," in *2011 Annual International Conference of the IEEE Engineering in Medicine and Biology Society*, 2011: IEEE, pp. 1575-1578.

[7]   B. B. Kang, H. Lee, H. In, U. Jeong, J. Chung, and K.-J. Cho, "Development of a polymer-based tendon-driven wearable robotic hand," in *2016 IEEE International Conference on Robotics and Automation (ICRA)*, 2016: IEEE, pp. 3750-3755.

[8]   J. Arata, K. Ohmoto, R. Gassert, O. Lambercy, H. Fujimoto, and I. Wada, "A new hand exoskeleton device for rehabilitation using a three-layered sliding spring mechanism," in *2013 IEEE International Conference on Robotics and Automation*, 2013: IEEE, pp. 3902-3907.

[9]   M. Sarac, M. Solazzi, E. Sotgiu, M. Bergamasco, and A. Frisoli, "Design and kinematic optimization of a novel underactuated robotic hand exoskeleton," *Meccanica,* vol. 52, no. 3, pp. 749-761, 2017.

[10]   B. Allotta, R. Conti, L. Governi, E. Meli, A. Ridolfi, and Y. Volpe, "Development and experimental testing of a portable hand exoskeleton," in *2015 IEEE/RSJ International Conference on Intelligent Robots and Systems (IROS)*, 2015: IEEE, pp. 5339-5344.

[11]   L. Cui, A. Phan, and G. Allison, "Design and fabrication of a three dimensional printable non-assembly articulated hand exoskeleton for rehabilitation," in *2015 37th Annual International Conference of the IEEE Engineering in Medicine and Biology Society (EMBC)*, 2015: IEEE, pp. 4627-4630.

[12]   L. H. Fuhai Zhang, Yili Fu, Hongwei Chen, Shuguo Wang, "Design and development of a hand exoskeleton for rehabilitation of hand injuries," *Mechanism and Machine Theory,* 2014.

[13]   H. K. Yap, J. H. Lim, F. Nasrallah, J. C. Goh, and R. C. Yeow, "A soft exoskeleton for hand assistive and rehabilitation application using pneumatic actuators with variable stiffness," in *2015 IEEE international conference on robotics and automation (ICRA)*, 2015: IEEE, pp. 4967-4972.

[14]   N. Fukaya, S. Toyama, T. Asfour, and R. Dillmann, "Design of the TUAT/Karlsruhe humanoid hand," in *Proceedings. 2000 IEEE/RSJ International Conference on Intelligent Robots and Systems (IROS 2000)(Cat. No. 00CH37113)*, 2000, vol. 3: IEEE, pp. 1754-1759.

[15]   I. Sarakoglou, A. Brygo, and D. Mazzanti, "HEXOTRAC: A highly under-actuated hand exoskeleton for finger tracking and force feedback. In 2016 IEEE," in *RSJ International Conference on Intelligent Robots and Systems (IROS)*, 2016, pp. 1033-1040.

[16]   C. J. Nycz, T. Bützer, O. Lambercy, J. Arata, G. S. Fischer, and R. Gassert, "Design and characterization of a lightweight and fully portable remote actuation system for use with a hand exoskeleton," *IEEE Robotics and Automation Letters,* vol. 1, no. 2, pp. 976-983, 2016.

[17]   M. Cempini, M. Cortese, and N. Vitiello, "A powered finger–thumb wearable hand exoskeleton with self-aligning joint axes," *IEEE/ASME Transactions on mechatronics,* vol. 20, no. 2, pp. 705-716, 2014.

[18]   A. Abbasimoshaei, M. Mohammadimoghaddam, and T. A. Kern, "Adaptive fuzzy sliding mode controller design for a new hand rehabilitation robot," in *International Conference on Human Haptic Sensing and Touch Enabled Computer Applications*, 2020: Springer, pp. 506-517.

[19]   N. Kladovasilakis *et al.*, "A novel soft robotic exoskeleton system for hand rehabilitation and assistance purposes," *Applied Sciences,* vol. 13, no. 1, p. 553, 2023.

[20]   A. Mandeljc, A. Rajhard, M. Munih, and R. Kamnik, "Robotic device for out-of-clinic post-stroke hand rehabilitation," *Applied Sciences,* vol. 12, no. 3, p. 1092, 2022.

[21]   N. Singh, M. Saini, N. Kumar, M. P. Srivastava, and A. Mehndiratta, "Evidence of neuroplasticity with robotic hand exoskeleton for post-stroke rehabilitation: a randomized controlled trial," *Journal of neuroengineering and rehabilitation,* vol. 18, no. 1, p. 76, 2021.

[22]   M. Li *et al.*, "A soft robotic glove for hand rehabilitation training controlled by movements of the healthy hand," in *2020 17th International Conference on Ubiquitous Robots (UR)*, 2020: IEEE, pp. 62-67.

[23]   M. Sandison *et al.*, "HandMATE: wearable robotic hand exoskeleton and integrated android app for at home stroke rehabilitation," in *2020 42nd Annual International Conference of the IEEE Engineering in Medicine & Biology Society (EMBC)*, 2020: IEEE, pp. 4867-4872.

[24]   A. Cisnal, J. Pérez-Turiel, J.-C. Fraile, D. Sierra, and E. de la Fuente, "Robhand: A hand exoskeleton with real-time emg-driven embedded control. quantifying hand gesture recognition delays for bilateral rehabilitation," *IEEE Access,* vol. 9, pp. 137809-137823, 2021.

[25]   K. Guo, J. Lu, C. Liu, and H. Yang, "Development, Research, Optimization and Experiment of Exoskeleton Robot for Hand Rehabilitation Training," *Applied Sciences,* vol. 12, no. 20, p. 10580, 2022.

[26]   M. Dragusanu, M. Z. Iqbal, T. L. Baldi, D. Prattichizzo, and M. Malvezzi, "Design, development, and control of a hand/wrist exoskeleton for rehabilitation and training," *IEEE Transactions on Robotics,* vol. 38, no. 3, pp. 1472-1488, 2022.

[27]   T. Ahmed *et al.*, "Flexohand: A hybrid exoskeleton-based novel hand rehabilitation device," *Micromachines,* vol. 12, no. 11, p. 1274, 2021.

[28]   F. C.-J. P.E. Ávila-Hernández, "Design and synthesis of a 2 DOF 9-bar spatial mechanism for a prosthetic thumb," *Mechanism and Machine Theory,* 2018.

[29]   *ROS*. [Online]. Available: https://www.ros.org/

[30]   N. M. Parent-Weiss and J. C. King, "Static progressive forearm rotation contracture management orthosis design: a study of 28 patients," *JPO: Journal of Prosthetics and Orthotics,* vol. 18, no. 3, pp. 63-67, 2006.

[31]   J. Li, R. Zheng, Y. Zhang, and J. Yao, "iHandRehab: An interactive hand exoskeleton for active and passive rehabilitation," in *2011 IEEE International Conference on Rehabilitation Robotics*, 2011: IEEE, pp. 1-6.

[32]   *fusion2urdf*. (2018). [Online]. Available: https://github.com/syuntoku14/fusion2urdf

[33]   T. P. Singh, P. Suresh, and S. Chandan, "Forward and inverse kinematic analysis of robotic manipulators," *International Research Journal of Engineering and Technology (IRJET),* vol. 4, no. 2, pp. 1459-1468, 2017.

[34]   Y. Jung and J. Bae, "Kinematic analysis of a 5-DOF upper-limb exoskeleton with a tilted and vertically translating shoulder joint," *IEEE/ASME Transactions on Mechatronics,* vol. 20, no. 3, pp. 1428-1439, 2014.

[35]   M. Sposito, C. Di Natali, S. Toxiri, D. G. Caldwell, E. De Momi, and J. Ortiz, "Exoskeleton kinematic design robustness: An assessment method to account for human variability," *Wearable Technologies,* vol. 1, p. e7, 2020.

[36]   D. Huamanchahua, J. Sierra-Huertas, D. Terrazas-Rodas, A. Janampa-Espinoza, J. Gonzáles, and S. Huamán-Vizconde, "Kinematic analysis of an 4 DOF upper-limb exoskeleton," in *2021 IEEE 12th Annual Ubiquitous Computing, Electronics & Mobile Communication Conference (UEMCON)*, 2021: IEEE, pp. 0914-0923.

[37]   K.-N. An, "Kinematic analysis of human movement," *Annals of biomedical engineering,* vol. 12, pp. 585-597, 1984.

[38]   I. Jo, Y. Park, J. Lee, and J. Bae, "A portable and spring-guided hand exoskeleton for exercising flexion/extension of the fingers," *Mechanism and Machine Theory,* vol. 135, pp. 176-191, 2019.

[39]   M. Sarac, M. Solazzi, and A. Frisoli, "Design requirements of generic hand exoskeletons and survey of hand exoskeletons for rehabilitation, assistive, or haptic use," *IEEE transactions on haptics,* vol. 12, no. 4, pp. 400-413, 2019.

[40]   R. J. Schwarz and C. Taylor, "The anatomy and mechanics of the human hand," *Artificial limbs,* vol. 2, no. 2, pp. 22-35, 1955.

[41]   P. Tran, S. Jeong, K. R. Herrin, and J. P. Desai, "Hand exoskeleton systems, clinical rehabilitation practices, and future prospects," *IEEE Transactions on Medical Robotics and Bionics,* vol. 3, no. 3, pp. 606-622, 2021.

Bibliography

[1]   P. B.-T. Zhou MA, "Hand Rehabilitation Learning System With an Exoskeleton Robotic Glove," *IEEE Transactions on Neural Systems and Rehabilitation Engineering,* 2015.

[2]   P. B.-T. Zhou MA, "RML Glove - An Exoskeleton Glove Mechanism with Haptics Feedback," 2015.

[3]   F. Zacharias, "Knowledge Representations for Planning Manipulation Tasks," 2011.

[4]   A. Yurkewich, D. Hebert, R. H. Wang, and A. Mihailidis, "Hand Extension Robot Orthosis (HERO) Glove: Development and Testing With Stroke Survivors With Severe Hand Impairment," *IEEE Transactions on Neural Systems and Rehabilitation Engineering,* vol. 27, no. 5, pp. 916-926, 2019.

[5]   K. Xing, Q. Xu, J. He, Y. Wang, Z. Liu, and X. Huang, "A wearable device for repetitive hand therapy," in *2008 2nd IEEE RAS & EMBS International Conference on Biomedical Robotics and Biomechatronics*, 2008: IEEE, pp. 919-923.

[6]   K. Xing, J. Huang, Q. Xu, and Y. Wang, "Design of a wearable rehabilitation robotic hand actuated by pneumatic artificial muscles," in *2009 7th Asian Control Conference*, 2009: IEEE, pp. 740-744.

[7]   T. Worsnopp, M. Peshkin, J. Colgate, and D. Kamper, "An actuated finger exoskeleton for hand rehabilitation following stroke," in *2007 IEEE 10th international conference on rehabilitation robotics*, 2007: IEEE, pp. 896-901.

[8]   S. Wen, J. Chen, S. Wang, H. Zhang, and X. Hu, "Path Planning of Humanoid Arm Based on Deep Deterministic Policy Gradient," in *2018 IEEE International Conference on Robotics and Biomimetics (ROBIO)*, 2018: IEEE, pp. 1755-1760.

[9]   A. Wege, K. Kondak, and G. Hommel, "Force control strategy for a hand exoskeleton based on sliding mode position control," in *2006 IEEE/RSJ International Conference on Intelligent Robots and Systems*, 2006: IEEE, pp. 4615-4620.

[10]   A. Wege, K. Kondak, and G. Hommel, "Mechanical design and motion control of a hand exoskeleton for rehabilitation," in *IEEE International Conference Mechatronics and Automation, 2005*, 2005, vol. 1: IEEE, pp. 155-159.

[11]   A. Wege and G. Hommel, "Development and control of a hand exoskeleton for rehabilitation of hand injuries," in *2005 IEEE/RSJ International Conference on Intelligent Robots and Systems*, 2005: IEEE, pp. 3046-3051.

[12]   F. Wang, "Design and Control of Robotic Systems for Upper Extremity Rehabilitation Following Stroke," Doctor of Philosophy, Mechanical Engineering, Vanderbilt, 2011.

[13]   H. Tuy, *Convex Analysis and Global Optimization*. Springer Nature, 2016.

[14]   S. Tortora, M. Moro, and E. Menegatti, "Dual-Myo Real-Time Control of a Humanoid Arm for Teleoperation," in *2019 14th ACM/IEEE International Conference on Human-Robot Interaction (HRI)*, 2019: IEEE, pp. 624-625.

[15]   K. Tong *et al.*, "An intention driven hand functions task training robotic system," in *2010 Annual International Conference of the IEEE Engineering in Medicine and Biology*, 2010: IEEE, pp. 3406-3409.

[16]   B. Tondu, S. Ippolito, J. Guiochet, and A. Daidie, "A seven-degrees-of-freedom robot-arm driven by pneumatic artificial muscles for humanoid robots," *The International Journal of Robotics Research,* vol. 24, no. 4, pp. 257-274, 2005.

[17]   A. Stilli. "Inflatable variable stiffness soft robots " https://ethos.bl.uk/OrderDetails.do?uin=uk.bl.ethos.769957 (accessed.

[18]   K. Stepanova, T. Pajdla, and M. Hoffmann, "Robot Self-Calibration Using Multiple Kinematic Chains—A Simulation Study on the iCub Humanoid Robot," *IEEE Robotics and Automation Letters,* vol. 4, no. 2, pp. 1900-1907, 2019.

[19] C. N. Schabowsky, S. B. Godfrey, R. J. Holley, and P. S. Lum, "Development and pilot testing of HEXORR: hand EXOskeleton rehabilitation robot," *Journal of neuroengineering and rehabilitation,* vol. 7, no. 1, p. 36, 2010.

[20] I. Sarakoglou, N. G. Tsagarakis, and D. G. Caldwell, "Occupational and physical therapy using a hand exoskeleton based exerciser," in *2004 IEEE/RSJ International Conference on Intelligent Robots and Systems (IROS)(IEEE Cat. No. 04CH37566)*, 2004, vol. 3: IEEE, pp. 2973-2978.

[21] S. P. S. Sumathi, *Computational Intelligence Paradigms Theory and Applications Using MATLAB*. 2010.

[22] S. C. Roll and M. E. Hardison, "Effectiveness of occupational therapy interventions for adults with musculoskeletal conditions of the forearm, wrist, and hand: A systematic review," *American Journal of Occupational Therapy,* vol. 71, no. 1, pp. 7101180010p1-7101180010p12, 2017.

[23] Z. L. Richard M. Murray, S. Shankar Sastry, *A Mathematical Introduction to Robotic Manipulation*. 1994.

[24] D. S. V. B. R.A.R.C. Gopura, Kazuo Kiguchi, G.K.I. Mann, "Developments in hardware systems of active upper-limb exoskeleton robots: A review," *Robotics and Autonomous Systems,* 2016.

[25] S.-W. Pu and J.-Y. Chang, "Robotic hand system design for mirror therapy rehabilitation after stroke," *Microsystem Technologies,* pp. 1-9, 2020.

[26] Z. M. Pinhas Ben-Tzvi, "Sensing and Force-Feedback Exoskeleton (SAFE) Robotic Glove," *IEEE Transactions on Neural Systems and Rehabilitation Engineering,* 2014.

[27] P. K. Parida, "Kinematic Analysis of Multi-Fingered, Anthropomorphic Robotic Hands," 2013.

[28] S. Pareek, H. Manjunath, E. T. Esfahani, and T. Kesavadas, "MyoTrack: Tracking subject participation in robotic rehabilitation using sEMG and IMU," in *2019 International Symposium on Medical Robotics (ISMR)*, 2019: IEEE, pp. 1-7.

[29] C. Ockenfeld, R. K. Tong, E. A. Susanto, S.-K. Ho, and X.-l. Hu, "Fine finger motor skill training with exoskeleton robotic hand in chronic stroke: Stroke rehabilitation," in *2013 IEEE 13th International Conference on Rehabilitation Robotics (ICORR)*, 2013: IEEE, pp. 1-4.

[30] M. Mohan and K. J. Kuchenbecker, "A Design Tool for Therapeutic Social-Physical Human-Robot Interactions," in *2019 14th ACM/IEEE International Conference on Human-Robot Interaction (HRI)*, 2019: IEEE, pp. 727-729.

[31] P. D. Marasco *et al.*, "Illusory movement perception improves motor control for prosthetic hands," *Science translational medicine,* vol. 10, no. 432, p. eaao6990, 2018.

[32] M. Li *et al.*, "Attention-controlled assistive wrist rehabilitation using a low-cost EEG Sensor," *IEEE Sensors Journal,* 2019.

[33] D. Leonardis *et al.*, "An EMG-controlled robotic hand exoskeleton for bilateral rehabilitation," *IEEE transactions on haptics,* vol. 8, no. 2, pp. 140-151, 2015.

[34] T. C. KOON, "A Task Oriented Robotic Hand Rehabilitation System for Post-Stroke Recovery," 2015.

[35] S. Kim, C. Kim, and J. H. Park, "Human-like arm motion generation for humanoid robots using motion capture database," in *2006 IEEE/RSJ International Conference on Intelligent Robots and Systems*, 2006: IEEE, pp. 3486-3491.

[36] G. J. Kim, M. Taub, C. Creelman, C. Cahalan, M. W. O'Dell, and J. Stein, "Feasibility of an Electromyography-Triggered Hand Robot for People After Chronic Stroke," *American Journal of Occupational Therapy,* vol. 73, no. 4, pp. 7304345040p1-7304345040p9, 2019.

[37] J. Khan, "Hand Therapy Needs," D. Benson, Ed., ed, 2019.

[38] H. Kawasaki *et al.*, "Development of a hand motion assist robot for rehabilitation therapy by patient self-motion control," in *2007 IEEE 10th International Conference on Rehabilitation Robotics*, 2007: IEEE, pp. 234-240.

[39] K. Kaneko *et al.*, "Humanoid Robot HRP-5P: An Electrically Actuated Humanoid Robot With High-Power and Wide-Range Joints," *IEEE Robotics and Automation Letters,* vol. 4, no. 2, pp. 1431-1438, 2019.

[40] C. L. Jones, F. Wang, C. Osswald, X. Kang, N. Sarkar, and D. G. Kamper, "Control and kinematic performance analysis of an Actuated Finger Exoskeleton for hand rehabilitation following stroke," in *2010 3rd IEEE RAS & EMBS International Conference on Biomedical Robotics and Biomechatronics*, 2010: IEEE, pp. 282-287.

[41] H. K. Jamshed Iqbal, Nikos G. Tsagarakis, and D. G. Caldwell, "A novel exoskeleton robotic system for hand rehabilitation – Conceptualization to prototyping," *ScienceDirect,* 2014.

[42] G. Jackson, "Development of a Pneumatic Hand Training Device for Stroke Rehabilitation," 2013.

[43] J. Iqbal, N. G. Tsagarakis, A. E. Fiorilla, and D. G. Caldwell, "A portable rehabilitation device for the hand," in *2010 Annual International Conference of the IEEE Engineering in Medicine and Biology*, 2010: IEEE, pp. 3694-3697.

[44] J. B. Inseong Jo, "Design and control of a wearable and force-controllable hand exoskeleton system," *Mechatronics,* 2017.

[45] M. Haghshenas-Jaryani, R. M. Patterson, N. Bugnariu, and M. B. Wijesundara, "A pilot study on the design and validation of a hybrid exoskeleton robotic device for hand rehabilitation," *Journal of Hand Therapy,* vol. 33, no. 2, pp. 198-208, 2020.

[46] M. Grebenstein *et al.*, "The DLR hand arm system," in *2011 IEEE International Conference on Robotics and Automation*, 2011: IEEE, pp. 3175-3182.

[47] S. Garcia-Vergara, "Coupling of an Oobjective And Quantifiable Methodology for Assessing Upper-Body Movements with Virtual Reality Gaming Platforms," 2017.

[48] Y. Fu, P. Wang, and S. Wang, "Development of a multi-DOF exoskeleton based machine for injured fingers," in *2008 IEEE/RSJ International Conference on Intelligent Robots and Systems*, 2008: IEEE, pp. 1946-1951.

[49] S. Fan. "Thought-Controlled Prosthetic Hand Restores 100 Realistic Touch Sensations." https://singularityhub.com/2017/11/27/thought-controlled-prosthetic-hand-delivers-100-realistic-sensations/#sm.00000et87ap4jddb0qnbjynyr11pd (accessed.

[50] S. Fan. "New Bionic Arm Blurs Line Between Self And Machine For Wearers." https://singularityhub.com/2018/04/04/new-bionic-arm-blurs-line-between-self-and-machine-for-wearers/#sm.00000et87ap4jddb0qnbjynyr11pd (accessed.

[51] P.-H. C. Erkin Gezgin, Ahmet Faruk Akhan, "Synthesis of a Watt II six-bar linkage in the design of a hand rehabilitation robot," *Mechanism and Machine Theory,* 2016.

[52] S. H. Chua, J. S. Limqueco, E. L. Lu, S. W. Que, and D. Abuan, "Development of a Microcontroller-based Wireless Writing Robotic Arm Controlled by Skeletal Tracking," in *2018 IEEE 10th International Conference on Humanoid, Nanotechnology, Information Technology, Communication and Control, Environment and Management (HNICEM)*, 2018: IEEE, pp. 1-6.

[53] M. A. R. Christian Ott, Florian Schmidt,Werner Friedl,, R. B. Johannes Englsberger, Alexander Werner,, D. L. Alexander Dietrich, Bernd Henze, Oliver Eiberger,, B. B. Alexander Beyer, Christoph Borst,, and a. A. Albu-Schäffer, "Mechanism Design of DLR Humanoid Robots," in *Humanoid Robotics: A Reference*, 2019.

[54] A. Chiri, N. Vitiello, F. Giovacchini, S. Roccella, F. Vecchi, and M. C. Carrozza, "Mechatronic design and characterization of the index finger module of a hand exoskeleton for post-stroke rehabilitation," *IEEE/ASmE Transactions on mechatronics,* vol. 17, no. 5, pp. 884-894, 2011.

[55] G. Cannata, M. Maggiali, G. Metta, and G. Sandini, "An embedded artificial skin for humanoid robots," in *2008 IEEE International Conference on Multisensor Fusion and Integration for Intelligent Systems*, 2008: IEEE, pp. 434-438.

[56]   C. Bütefisch, H. Hummelsheim, P. Denzler, and K.-H. Mauritz, "Repetitive training of isolated movements improves the outcome of motor rehabilitation of the centrally paretic hand," *Journal of the neurological sciences,* vol. 130, no. 1, pp. 59-68, 1995.

[57]   D. A. Brooks, "Towards Quantifying Upper-Arm Rehabilitation Metrics for Children Through Interaction With a Humanoid Robot," 2012.

[58]   L. Bing *et al.*, "System Design and Experiment of Bionics Robotic Arm with Humanoid Characteristics," in *2018 WRC Symposium on Advanced Robotics and Automation (WRC SARA)*, 2018: IEEE, pp. 90-95.

[59]   D. Berenson, "Constrained Manipulation Planning," 2011.

[60]   B. Bäuml, "Bringing a Humanoid Robot Closer to Human Versatility: Hard Realtime Software Architecture and Deep Learning Based Tactile Sensing," Universität Bremen, 2018.

[61]   T. Asfour and R. Dillmann, "Human-like motion of a humanoid robot arm based on a closed-form solution of the inverse kinematics problem," in *Proceedings 2003 IEEE/RSJ International Conference on Intelligent Robots and Systems (IROS 2003)(Cat. No. 03CH37453)*, 2003, vol. 2: IEEE, pp. 1407-1412.

[62]   B. Adams, "Evolutionary, Developmental Neural Networks for Robust Robotic Control," 2006.

[63]   "Hero Arm - An Affordable, Advanced And Intuitive Bionic Arm." https://openbionics.com/hero-arm/ (accessed.

[64]   "Robotic Hand Orthosis for Therapy and Assistance in Activities of Daily Living." https://relab.ethz.ch/research/current-research-projects/robotic-hand-orthosis-for-therapy-and-assistance-in-activities-of-daily-living.html (accessed.

[65]   "Hand Exercises After Surgery." https://www.spectrumortho.com/2018/03/02/hand-exercises-after-surgery/ (accessed.

[66]   "LUKE Arm." http://www.mobiusbionics.com/luke-arm/ (accessed.

[67]   "Hackberry |3D-Printable Open-Source Bionic Arm." http://exiii-hackberry.com/ (accessed.

[68]   "Bionic Arms | Limbitless Solutions." https://limbitless-solutions.org/ourResearch (accessed.
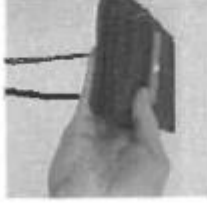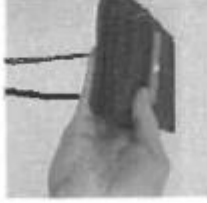
School of Occupational Therapy, Social Work & Speech Pathology
Range of Motion Assessment Chart

Curtin University

		Right	Left
Shoulder 0° to 180°	Flexion		
Shoulder 0° to 60°	Extension		
Elbow 0° to 150°	Ext/Flex		
Forearm 0° to 80°	Supination		
Forearm 0° to 80°	Pronation		
Wrist 0° to 80°	Flexion		
Wrist 0° to 70°	Extension		
Wrist 0° to 20°	Radial Dev		
Wrist 0° to 30°	Ulnar Dev		
Thumb CMC no norms	Radial Abd		
Thumb CMC no norms	Palmar Abd		
Thumb MCP 0° to 50°	Ext/Flex		
Thumb IP 0° to 80°	Ext/Flex		

		Right	Left
Index Finger 0° to 90°	MP Ext/Flex		
Index Finger 0° to 100°	PIP Ext/Flex		
Index Finger	DIP Ext/Flex		
Middle Finger 0° to 90°	MP Ext/Flex		
Middle Finger 0° to 100°	PIP Ext/Flex		
Middle Finger	DIP Ext/Flex		
Ring Finger 0° to 90°	MP Ext/Flex		
Ring Finger 0° to 100°	PIP Ext/Flex		
Ring Finger	DIP Ext/Flex		
Little Finger 0° to 90°	MP Ext/Flex		
Little Finger 0° to 100°	PIP Ext/Flex		
Little Finger 0° to 90°	DIP Ext/Flex		

Appendix B: Therapeutic Grasp Exercises

		Power		Precision	
Cylindrical	Spherical	Hook	Pinch	Tripod	Lumbrical

Appendix C: Exercise Pose Subject Joint Angles

		Pose Name: Row:	1	1	1	1	1	1	2	2	2	2	2	2	3	3	3	3	3	3
		Column:	1	2	3	4	5	6	1	2	3	4	5	6	1	2	3	4	5	6
		Joint Angle:																		
index	dip	1	30	5	80	0	5	0	0	10	85	0	0	0	65	20	80	5	0	0
middle		2	20	5	85	0	10	0	10	5	90	0	0	0	65	25	90	5	0	5
ring		3	20	5	85	0	20	0	0	15	90	0	0	0	65	20	80	0	0	0
little		4 *				70	15	20	0	5	45	90	30	0	65	5	80	45	70	70
index	pip	5	40	30	90	30	45	30	30	30	90	40	35	0	90	60	90	60	40	40
middle		6	35	35	90	30	60	0	45	80	90	90	45	45	90	50	90	30	45	45
ring		7	35	35	90	90	35	35	45	45	90	90	90	0	90	50	90	30	45	0
little		8	25	25	90	90	90	0	90	45	90	90	90	0	90	50	90	90	90	0
index	mcp	9	20	50	85	80	80	80	0	45	90	85	45	30	85	25	85	80	80	85
middle		10	25	40	90	80	30	75	0	5	90	90	45	30	90	0	90	30	80	80
ring		11	20	10	90	90	80	80	0	0	90	90	45	30	90	0	90	0	5	85
little		12	20	45	90	90	0	85	0	15	90	90	45	30	90	30	90	0	90	35
index	mcpa	13	0	0	0	0	-10	0	15	15	0	-5	-5	0	-5	5	-5	5	-5	-5
middle		14	0	0	0	0	0	0	0	0	0	0	0	0	0	0	0	0	0	0
ring		15	0	0	0	0	0	0	0	0	0	0	0	0	0	0	0	0	0	0
little		16	0	0	0	0	0	0	0	0	0	0	0	0	0	-10	0	0	0	0
thumb	dp	17	10	5	60	85	0	90	10	15	50	10	5	0	90	35	50	0	25	0
thumb	mcp	18	x	x	x	x	x	x	x	x	x	x	x	x	x	x	x	x	x	x
thumb	mcpa	19	x	x	x	x	x	x	x	x	x	x	x	x	x	x	x	x	x	x
thumb	cmc	20	x	x	x	x	x	x	x	x	x	x	x	x	x	x	x	x	x	x
thumb	cmcr	21	x	x	x	x	x	x	x	x	x	x	x	x	x	x	x	x	x	x
ring	cmc	22	5	0	0	0	0	0	0	0	0	0	0	5	0	0	0	0	0	0
little	cmc	23	10	0	0	0	0	0	0	0	0	0	0	0	0	0	0	0	0	0
wrist	abd	24	10	0	-20	0	0	20	20	15	10	-5	5	-10	-30	0	-20	0	15	20
wrist	flex	25	10	0	45	0	0	40	40	0	0	0	-10	45	-20	-70	-45	0	15	0
forearm	rota	26	80	0	30	0	0	180	90	0	90	90	0	180	45	-10	90	10	45	0

85

Appendix D: Subject Hand Measurements

Link	-	Length (mm)
L1	-	162
L2	-	96
L3	-	45
L4	-	41
L5	-	41
L6	-	45
L7	-	38
L8	-	46
L9	-	51
L10	-	28
L11	-	38
L12	-	43
L13	-	42
L14	-	33
L15	-	20
L16	-	33
L17	-	32
L18	-	23
L19	-	32
L20	-	20
L21	-	26
L22	-	23
L23	-	27
L24	-	28
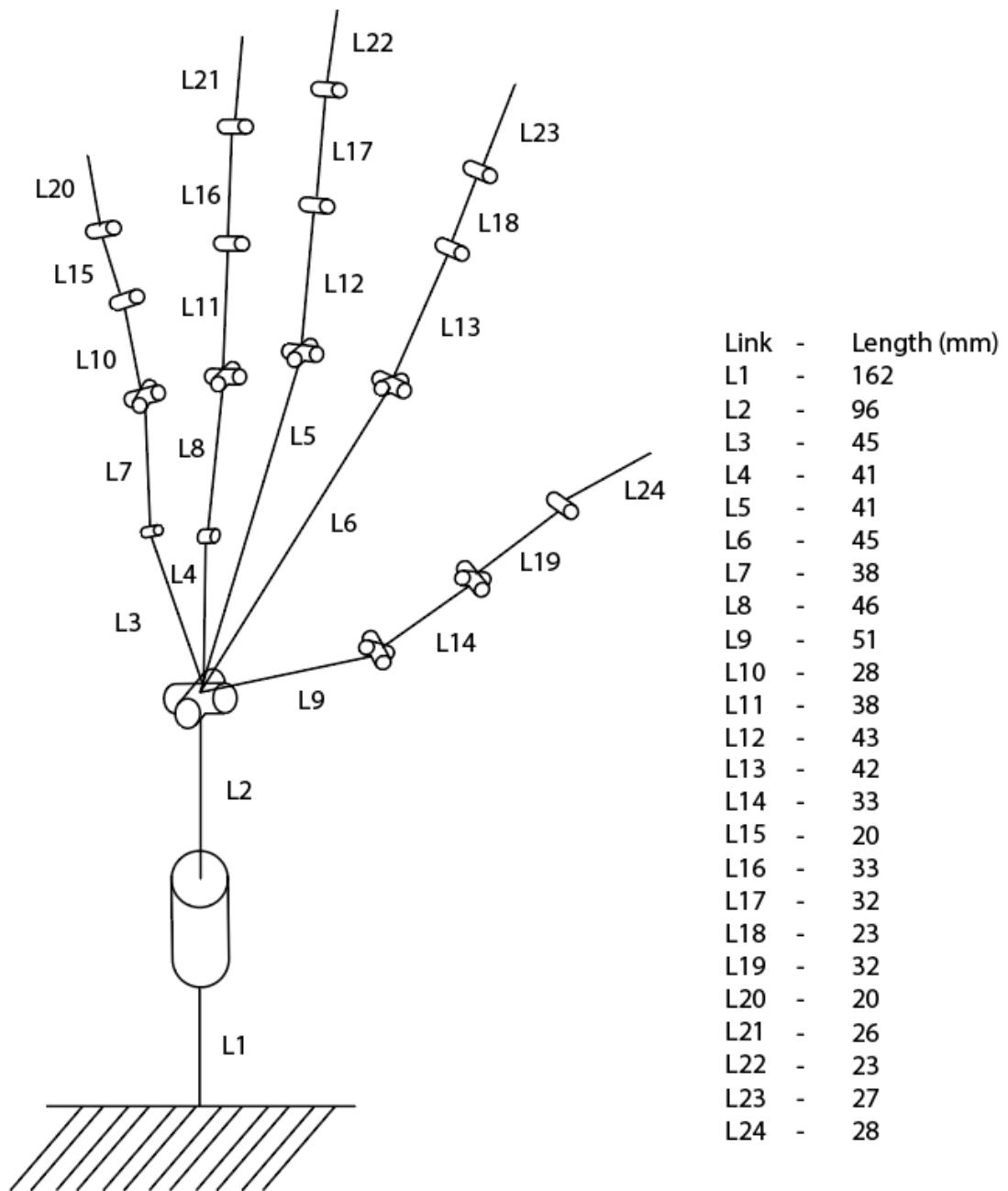
Analysis and Comparison of Modern Hand Exoskeleton Designs for Rehabilitation Therapy

Daniel Aidan Benson

Abstract

Exoskeleton design is a growing area of engineering investigation. The diverse needs for hand rehabilitation have inspired designing a variety of exoskeletons. This work analyses existing designs for understanding different processes of achieving sensing, control, and structural flexibility in exoskeletons. Through an objective analysis, this work tries to identify how structural, sensing and control elements work in synchrony to meet the rehabilitation requirements. The diverse actuation, volumetrics, sensing, and range of motion are studied to understand how applications influence optimizing designs for achieving the joint mobility and sensory requirement.

Hypothesis: Identify complexities in existing motion planning schemes and propose a simplified motion planning method.

Objectives

This work aims to explore theoretical and experimental challenges associated with the design of robotic exoskeleton orthoses in occupational hand therapy. The analyses required for planning and designing exoskeletons' interactions and functionality would help in achieving the following objectives:

    a. Building a robust model of a therapeutic hand exoskeleton;

    b. Developing a novel robotic system that can act upon, partially substitute and assist human beings in hand therapy;

    c. Designing and constructing therapeutic robots;

    d. Implementing sophisticated behavioural routines that replicate human motion; and

    e. Simplifying the motion planning scheme and incorporating a distributed, low profile sensory system for reporting behavioural data in a diverse selection of sites.

Introduction

The primary focus of this paper is to provide an overview of the subject of current and recent trends in the development of hand exoskeletons for the rehabilitation of the human hand. In this paper we will be reviewing the design functionality and capabilities as well as the size and scale of past exoskeletons, this will permit us to make an informed decision on possible designs, revisions and potential improvements to provide future designs that are capable of achieving a greater form of operation and greater means of control.

The process of review for designs involves locating appropriate papers which contain adequate display and discussion of individual excellent designs as well as their usage and rehabilitation this results in any papers which produce insufficient results or incomplete designs being disregarded due to not being able to provide meaningful information or being insufficient to provide a meaningful view. In addition to the base papers further data has been acquired and discussed to
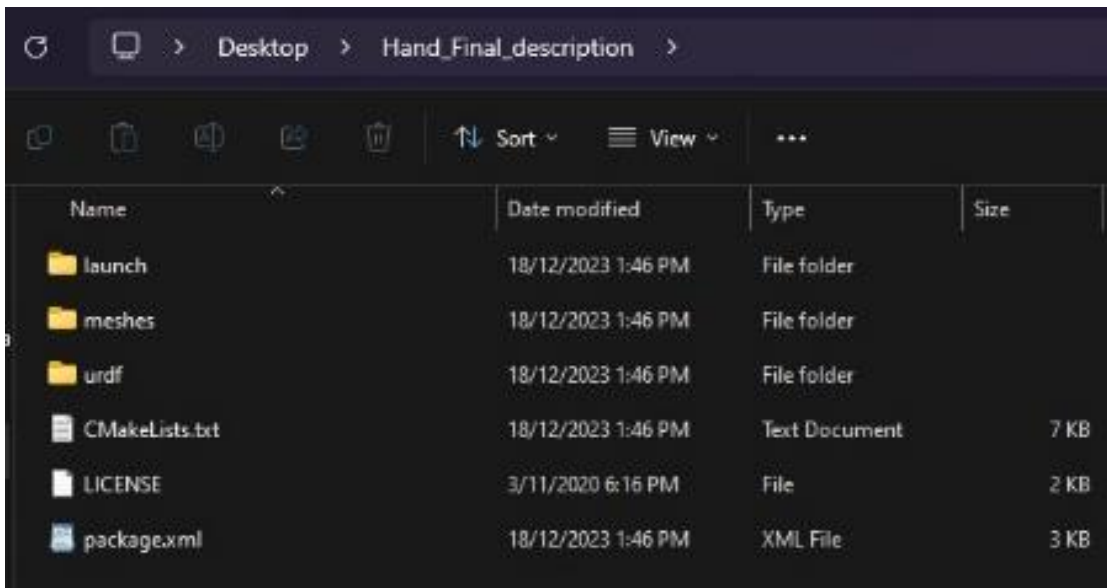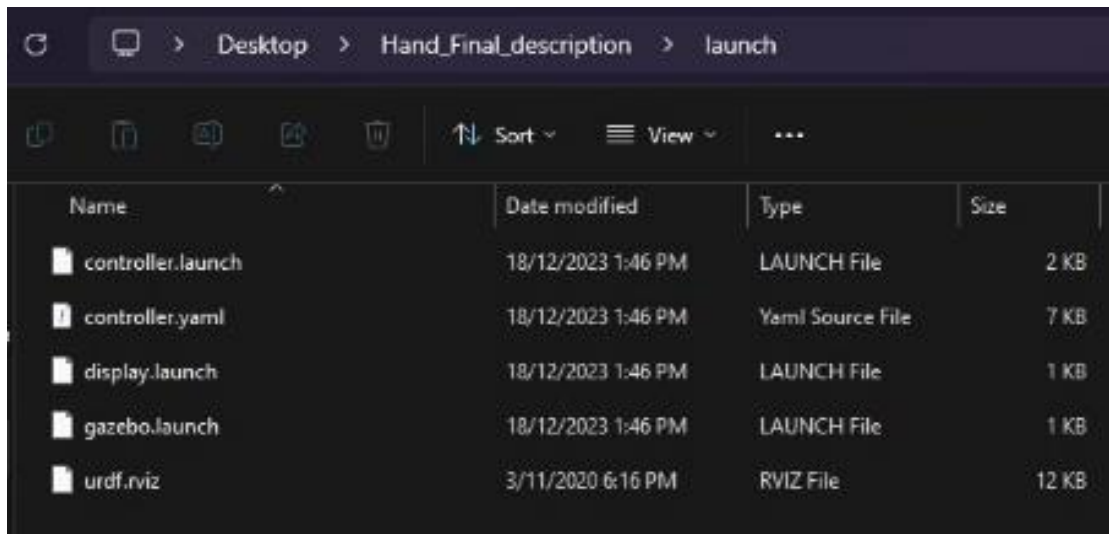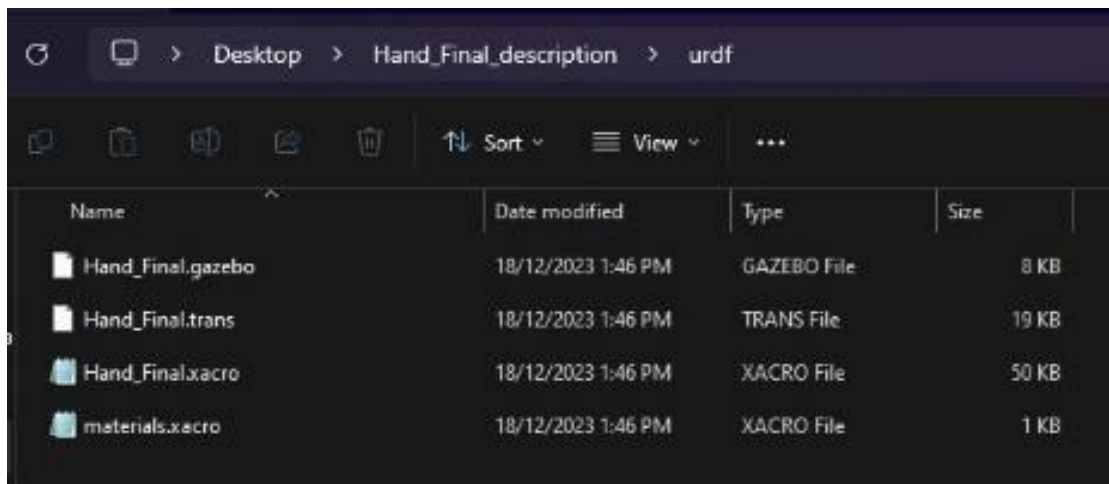
Appendix F: ROS Export Process

(1)

(2)

(3)

(4)

(5)

⮐ Sort ˅   ≡ View ˅   •••
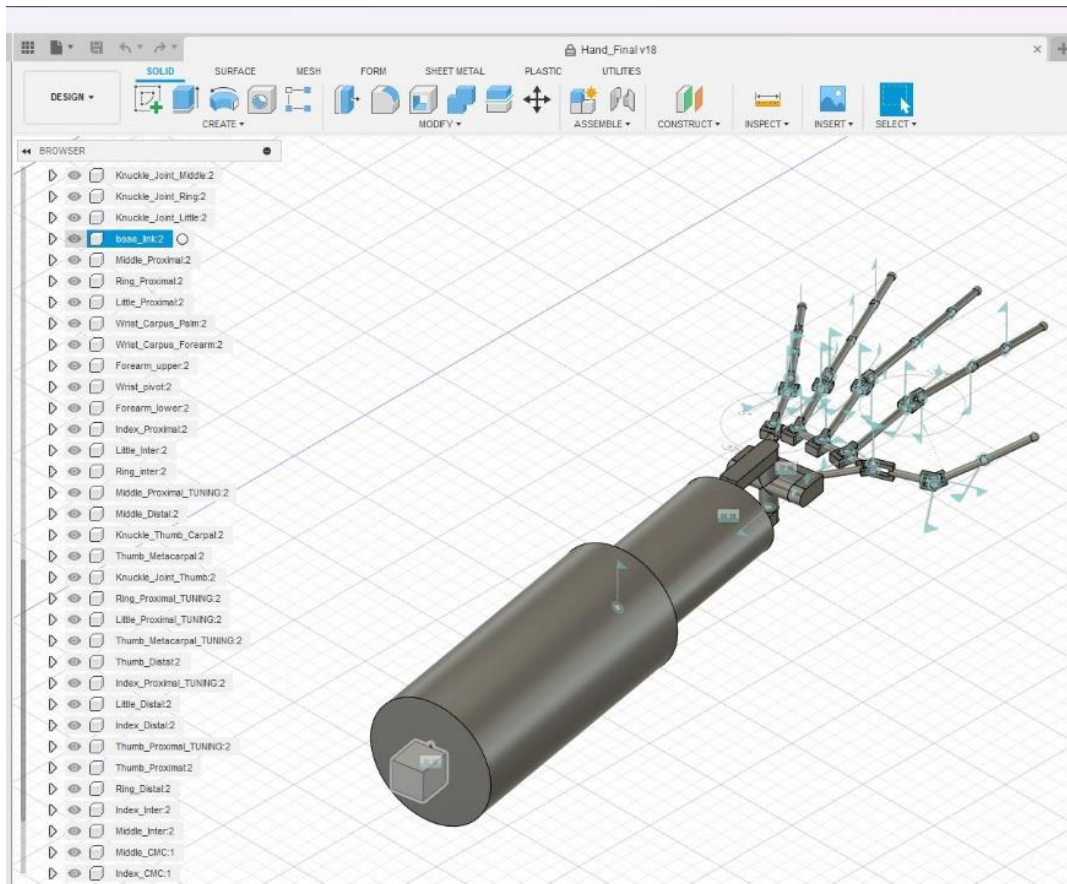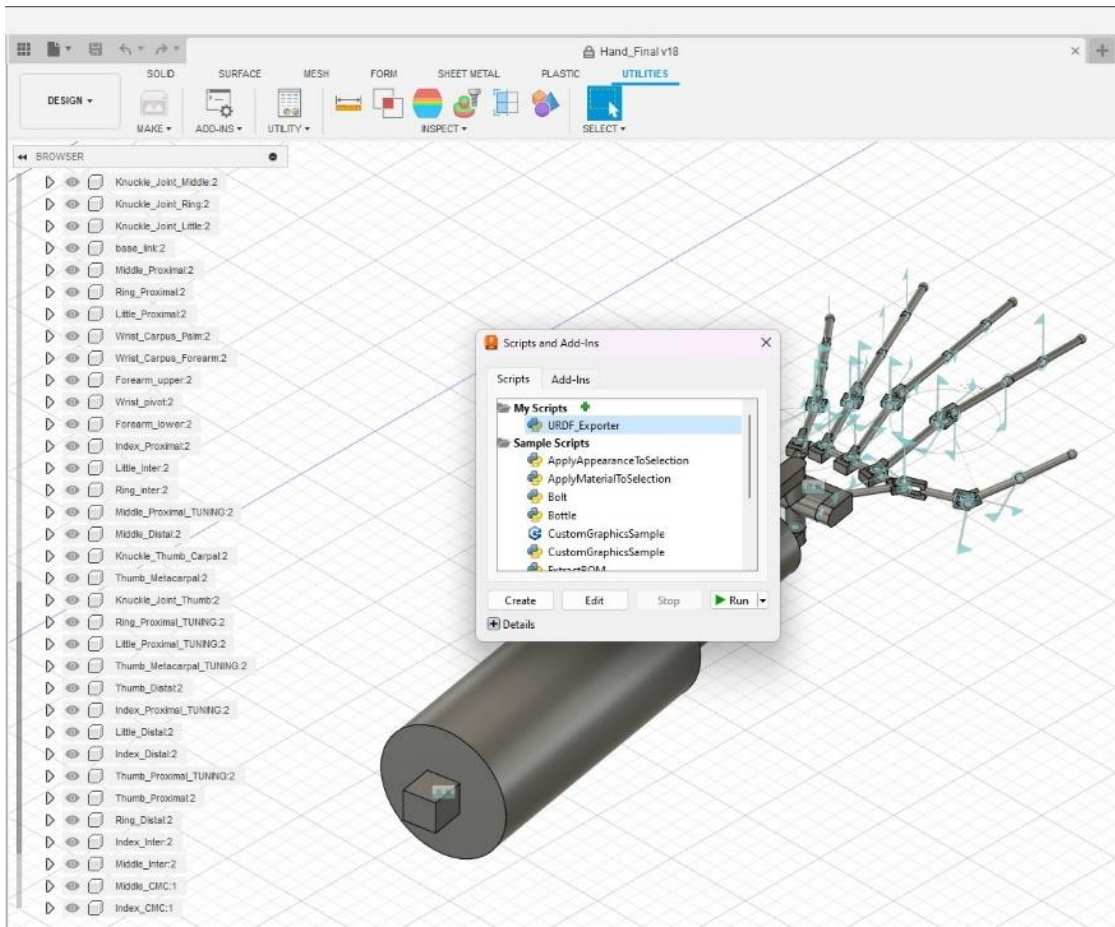
Name	Date modified	Type	Size
base_link.stl	18/12/2023 1:46 PM	Program Photon...	1 KB
Forearm_lower_2.stl	18/12/2023 1:46 PM	Program Photon...	19 KB
Forearm_upper_2.stl	18/12/2023 1:46 PM	Program Photon...	14 KB
Index_CMC_1.stl	18/12/2023 1:46 PM	Program Photon...	31 KB
Index_Distal_2.stl	18/12/2023 1:46 PM	Program Photon...	79 KB
Index_Inter_2.stl	18/12/2023 1:46 PM	Program Photon...	70 KB
Index_Metacarpal_2.stl	18/12/2023 1:46 PM	Program Photon...	17 KB
Index_Metacarpal_TUNING_2.stl	18/12/2023 1:46 PM	Program Photon...	13 KB
Index_Proximal_2.stl	18/12/2023 1:46 PM	Program Photon...	36 KB
Index_Proximal_TUNING_2.stl	18/12/2023 1:46 PM	Program Photon...	14 KB
Knuckle_Joint_Index_2.stl	18/12/2023 1:46 PM	Program Photon...	31 KB
Knuckle_Joint_Little_2.stl	18/12/2023 1:46 PM	Program Photon...	30 KB
Knuckle_Joint_Middle_2.stl	18/12/2023 1:46 PM	Program Photon...	31 KB
Knuckle_Joint_Ring_2.stl	18/12/2023 1:46 PM	Program Photon...	31 KB
Knuckle_Joint_Thumb_2.stl	18/12/2023 1:46 PM	Program Photon...	30 KB
Knuckle_Thumb_Carpal_2.stl	18/12/2023 1:46 PM	Program Photon...	30 KB
Little_CMC_1.stl	18/12/2023 1:46 PM	Program Photon...	31 KB
Little_Distal_2.stl	18/12/2023 1:46 PM	Program Photon...	87 KB
Little_Inter_2.stl	18/12/2023 1:46 PM	Program Photon...	71 KB
Little_Metacarpal_2.stl	18/12/2023 1:46 PM	Program Photon...	17 KB
Little_Metacarpal_TUNING_2.stl	18/12/2023 1:46 PM	Program Photon...	12 KB
Little_Proximal_2.stl	18/12/2023 1:46 PM	Program Photon...	42 KB
Little_Proximal_TUNING_2.stl	18/12/2023 1:46 PM	Program Photon...	13 KB
Middle_CMC_1.stl	18/12/2023 1:46 PM	Program Photon...	32 KB
Middle_Distal_2.stl	18/12/2023 1:46 PM	Program Photon...	87 KB
Middle_Inter_2.stl	18/12/2023 1:46 PM	Program Photon...	57 KB
Middle_Metacarpal_2.stl	18/12/2023 1:46 PM	Program Photon...	17 KB

(6)

Appendix G: Copyright Permissions

Thesis / Dissertation Reuse

The IEEE does not require individuals working on a thesis to obtain a formal reuse license, however, you may print out this statement to be used as a permission grant:

Requirements to be followed when using any portion (e.g., figure, graph, table, or textual material) of an IEEE copyrighted paper in a thesis:

1) In the case of textual material (e.g., using short quotes or referring to the work within these papers) users must give full credit to the original source (author, paper, publication) followed by the IEEE copyright line © 2011 IEEE.
2) In the case of illustrations or tabular material, we require that the copyright line © [Year of original publication] IEEE appear prominently with each reprinted figure and/or table.
3) If a substantial portion of the original paper is to be used, and if you are not the senior author, also obtain the senior author's approval.

Requirements to be followed when using an entire IEEE copyrighted paper in a thesis:

1) The following IEEE copyright/ credit notice should be placed prominently in the references: © [year of original publication] IEEE. Reprinted, with permission, from [author names, paper title, IEEE publication title, and month/year of publication]
2) Only the accepted version of an IEEE copyrighted paper can be used when posting the paper or your thesis on-line.
3) In placing the thesis on the author's university website, please display the following message in a prominent place on the website: In reference to IEEE copyrighted material which is used with permission in this thesis, the IEEE does not endorse any of [university/educational entity's name goes here]'s products or services. Internal or personal use of this material is permitted. If interested in reprinting/republishing IEEE copyrighted material for advertising or promotional purposes or for creating new collective works for resale or redistribution, please go to http://www.ieee.org/publications_standards/publications/rights/rights_link.html to learn how to obtain a License from RightsLink.

If applicable, University Microfilms and/or ProQuest Library, or the Archives of Canada may supply single copies of the dissertation.